

A Novel Naphthalene Polymer Based on the 1, 3, 5 -Triazines

Kawa Hama Sharif Mahmood

Submitted to the
Institute of Graduate Studies and Research
in partial fulfillment of the requirement for the degree of

Master of Science
in
Chemistry

Eastern Mediterranean University
July 2015
Gazimağusa, North Cyprus

Approval of the Institute of Graduate Studies and Research

Prof. Dr. Serhan Çiftçiođlu
Acting Director

I certify that this thesis satisfies the requirements as a thesis for the degree of Master of Science in Chemistry.

Prof. Dr. Mustafa Halilsoy
Chair, Department of Chemistry

We certify that we have read this thesis and that in our opinion it is fully adequate in scope and quality as a thesis for the degree of Master of Science in Chemistry.

Prof. Dr. Huriye İcil
Supervisor

Examining Committee

1. Prof. Dr. Huriye İcil

2. Asst.Prof.Dr.Nur P. Aydinlik

3. Asst.Prof.Dr.Hürmüz Refik

ABSTRACT

Naphthalene diimide-based polymers used as acceptors in organic photovoltaic cells due to their perfect thermal, chemical, and photochemical stability and high electron affinity.

In the present study, a novel naphthalene polymer (TANPI) was synthesized by polycondensation of 1,4,5,8-naphthalene tetracarboxylic dianhydride (NDA) with hindered aromatic diamine, 2,4-diamino-6-phenyl-1,3,5-triazine in isoquinoline and m-cresol solvents mixture and under argon atmosphere. The synthesized product purity was confirmed using elemental analysis, IR and UV-vis spectroscopy.

The product TANPI is soluble mainly in polar solvents such as pyridine, NMP, DMF, DMSO, m-cresol and TFAC in brown colour. The product was insoluble in polar protic solvents such ethanol and methanol.

The optical properties for the polymer were investigated using absorption and emission spectrophotometric measurements. Observed different properties indicate different intermolecular interactions in different solvent which can be important in photonic applications. It is important to note that, excimer emission were observed in pyridine, NMP, DMF, DMSO, m-cresol and TFAC with long Stoke Shifts.

Fluorescence quantum yields in different solvents were determined using anthracene in ethanol as standard (NMP: 2%, DMF: 5% and DMSO: 1%).

Keywords: Naphthalene polymers, hindered diamine, photonics, solar cells.

ÖZ

Naftalen diimid esaslı polimerler termal, kimyasal ve fotokimyasal kararlılıkları ve yüksek elektron ilgileri nedeniyle Organik Fotovoltaik Hücrelerde electron akseptörler olarak kullanılmaktadırlar.

Bu çalışmada, ,1,4,5,8-naftalen tetrakarboksilik dianhidrit (NDA) ve engelli diamin 2,4-diamino-6-fenil-1,3,5-triazin kullanımı ile isokinolin ve m-kresol çözen karışımında yeni bir naftalen polimeri, argon atmosferinde sentezlenmiştir (TANPI). Sentezlenen ürünün saflığı elemental analiz, IR ve UV-vis spektroskopi ölçümleri ile doğrulanmıştır.

Sentezlenen polimer NMP, DMF, DMSO, m-kresol ve TFAC gibi polar çözenlerde kahve renkte çözünmektedir. Ürün etanol ve methanol gibi polar protik çözenlerde ise çözünmemektedir.

Polimer ürününün optik özellikleri absorpsiyon ve emisyon spektroskopik ölçümleri ile araştırılmıştır. Gözlenen farklı özellikler değişik çözenler içerisinde moleküller arası ilişkinin farklı olduğunu işaret etmektedir. Bu özellikler fotonik uygulamalar için önemli avantajlar sağlayabilecek niteliktedir.

Piridin, NMP, DMF, DMSO, m-kresol ve TFAC çözenlerinde alınan emisyon spektrumlarında ekzimer emisyonu ve uzun Stoke Shift gözlenmiş olması önemli bulgulardır.

Fluoresans kuantum verimler deęişik özgenler içerisinde antrasen (etanolda) standardına göre ölçülmüşlerdir (NMP: 2%, DMF: 5% and DMSO: 1%).

Anahtar kelimeler: Naftalen polimeri, engelli diamin, fotonik, solar hücre.

To Prof.Dr.H.IciL

ACKNOWLEDGMENT

First of all, I would like to express my appreciation thanks to my supervisor Prof. Dr. Huriye Icil for giving me the great opportunity to study in her research group and for her excellent guidance, caring, patience and providing me with an excellent atmosphere my master thesis. I will always remember her as a distinguished scientist. I am really lucky because I was her student.

I would like to sincerely thank to the jury members.

I would like to thank Dr. Duygu Uzun for her supports and help me during my research.

Also very special thanks to Icil's Organic Group at Eastern Mediterranean University.

Finally, I am grateful to my wife (Ilham) and my son (Sina) for their endless encouragements and abundant love during my studies

TABLE OF CONTENTS

ABSTRACT.....	iii
ÖZ.....	iv
DEDICATION.....	vi
ACKNOWLEDGMENT	vii
LIST OF TABLES.....	x
LIST OF FIGURES	xi
LIST OF ILLUSTRATIONS.....	xviii
LIST OF ABBREVIATIONS/ SYMBOLS.....	xix
1 INTRODUCTION	1
2 THEORETICAL.....	6
2.1 Naphthalene Dyes in Applications.....	6
2.2 Energy Transfer.....	8
2.3 Electron Transfer.....	9
2.4 Supramolecular Systems.....	11
2.5 Naphthalene Dyes in Photonic Applications.....	12
3 EXPERIMENTAL.....	14
3.1 Materials.....	14
3.2 Instruments.....	14
3.3 Method of Synthesis.....	15
3.4 Synthesis of TANPI.....	16
3.5 General Synthetic Mechanisms.....	17
4 DATA AND CALCULATION.....	20
4.1 Photophysical Properties.....	20

4.1.1 Absorptivity Coefficients.....	20
4.1.2 Fluorescence Quantum Yield (Φ_f).....	21
4.1.3 The Selected Maximum Absorption Half-width ($\Delta\bar{\nu}_{1/2}$).....	23
4.1.4 Theoretical Radiative Lifetimes (τ_0).....	25
4.1.5 Theoretical Fluorescence Lifetime (τ_f).....	26
4.1.6 Theoretical Fluorescence Rate constant (k_f).....	27
4.1.7 Rate Constant of Radiationless Deactivation (k_d).....	28
4.1.8 Oscillator Strengths (f)	28
4.1.9 Singlet Energy (E_s).....	29
4.1.10 Optical Band Gap Energy (E_g).....	30
5 RESULT AND DISCUSSION.....	109
5.1 Synthesis of the compound TANDI.....	109
5.2 Solubility of TANPI	109
5.3 Analysis of FT-IR Spectra.....	110
5.4 Optical Properties.....	113
6 CONCLUSION.....	115
REFERENCES.....	116
APPENDIX.....	123
Appendix A : Curriculum Vitae.....	124

LIST OF TABLES

Table 4.1: Absorbance and concentration data of TANPI in NMP.....	20
Table 4.2: Absorptivity coefficient data of TANPI in different solvents.....	21
Table 4.3: Fluorescence quantum yields of TANPI in different solvents.....	22
Table 4.4: Half-width of TANPI in different solvents.....	24
Table 4.5: In different solvents Theoretical radiative lifetimes data of TANPI.....	25
Table 4.6: In different solvents theoretical fluorescence lifetime of TANPI.....	26
Table 4.7: Calculated theoretical fluorescence lifetime of TANPI in different solvents.....	26
Table 4.8: Radiationless deactivation Rate constant of TANPI in different solvents.....	27
Table 4.9: Oscillator strength data of TANPI in different solvents.....	28
Table 4.10: Singlet energy of TANPI in different solvents.....	29
Table 4.11: Band gap energy of TANPI in different solvents.....	30
Table 5.1: Solubility properties of TANPI in different solvents.....	108
Table 5.2: Stokes shifts of TANPI ($C = 1 \times 10^{-5}$ M) in different solvents.....	113
Table 5.3: Optical and photochemical constant.....	114

LIST OF FIGURES

Figure 1.1: Cyclophane Based on Cram, Schubert, and Smith.	1
Figure 1.2: N, N-Di (2 -amino - 4 - phenyl -1, 3, 5-triazine) -1, 4, 5, 8 Naphthalene Tetracarboxylic Diimide.....	4
Figure 1.3: Para-cyclophane.....	5
Figure 1.4: Naphthalene-1, 4, 5, 8-tetracarboxylicacid-bis - (N, N` - bis -6-Phenyl-1, 3, 5 Triaznylpolyimide.....	5
Figure 2.1: Application of Naphthalene Dyes in organic solar cell.....	7
Figure 2.2: Jablonski Diagram Illustrating Fluorescence Resonance Energy Transfer	8
Figure 2.3: Energy Transfer According To Dexter and Forster Mechanism.....	9
Figure 2.4: Donor-Bridge-Acceptor Model Systems.....	10
Figure 2.5: Quenching by Electron Transfer Due to Charge Transfer Complex.....	11
Figure 2.6: Supramolecular Assemblies of Non-Covalent Bonds.....	12
Figure 4.1: Plot Absorbance And Concentration Of TANPI In NMP.....	21
Figure 4.2: Absorption Spectrum of TANPI in NMP.....	23
Figure 4.3: Absorption Spectrum Of TANPI In NMP.....	30
Figure 4.4: FT-IR Spectrum of TANPI	31
Figure 4.5: Absorption Spectrum Of TANPI in DMSO (C = 1×10^{-5} M, Inset: Enlarged Spectrum, 450-800 Nm).....	32
Figure 4.6: Absorption Spectrum of TANPI in DMSO (Microfiltered, Inset: Enlarged Spectrum, 450-800 nm).....	33
Figure 4.7: Absorption Spectrum of TANPI in DMSO (—: C = 1×10^{-5} M ; - - : Microfiltered; Inset: Enlarged Spectra 450-800 nm).....	34

Figure 4.8: Emission Spectrum of TANPI in DMSO ($C = 1 \times 10^{-5}$ M; $\lambda_{exc} = 360$ nm).....	35
Figure 4.9: Emission Spectrum of TANPI in DMSO (Microfiltered; $\lambda_{exc} = 360$ nm).....	36
Figure 4.10: Emission Spectrum of TANPI in DMSO (— : $C = 1 \times 10^{-5}$ M; - - : Microfiltered; $\lambda_{exc} = 360$ nm).....	37
Figure 4.11: Emission Spectrum of TANPI in DMSO ($C=1 \times 10^{-5}$ M; $\lambda_{exc} = 485$ nm).....	38
Figure 4.12: Emission Spectrum of TANPI in DMSO (Microfiltered ; $\lambda_{exc} = 485$ nm).....	39
Figure 4.13: Emission Spectrum of TANPI in DMSO (— : $C = 1 \times 10^{-5}$ M; - - : Microfiltered; $\lambda_{exc} = 485$ nm).....	40
Figure 4.14: Excitation Spectrum of TANPI in DMSO ($C = 1 \times 10^{-5}$ M; $\lambda_{emis} = 650$ nm).....	41
Figure 4.15: Excitation Spectrum of TANPI in DMSO (Microfiltered; $\lambda_{emis} = 650$ nm).....	42
Figure 4.16: Excitation Spectrum of TANPI in DMSO (— : $C= 1 \times 10^{-5}$ M ; - - : Microfiltered; $\lambda_{emis} = 650$ nm).....	43
Figure 4.17: Absorption Spectrum of TANPI in DMF ($C = 1 \times 10^{-5}$ M, Inset: Enlarged Spectrum, 450-800 nm).....	44
Figure 4.18: Absorption Spectrum of TANPI in DMF (Microfiltered; Inset: Enlarged Spectrum; 450-800 nm).....	45
Figure 4.19: Absorption Spectrum of TANPI in DMF (— : $C = 1 \times 10^{-5}$ M; - - : Microfiltered; Inset: Enlarged spectra 450-800 nm).....	46
Figure 4.20: Emission Spectrum of TANPI in DMF ($C = 1 \times 10^{-5}$ M; $\lambda_{exc} = 360$ nm).....	

nm).....	47
Figure 4.21: Emission Spectrum of TANPI in DMF (Microfiltered; $\lambda_{exc} = 360$ nm)	
.....	48
Figure 4.22: Emission Spectrum of TANPI in DMF (—: $C = 1 \times 10^{-5}$ M; - - : Microfiltered; $\lambda_{exc} = 360$ nm).....	49
Figure 4.23: Emission Spectrum of TANPI in DMF ($C = 1 \times 10^{-5}$ M; $\lambda_{exc} = 485$ nm).....	50
Figure 4.24: Emission Spectrum of TANPI in DMF (Microfiltered; $\lambda_{exc} = 485$ nm).....	51
Figure 4.25: Emission Spectrum of TANPI in DMF (—: $C = 1 \times 10^{-5}$ M; - - : Microfiltered; $\lambda_{exc} = 485$ nm).....	52
Figure 4.26: Excitation Spectrum of TANPI in DMF ($C = 1 \times 10^{-5}$ M; $\lambda_{emis} = 650$ nm).....	53
Figure 4.27: Excitation Spectrum of TANPI in DMF (Microfiltered; $\lambda_{emis} = 650$ nm).....	54
Figure 4.28: Excitation Spectrum of TANPI in DMF (—: $C = 1 \times 10^{-5}$ M; - - : Microfiltered; $\lambda_{emis} = 650$ nm).....	55
Figure 4.29: Absorption spectrum of TANPI in NMP ($C = 1 \times 10^{-5}$ M, Inset: enlarged spectrum ,450-800 nm).....	56
Figure 4.30: Absorption spectrum of TANPI in NMP (Microfiltered, Inset: Enlarged Spectrum, 450-800 nm).....	57
Figure 4.31: Absorption Spectrum of TANPI in NMP (— : $C = 1 \times 10^{-5}$ M; - - : Microfiltered; Inset: Enlarged Spectrum 450-800 nm.....	58
Figure 4.32: Emission Spectrum of TANPI in DMF ($C=1 \times 10^{-5}$ M; $\lambda_{exc} = 360$ nm).....	59

Figure 4.33: Emission Spectrum of TANPI in NMP (Microfiltered; $\lambda_{\text{exc}} = 360$ nm).....	60
Figure 4.34: Emission Spectrum of TANPI in NMP (— : $C = 1 \times 10^{-5}$ M; - - : Microfiltered; $\lambda_{\text{exc}} = 360$ nm).....	61
Figure 4.35: Emission Spectrum of TANPI in NMP ($C = 1 \times 10^{-5}$ M; $\lambda_{\text{exc}} = 485$ nm).....	62
Figure 4.36: Emission Spectrum of TANPI in NMP (Microfiltered; $\lambda_{\text{exc}} = 485$ nm).....	63
Figure 4.37: Emission Spectrum of TANPI in NMP (—: $C = 1 \times 10^{-5}$ M; - - : Microfiltered; $\lambda_{\text{exc}} = 485$ nm).....	64
Figure 4.38: Excitation Spectrum of TANPI in NMP ($C = 1 \times 10^{-5}$ M; $\lambda_{\text{emis}} = 650$ nm).....	65
Figure 4.39: Excitation Spectrum of TANPI in NMP (Microfiltered; $\lambda_{\text{emis}} = 650$ nm).....	66
Figure 4.40: Excitation Spectrum of TANPI in NMP (—: $C = 1 \times 10^{-5}$ M; - - : Microfiltered; $\lambda_{\text{emis}} = 650$ nm).....	67
Figure 4.41: Absorption Spectrum of TANPI in TCE ($C = 1 \times 10^{-5}$ M, Inset: Enlarged Spectrum, 450-800 nm).....	68
Figure 4.42: Absorption Spectrum of TANPI in TCE (Microfiltered, Inset: Enlarged Spectrum, 450-800 nm).....	69
Figure 4.43: Absorption Spectrum of TANPI in TCE (— : $C = 1 \times 10^{-5}$ M; - - : Microfiltered; Inset: Enlarged Spectra 450-800 nm).....	70
Figure 4.44: Emission Spectrum of TANPI in TCE ($C = 1 \times 10^{-5}$ M; $\lambda_{\text{exc}} = 360$ nm).....	71
Figure 4.45: Emission Spectrum of TANPI in TCE (Microfiltered; $\lambda_{\text{exc}} = 360$	

nm).....	72
Figure 4.46: Emission Spectrum of TANPI in TCE (— : $C = 1 \times 10^{-5}$ M; - - : Microfiltered; $\lambda_{exc} = 360$ nm).....	73
Figure 4.47: Emission Spectrum of TANPI in TCE ($C = 1 \times 10^{-5}$ M; $\lambda_{exc} = 485$ nm).....	74
Figure 4.48: Emission Spectrum of TANPI in TCE (Microfiltered ; $\lambda_{exc} = 485$ nm).....	75
Figure 4.49: Emission Spectrum of TANPI in TCE (— : $C = 1 \times 10^{-5}$ M; - - : Microfiltered; $\lambda_{exc} = 485$ nm).....	76
Figure 4.50: Excitation Spectrum of TANPI in TCE ($C = 1 \times 10^{-5}$ M; $\lambda_{emis} = 650$ nm).....	77
Figure 4.51: Excitation Spectrum of TANPI in TCE (Microfiltered; $\lambda_{emis} = 650$ nm).....	78
Figure 4.52: Excitation Spectrum of TANPI in TCE (— : $C = 1 \times 10^{-5}$ M; - - : Microfiltered; $\lambda_{emis} = 650$ nm).....	79
Figure 4.53: Absorption Spectrum of TANPI in Pyridine ($C = 1 \times 10^{-5}$ M, Inset: Enlarged Spectrum, 450-800 nm).....	80
Figure 4.54: Absorption Spectrum of TANPI in Pyridine (Microfiltered, Inset: Enlarged Spectrum, 450-800 nm).....	81
Figure 4.55: Absorption Spectrum of TANPI in Pyridine (— : $C = 1 \times 10^{-5}$ M; - - : Microfiltered; Inset: Enlarged Spectra 450-800 nm).....	82
Figure 4.56: Emission Spectrum of TANPI in Pyridine ($C = 1 \times 10^{-5}$ M; $\lambda_{exc} = 360$ nm).....	83
Figure 4.57: Emission Spectrum of TANPI in Pyridine (Microfiltered; $\lambda_{exc} = 360$ nm).....	84

Figure 4.58: Emission Spectrum of TANPI in Pyridine (—: $C = 1 \times 10^{-5}$ M; - - : Microfiltered; $\lambda_{\text{exc}} = 360$ nm).....	85
Figure 4.59: Emission Spectrum of TANPI in Pyridine ($C = 1 \times 10^{-5}$ M; $\lambda_{\text{exc}} = 485$ nm)	86
Figure 4.60: Emission Spectrum of TANPI in Pyridine (Microfiltered; $\lambda_{\text{exc}} = 360$ nm)	87
Figure 4.61: Emission Spectrum of TANPI in Pyridine (—: $C = 1 \times 10^{-5}$ M; - - : Microfiltered; $\lambda_{\text{exc}} = 485$ nm).....	88
Figure 4.62: Excitation Spectrum of TANPI in Pyridine ($C = 1 \times 10^{-5}$ M; $\lambda_{\text{emis}} = 650$ nm).....	89
Figure 4.63: Excitation Spectrum of TANPI in Pyridine (Microfiltered; $\lambda_{\text{emis}} = 650$ nm).....	90
Figure 4.64: Excitation Spectrum of TANPI in Pyridine (—: $C = 1 \times 10^{-5}$ M; - - : Microfiltered; $\lambda_{\text{emis}} = 650$ nm).....	91
Figure 4.65: Absorption Spectrum of TANPI in m-cresol ($C = 1 \times 10^{-5}$ M, Inset: Enlarged Spectrum, 450-800 nm).....	92
Figure 4.66: Emission Spectrum of TANPI in m-cresol ($C = 1 \times 10^{-5}$ M; $\lambda_{\text{exc}} = 360$ nm).....	93
Figure 4.67: Emission Spectrum of TANPI in m-cresol ($C = 1 \times 10^{-5}$ M; $\lambda_{\text{exc}} = 485$ nm).....	94
Figure 4.68: Excitation Spectrum of TANPI in m-cresol ($C = 1 \times 10^{-5}$ M; $\lambda_{\text{emis}} = 650$ nm).....	95
Figure 4.69: Absorption Spectrum of TANPI in TFA ($C = 1 \times 10^{-5}$ M, Inset: Enlarged Spectrum, 450-800 nm).....	96
Figure 4.70: Emission Spectrum of TANPI in TFA ($C = 1 \times 10^{-5}$ M; $\lambda_{\text{exc}} = 360$	

nm).....	97
Figure 4.71: Emission Spectrum of TANPI in TFA ($C = 1 \times 10^{-5}$ M; $\lambda_{\text{exc}} = 485$ nm).....	98
Figure 4.72: Excitation Spectrum of TANPI in TFA ($C = 1 \times 10^{-5}$ M; $\lambda_{\text{emis}} = 650$ nm).....	99
Figure 4.73: Absorption Spectrum of TANPI in TFA, m-cresol, DMSO, DMF, NMP, Pyridine, and TCE ($C = 1 \times 10^{-5}$ M).....	100
Figure 4.74: Absorption Spectrum of TANPI in DMSO, DMF, NMP, Pyridine, and TCE (Microfiltered).....	101
Figure 4.75: Emission Spectrum of TANPI in TFA, M-cresol, DMSO, DMF, NMP, Pyridine, and TCE ($C = 1 \times 10^{-5}$ M; $\lambda_{\text{exc}} = 360$ nm).....	102
Figure 4.76: Emission Spectrum of TANPI in DMSO, DMF, NMP, Pyridine, and TCE (Microfiltered; $\lambda_{\text{exc}} = 360$ nm).....	103
Figure 4.77: Emission Spectrum of TANPI in TFA, m-cresol, DMSO, DMF, NMP, Pyridine, and TCE ($C = 1 \times 10^{-5}$ M; $\lambda_{\text{exc}} = 485$ nm).....	104
Figure 4.78: Emission spectrum of TANPI in DMSO, DMF, NMP, Pyridine, and TCE (Microfiltered; $\lambda_{\text{exc}} = 485$ nm).....	105
Figure 4.79: Excitation Spectrum of TANPI in TFA, m-cresol, DMSO, DMF, NMP, Pyridine, and TCE ($C = 1 \times 10^{-5}$ M; $\lambda_{\text{emis}} = 650$ nm).....	106
Figure 4.80: Excitation Spectrum of TANPI in DMSO, DMF, NMP, Pyridine, and TCE (Microfiltered; $\lambda_{\text{emis}} = 650$ nm).....	107

LIST OF ILLUSTRATIONS

Scheme 3.1: Synthetic of Naphthalene-1, 4, 5, 8-tetracarboxylicacid-bis - (N, N` - bis - 6-phenyl-1, 3, 5 triaznylpolyimide).....	14
--	----

LIST OF ABBREVIATIONS/SYMBOLS

Å	Armstrong
A	Absorbance
cm	Centimeter
°C	Degree Celsius
ϵ_{\max}	Maximum Extinction Coefficient
E_s	Singlet Energy
λ_{exc}	Excitation Wavelength
λ_{emis}	Emission wavelength
λ_{max}	Maximum Absorption Wavelength
TCE	1, 1, 2, 2- tetrachloroethane
TFAc	Trifluoroacetic acid
τ_0	Theoretical Radiative Lifetime
τ_f	Fluorescence Lifetime
Φ_f	Fluorescence Quantum Yield
nm	Nanometer
c	Concentration
DMF	N, N-dimethylformamide
DMSO	Dimethyl Sulfoxide
FT-IR	Fourier Transform Infrared Spectroscopy
FRET	Fluorescence Resonance Energy Transfer
h	Hour
HOMO	Highest Occupied Molecular Orbital

K_d	Rate Constant of Radiationless Deactivation
k_f	Fluorescence Rate Constant
LUMO	Lowest Unoccupied Molecular Orbital
M	Molar concentration
NDI	Naphthalene diimide
NMP	N-Methylpyrrolidone
Std	Standard
UV/VIS	Ultra violet visible spectroscopy
ν	Wavenumber
$\Delta\bar{\nu}_{1/2}$	Half-width of the selected Absorption
$\bar{\nu}_{\max}$	Mean frequency
MeOH	Methanol
f	Oscillator Strengths
mol	Mole
l	Path length
TGA	Thermogravimetric analysis
TANPI	Naphthalene-1, 4, 5, 8-tetracarboxylicacid-bis - (N, N' - bis -6-phenyl-1, 3, 5 triaznylpolyimide

Chapter 1

INTRODUCTION

From the last century, the interests of scientists have been captured towards the discovery of the concept of matters that are optically and spectroscopically active. Areas such as physics, chemistry, medicine and biology have witnessed unprecedented advancement with a continuing progress scientifically and technologically.

A cyclophane are known to consist of an aromatic ring and an aliphatic chain, forming a bridge at two positions of the aromatic unit [1] (Figure 1.1).

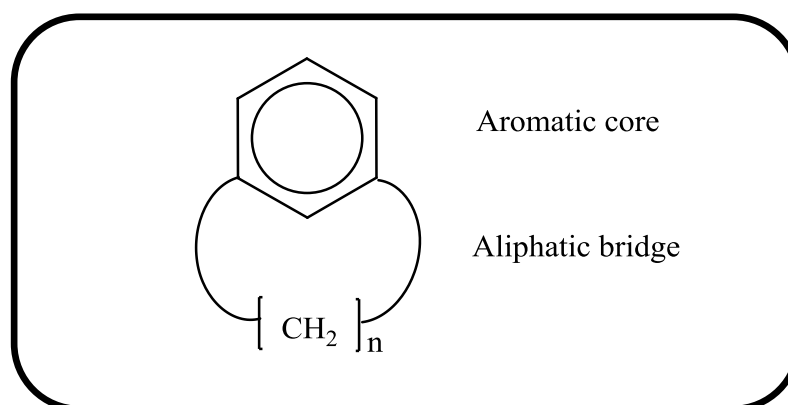


Figure 1.1: Cyclophane Based on Cram, Schubert, and Smith.

The field of supramolecular chemistry has kept the interest in cyclophanes due to their applicability in photonic devices [2]. Additionally, naphthalene diimides (NDIs) have been biologically and medically as well as in supramolecular chemistry. NDI's investigated for biological and supramolecular aspects applications as laser dyes,

structural models for photosynthetic reaction centers and DNA intercalators have also been reported [3].

1, 4, 5, 8-naphthalene tetracarboxylic diimides (NDIs) are planar and heteroaromatic compounds which act as acceptors and linker in electron transfer system (Figure 1.2) [4]. Applications of NDIs in optical and electronic devices have been investigated due to their promising n-type semiconducting properties [5]. Notably, the NDIs have shown outstanding photochemical and electrochemical properties [6]. They form triplet state efficiently and generate singlet state oxygen in high yields. They undergo two reversible and electrostable reduction processes to produce monoanions and dianions. Electrochemical properties of NDIs make them attractive for conducting materials and other optical devices [2].

In general, NDIs are soluble in low-polar (CHL, DCM, Toluene) and polar-aprotic (DMF, DMSO) organic solvents [2]. Scientists have studied the intercalation of diimides into DNA which have given more insight into explanation of photoinduced charge separation and recombination processes [7]. In general, the $\pi - \pi$ formed due to the planar structure reduce the solubility. On the other hand, different kinds of intermolecular interactions could generate various important optical properties [8].

Recently, scientists have been involved in the investigations on the supramolecular properties of Naphthalene diimides (NDIs) cyclophanes. The investigation of aromaticity of strained cyclic compounds and their electronic interactions were a challenge for researchers [9-10].

In supramolecular chemistry, structural building blocks are being assembled into regular arrays with new properties that could improve our knowledge on non-covalent interactions. NDIs undergo many effective host-guest interactions depending to their chemical structures (donor – acceptor moieties). NDIs with electron donor moieties are capable of making face to face intermolecular interactions. Further, the naphthalene diimides properties in intercalation, catenanes, rotaxanes, ion channel and foldamers have been investigated in detail in literature [11-12].

The cyclic compounds with aromatic rings as part of the cycle studied for new receptor designs. Metacyclophane and paracyclophane were the simplest cyclophanes (Figure 1.3). Furthermore, the commercially available paracyclophanes could be additionally functionalized through its aromatic core [13]. The properties of these cavities such as shape, size, charge, hydrophobicity become synthetically tunable [2]. In the past decade, several cyclophanes with guest molecules in their cavities have been reported. The interaction between “face to face” organized chromophores, with relation to the space and orientation to cyclophanes has been studied in detail for paracyclophanes, pyrenophanes and donor-acceptor cyclophanes [14].

The chemical and photochemical properties of several nitrogen-bridged cyclophanes have been investigated [15]. Many properties of them were affected by their rigid structure [16]. Their optical properties have attracted significant attention in view of their applications. They show lower excited energy state comparing their ligands. In general, the electron transfer properties of cyclophanes are investigated via photoelectron spectroscopy (PES), cyclic voltammetry (CV), ESR, UV/VIS and

emission spectra [17].

In this project, we have designed and synthesized a novel polymer based on the 1,3,5-triazines (Figure 1.4). The product was characterized and its optical and photophysical properties were investigated in detail. Expectively, related diimide product was obtained but could not be characterized completely due to its limited amount (Figure 1.2).

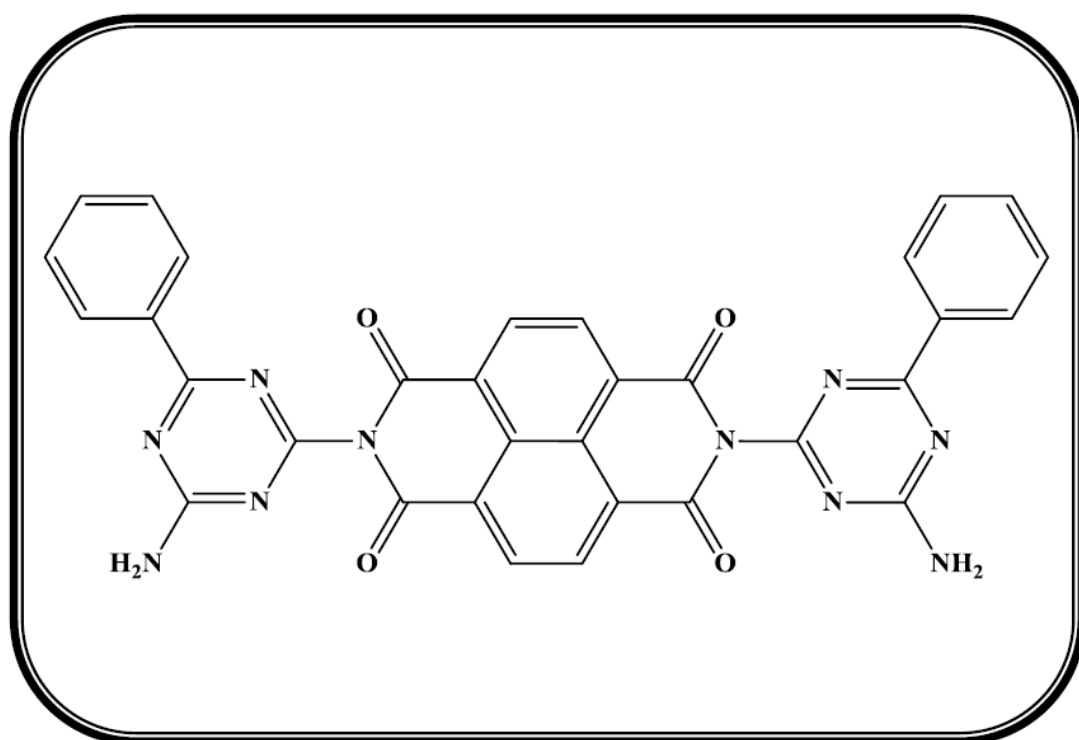


Figure 1.2: N, N-Di (2-Amino-4-Phenyl-1, 3, 5-Triazine)-1, 4, 5, 8 Naphthalene

Tetracarboxylic Diimide

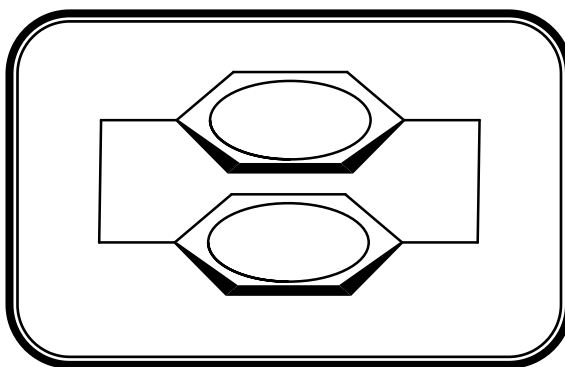


Figure 1.3: Para-Cyclophane

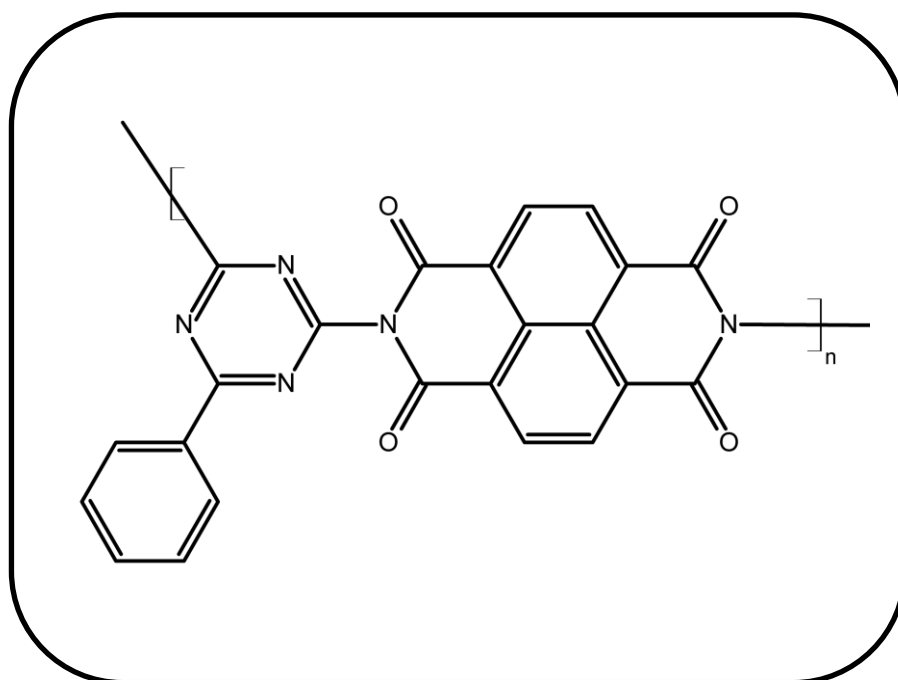


Figure 1.4: Naphthalene-1, 4, 5, 8-Tetracarboxylic acid-bis-(N, N'-bis-6-Phenyl-1, 3, 5-triaznylpolyimide)

Chapter 2

THEORETICAL

2.1 Naphthalene Dyes in Applications

Recent developments have shown tremendous advancement in the applications of naphthalene dimides (NDIs), especially in the field of supramolecular and material science [18]. Several many applications have been extensively studied by the functionalization of the naphthalene dimides through nitrogen atom [19]. In supramolecular building block-structures, naphthalene dimides (NDIs) act as redox active compounds for which scientists have been inspired to explore further [20].

Naphthalene dimides (NDIs) are easily and reversibly reducible because of the presence of carbonyl groups. Most of the simple NDIs derivatives have planar aromatic structure [21]. Nanorods obtained from amino acid containing NDIs through hydrogen bonding have been reported in literature. Their electron accepting properties and excellent photo and thermal stabilities make them attractive for photonic applications [22]. They have been investigated as rigid molecular cleft as linkers in electron-acceptor systems for DNA intercalators as UV absorbents [23-24].

Furthermore, their applications in organic solar cell systems studied (Figure 2.1) [25]. Biotechnologically the photolysis of naphthalene dimides (NDIs) have been utilized for heme protein, and used in the oxidation of protein and DNA [26].

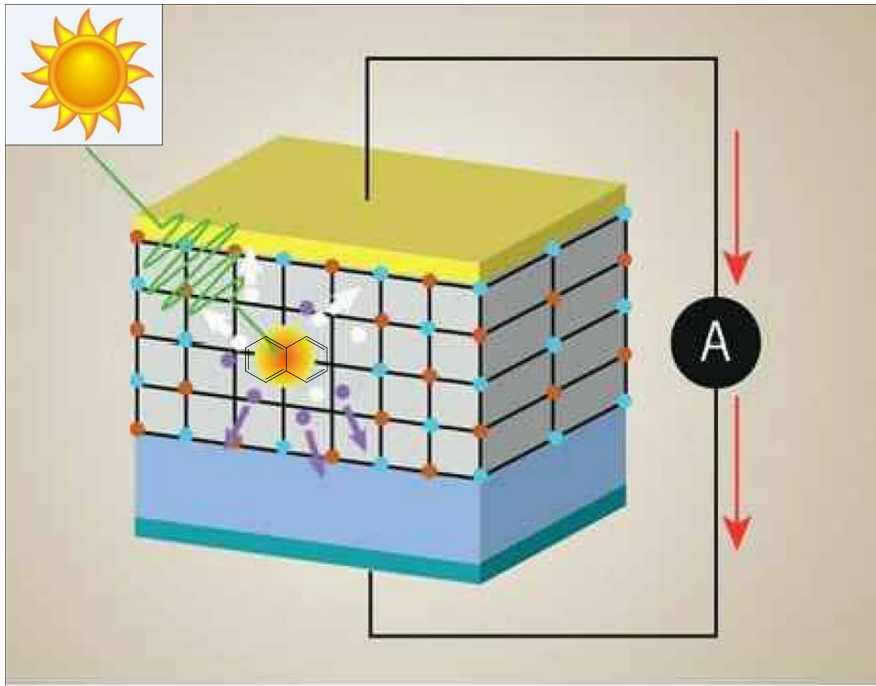


Figure 2.1: Application of Naphthalene Dyes in Organic Solar Cell

2.2 Fluorescence Resonance Energy Transfer (FRET)

Fluorescence resonance energy transfer (FRET) depends on distance. FRET is the radiationless transmission of energy from a donor molecule to an acceptor molecule.

An excited donor molecule transfers its energy to an acceptor molecule via nonradiative transmission (Figure 2.2) [27].

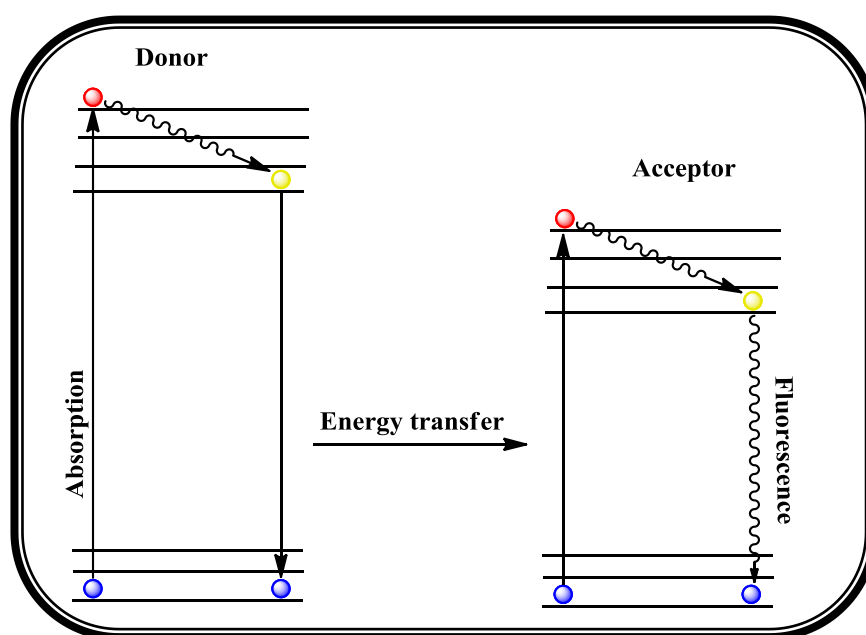


Figure 2.2: Jablonski Diagram Illustrating the FRET

The distance donor and acceptor molecules and donor emission and acceptor absorbance overlap are important factors for a successful fluorescence resonance energy transfer process [28].

Columbic (long range) or Dexter (short range) types energy transfers are possible. Evidently, both kinds of energy transfers are always both present. In general, Forster type energy transfer dominates for the distances (1-100 nm), while Dexter energy transfer taken over only at shorter than 1 nm distances (Figure 2.3) [29].

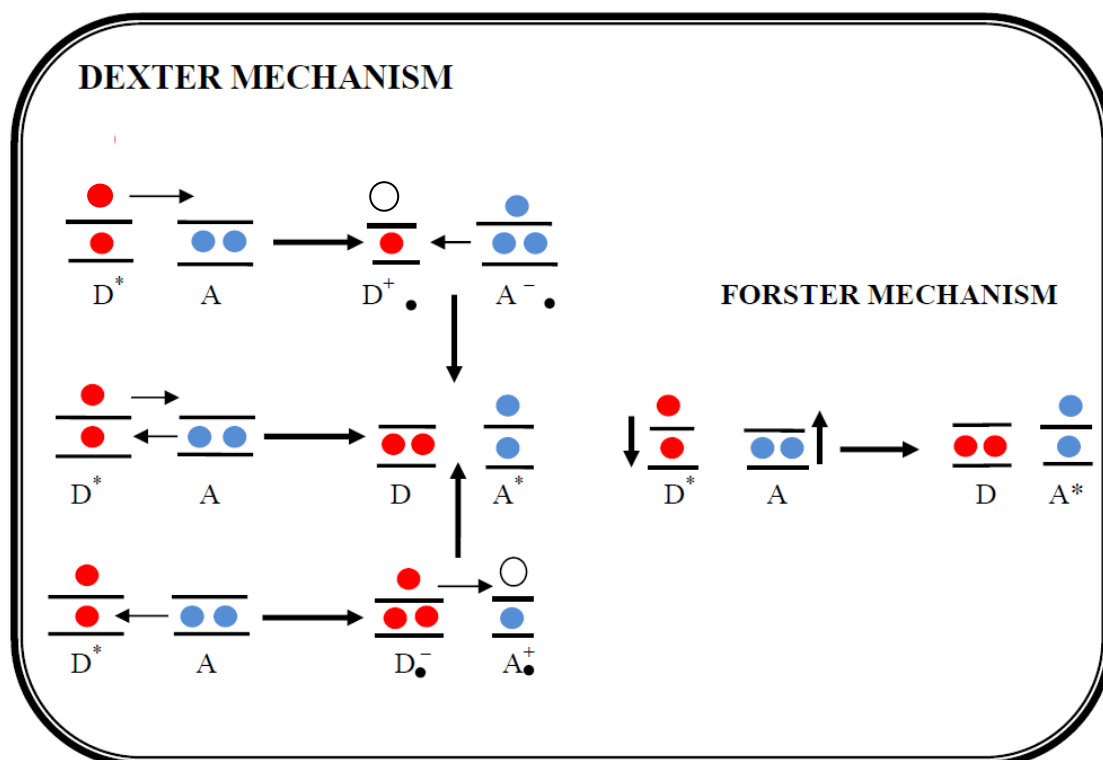
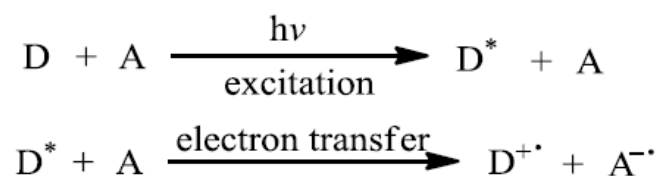


Figure 2.3: Energy Transfer According to Dexter and Förster Mechanism

2.3 Electron Transfer

The transfer of an electron from an electron donating specie (donor) to an electron accepting specie (acceptor) is known as electron transfer (ET) process [30].



Electron transfer can be explained by Marcus theory [36]. The rate of the electron transfer in reactions could be calculated according to Marcus theory, using the driving force of the reaction ($-\Delta G^\circ$), the reorganization energy which is associated with the unclear rearrangement upon electron transfer (λ) and electronic coupling matrix between donor and acceptor (V_{DA}) are known (Eq.2.1) [31].

$$K_{ET} = \sqrt{\frac{\pi}{h^2 l k_B T}} V_{DA} \exp\left(\frac{-\Delta G^\circ + \lambda}{4 \lambda k_B T}\right) \quad (\text{Eq.2.1})$$

There are two mechanisms in order to explain electron transfer over long range between donors and acceptors. When the electron moves in series of shorter electron transfer steps while reduction and oxidation of the bridging units occurs transiently, this is known as electron hopping. During charge transport bridging unit should have reduction potentials.

According to the second mechanism McConnell super exchange, electron donor and acceptors are mediated via coupling of the bridging units (Figure 2.4) [32].

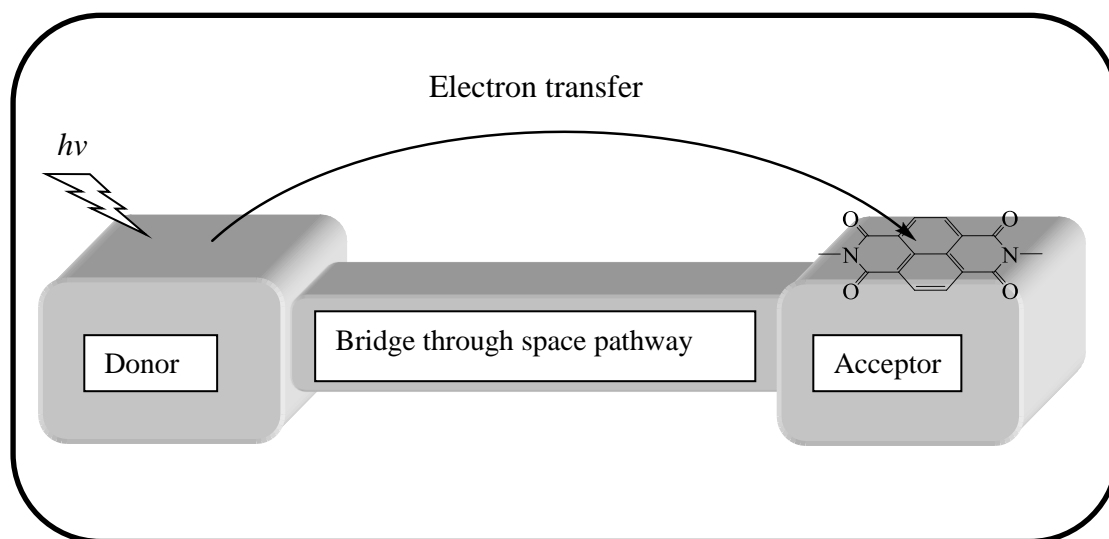


Figure 2.4: Donor-Bridge-Acceptor Model Systems

During electron transfer reactions, quenching (the deactivation of an excited state through a non-radiative process) generates radical ion pairs (charge transfer complex, Figure 2.5). This is usually from an occupied orbital of a donor to unoccupied orbital of an acceptor [33].

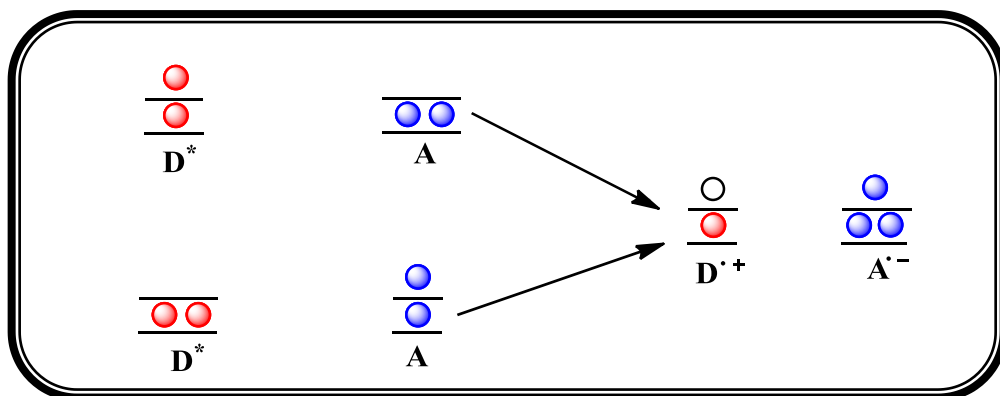
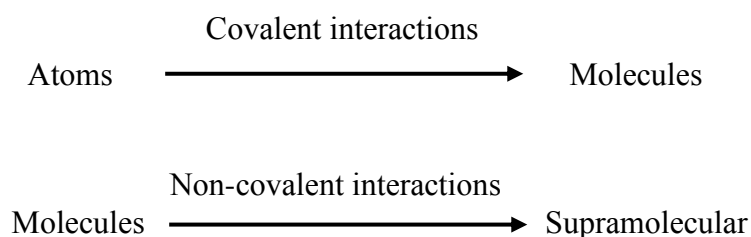


Figure 2.5: Quenching by Electron Transfer Due to Charge Transfer Complex

According to photo-oxidation studies, electron transfer processes are initiated through excited states (singlet or triplet excited states). Hence, movement of electrons (intramolecular and intermolecular charge transfer interactions) occurs in donor and acceptor chromophores on a same compound [34].

2.4 Supramolecular System

Self-organized systems that results from the association of two or more molecules held together by intermolecular forces (non-covalent bonds) are known as supramolecular systems (Figure 2.6) [35].



Recently, the fields of supramolecular chemistry have been developed exponentially. Novel structures could be prepared by using weak intermolecular interactions involving Vander Waals, π - π stacking, hydrogen bonding and dipole-dipole interactions [36].

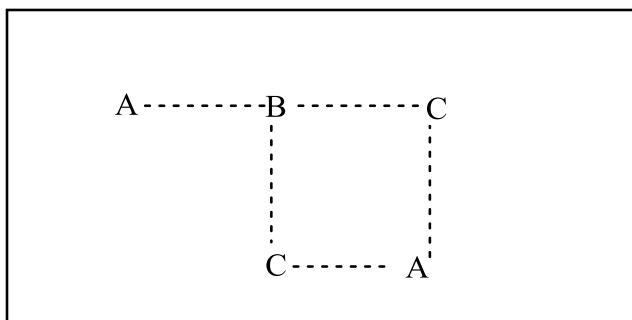


Figure 2.6: Supramolecular Assemblies of Non-Covalent Bonds

The aromatic NDI chromophores are well known for their important photonic properties [37]. Their applications in supramolecular systems are well described in literature. The controls of complex supramolecular molecules are formed by self-assembly [38]. Since most non-covalent interactions are relatively weak, without much activation barriers, many supramolecular systems can be controlled thermodynamically. Many novel materials obtained through self-organizations have been informed [39].

2.5 Naphthalene Dye in Photonic Application

Dye chemistry has been one of the oldest and most studied sections of industrial organic chemistry. Although commercial dyes are available, the developments of new functional chromophores are needed for high level photonic applications. Photonic devices are used in industry such as laser dyes, photodetectors and optical fiber [40]. In the past years, the use of dye assemblies in areas such as organic electronic and photonics have shown great success.

Dyes have excellent physical and chemical properties. They are important in photovoltaic devices like as laser markers and as fluorescent labels [41]. Naphthalene dyes possess high thermal photochemical and electrochemical stabilities. Hence, they are good candidates in photonic applications. They are used in smart films and fibers [42-43]. Also, they have been investigated for using in chromogenic polymer

systems and sensors. Their applications in liquid crystal displays reported in literature Furthermore, they have been investigated as intercalators for DNA, electron carrier units in organic light emitting diodes (OLED), a class of LED and near IR (NIR) fluorescent dyes [4-44].

Chapter 3

EXPERIMENTAL

3.1 Chemicals

1, 4, 5, 8-Naphthalene tetracarboxylic dianhydride ($C_{14}H_4O_6$), 2, 6-Diamino-4-phenyl-1, 3, 5-triazine ($C_9H_9N_5$), m-cresol, and isoquinoline were purchased from Aldrich. Spectroscopic grade solvents were used for spectroscopic measurements.

3.2 Instruments

Varian-Cary 100 spectrometer was used to measure ultraviolet absorption spectra (UV) in solutions.

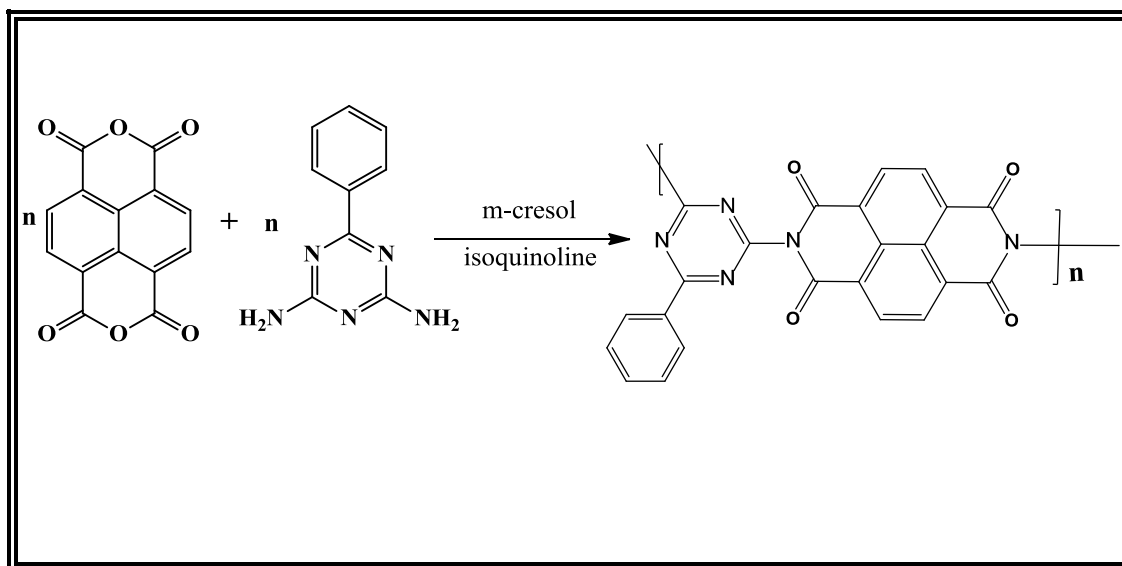
JASCO FT/IR- 6200 spectrometer was used to measure infrared spectra.

Varian Cary Eclipse Fluorescence spectrophotometer was used to record the emission and excitation spectra.

Elemental analysis was recorded by using Carol-Erba 1106 C, H and N-analyzer.

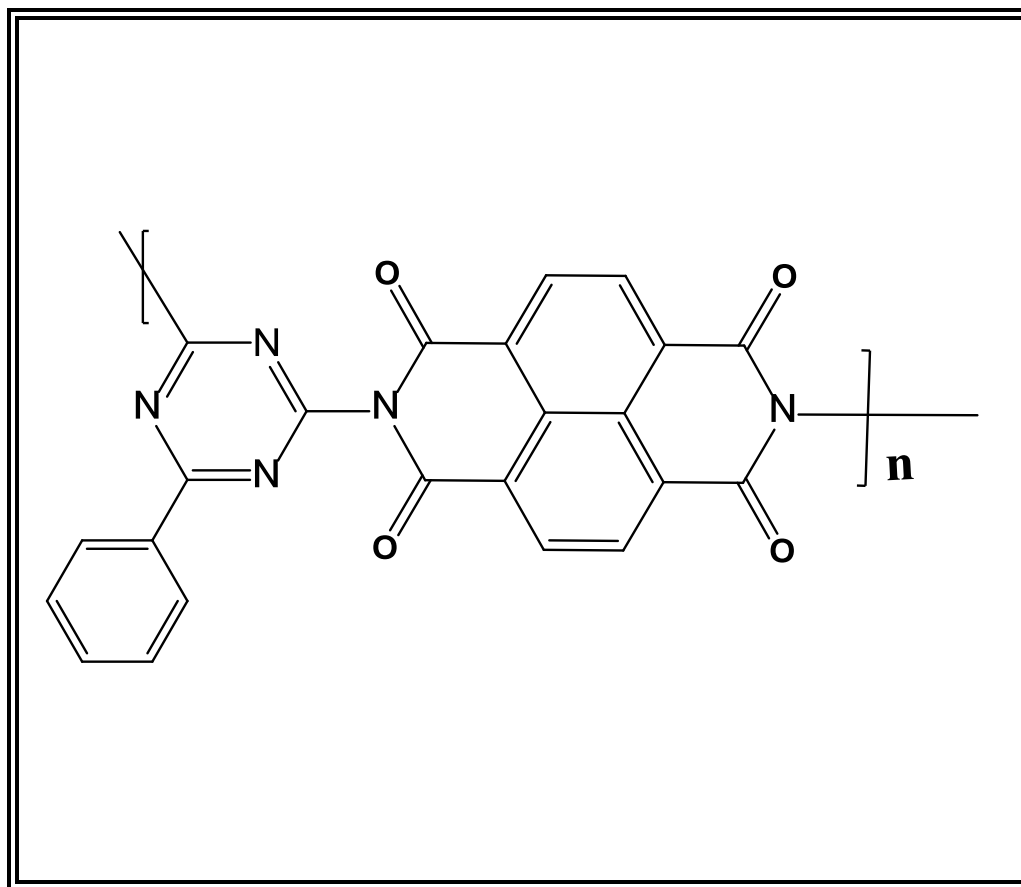
3.3 Synthetic Method

Naphthalene-1, 4, 5, 8-tetracarboxylicacid-bis - (N, N`- bis -6-phenyl-1, 3, 5 triaznylpolyimide was synthesized via condensation reaction obtained by one step as shown in Scheme 3.1. The product was purified with standard purification techniques.



Scheme 3.1: Synthetic Naphthalene-1, 4, 5, 8-tetracarboxylicacid-bis - (N, N`- bis -6-phenyl-1, 3, 5 triaznylpolyimide

3.4 Synthesis of TANPI



A mixture of both 1,4,5,8-Naphthalene tetracarboxylic dianhydride (1.004 g, 3.741 mmol) and 2,6-Diamino-4-phenyl-1,3,5-triazine (0.699 g, 3.737 mmol) in a solvent isoquinoline and m-cresol (40 ml) at 27 °C was continuously stirred in argon atmosphere. On further heating, the mixture was heated at 80 °C, 100 °C, 120 °C and 140 °C for 5 h, 4 h, 3 h and 6 h respectively. The temperature was then raised to 180 °C and stirred for 2h. Finally, the reaction was completed with heating 2 more hours at 200 °C. The reaction mixture at room temperature was poured into 200ml ethanol and the precipitate filtered using a suction filtration system. The crude product was purified from high-boiling point solvents and unreacted reactants by Soxhlet apparatus with chloroform for 50 hrs. The purified compound was dried at 100 °C in vacuum oven.

Yield: 60%

Color: Black.

FT-IR (KBr, cm^{-1}): 3443, 3173, 3070, 2860, 1696, 1632, 1526, 1443, 1270, 1100, 855, 768, 624

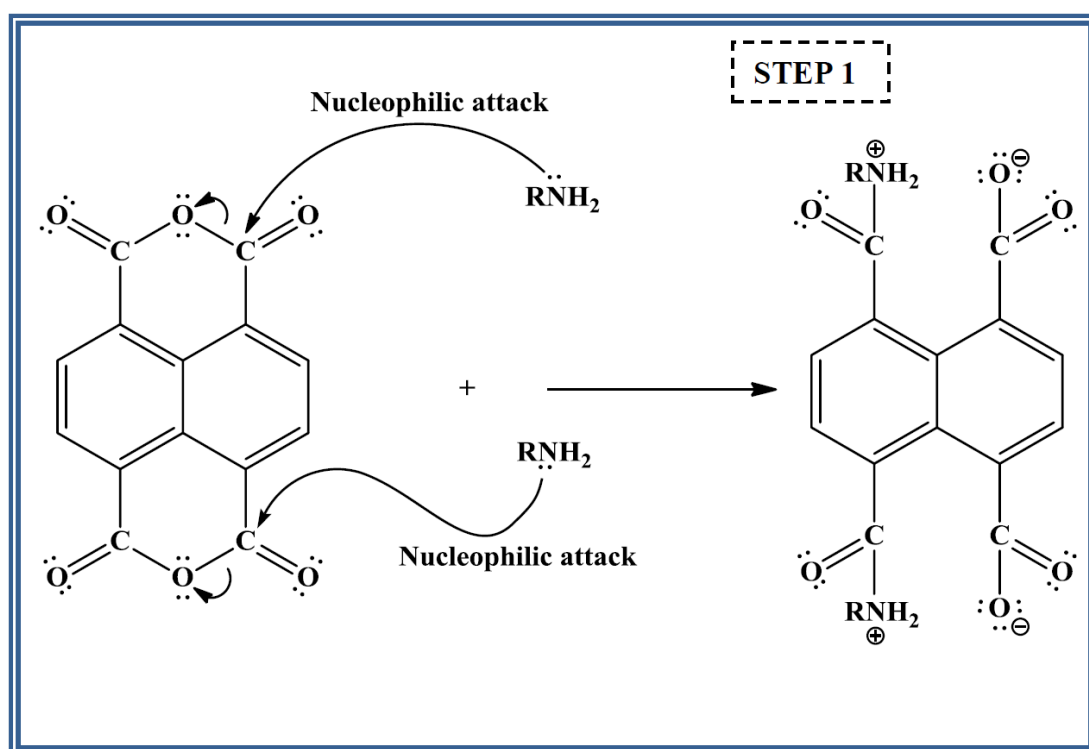
UV-vis (NMP) (λ_{max} , nm (ϵ_{max} , $\text{L}\cdot\text{mol}^{-1}\cdot\text{cm}^{-1}$): 342, 358, 379 (41648.80)

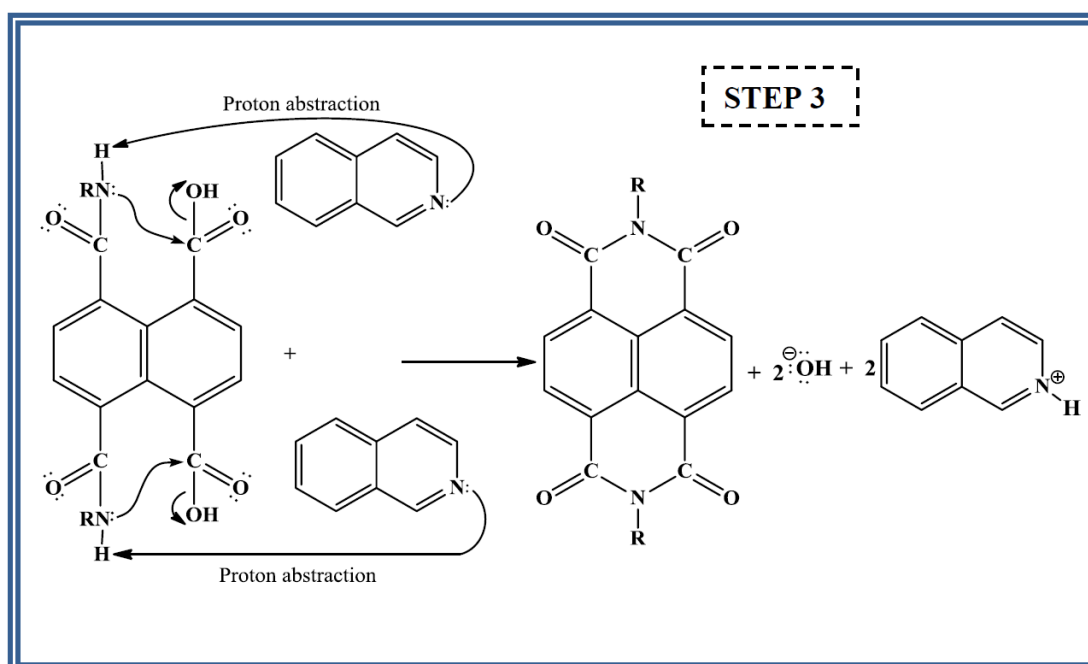
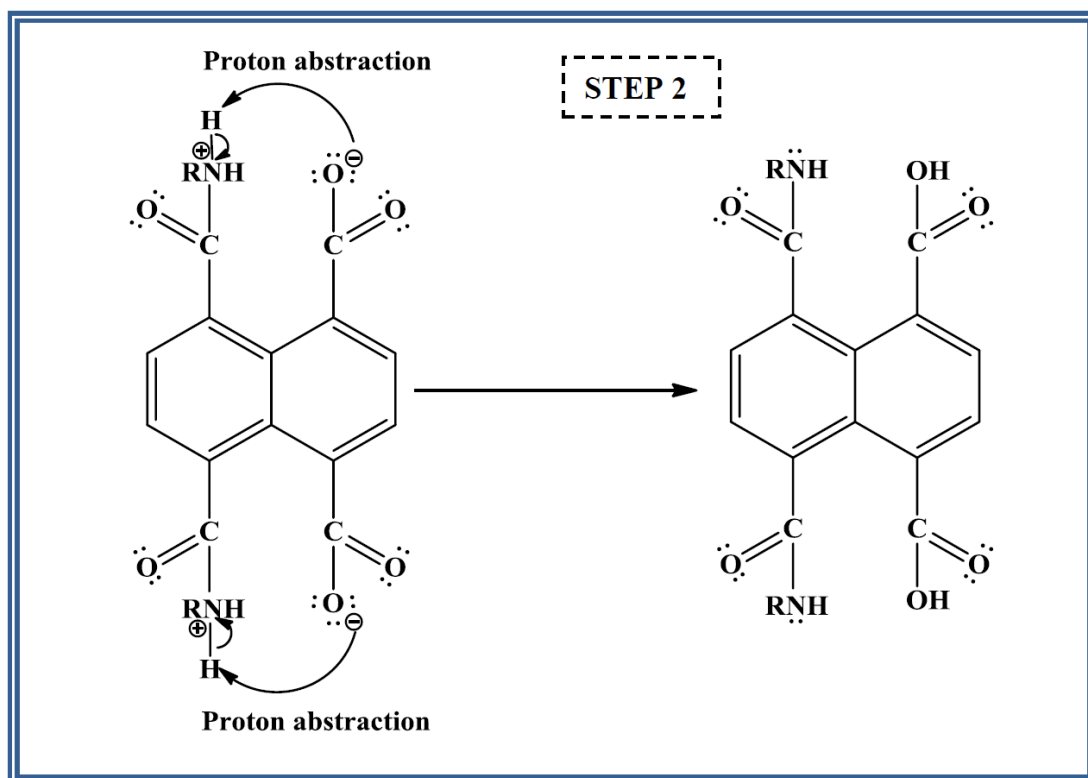
Fluorescence (NMP) (λ_{max} , nm): 408, 536, 577, 610

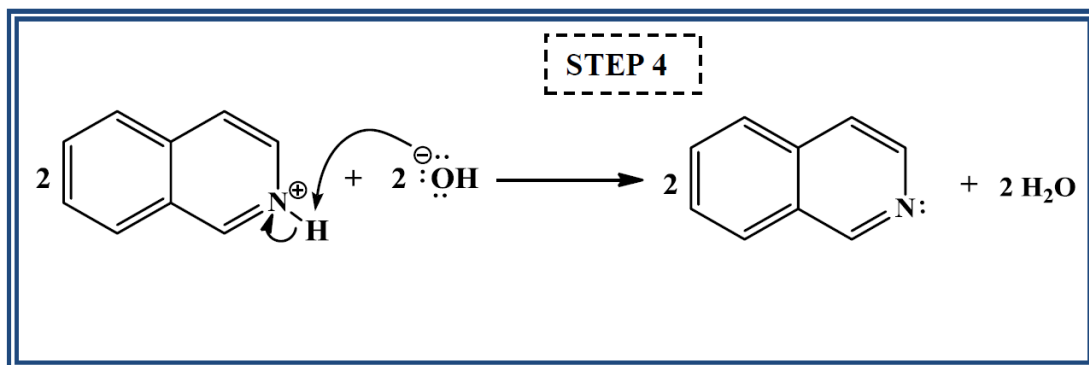
Anal. calcd. for $(\text{C}_{13}\text{H}_9\text{N}_5\text{O}_4)_n$ (Mw, $(419.35)_n$); C, 65.87 %; H, 2.16 %; N, 16.70%.

Found: C, 65.87 %; H, 2.06 %; N, 15.66 %

3.5 General Synthetic Mechanisms of Naphthalene Dyes







Chapter 4

DATA AND CALCULATION

4.1 Photophysical Properties

4.1.1 Absorptivity Coefficients

Absorbance versus Concentration Plot (A vs. C).

The slope of the absorbance versus concentration plot gives the absorptivity coefficient, ϵ_{max} , according to the Beer Lambert's Law, Eq. 4.1.

$$\epsilon_{max} = \frac{A}{C.l} \quad (\text{Eq.4.1})$$

First, six different concentrations were prepared from the synthesized compound. Then the maximum absorbances of the maximum absorption wavelengths were recorded for each concentration from their absorption spectrum. Finally, the absorbance versus concentration plotted. The slope of this plot gives the ϵ_{max} of the compound in that solvent.

ϵ_{max} Calculation of TANPI from the Plot of (A vs. C) in NMP.

Table 4.1: Absorbance and concentration data of TANPI in NMP

$\lambda_{max}(\text{nm})$	Absorbance	Concentration (M)
377	0.088	1.956×10^{-6}
377	0.158	3.912×10^{-6}
377	0.289	7.824×10^{-6}
377	0.533	1.564×10^{-5}
377	1.008	3.129×10^{-5}
377	1.978	6.25×10^{-5}

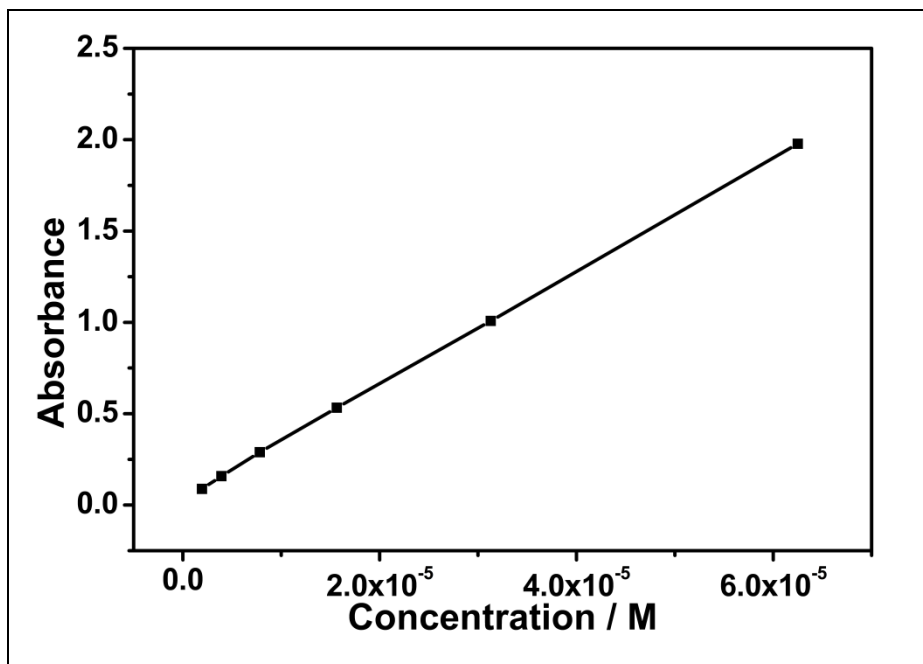


Figure 4.1: Absorbance versus Concentration Plot of TANPI in NMP

$$\text{Slope} = \epsilon_{\max} = 41648.8 \text{ M}^{-1} \cdot \text{cm}^{-1}$$

Table 4.2: Absorptivity coefficient data of TANPI in different solvents

Solvents	$\epsilon_{\max} (\text{M}^{-1} \cdot \text{cm}^{-1})$
DMSO	31062.10
NMP	41648.8
DMF	33987.32

4.1.2 Fluorescence Quantum Yield (Φ_f)

The TANPI fluorescence quantum yield was calculated by using the Eq.4.2 given below.

$$\Phi_f (u) = \frac{A_{\text{std}}}{A_u} \times \frac{S_u}{S_{\text{std}}} \times \left[\frac{n_u}{n_{\text{std}}} \right]^2 \times \Phi_f (\text{std}) \quad (\text{Eq.4.2})$$

Φ_f calculation of TANPI in NMP

The emission spectra of TANPI reported was excited at $\lambda_{exc} = 360$ nm and the anthracene in EtOH was used as reference for the fluorescence quantum yield measurements of TANPI ($\Phi_f = 0.27$; $\lambda_{exc} = 360$ nm).

$$\Phi_f (\text{std}) = 0.27 \text{ in EtOH}$$

$$A_{\text{std}} = 0.1055$$

$$A_u = 0.1018$$

$$S_u = 484.3$$

$$S_{\text{std}} = 7827.32$$

$$n_{\text{std}} = 1.3616$$

$$n_u = 1.4700$$

$$\Phi_f (u) = \frac{0.1055}{0.1018} \times \frac{484.3}{7827.32} \times \left[\frac{1.4700}{1.3616} \right]^2 \times 0.27$$

$$\Phi_f (u) = 0.02$$

Table 4.3: Fluorescence quantum yields of TANPI in DMSO, NMP and DMF solvents

Solvents	Φ_f
DMSO	0.01
NMP	0.02
DMF	0.01

4.1.3 The Selected Maximum Absorption Half-width ($\Delta\bar{\nu}_{1/2}$)

The half of the maximum intensity of the selected maximum absorption is called the half-width/full-width, ($\Delta\bar{\nu}_{1/2}$). It was calculated by using the Eq.4.3 given below.

$$\Delta\bar{\nu}_{1/2} = \bar{\nu}_1 - \bar{\nu}_2 \quad (\text{Eq.4.3})$$

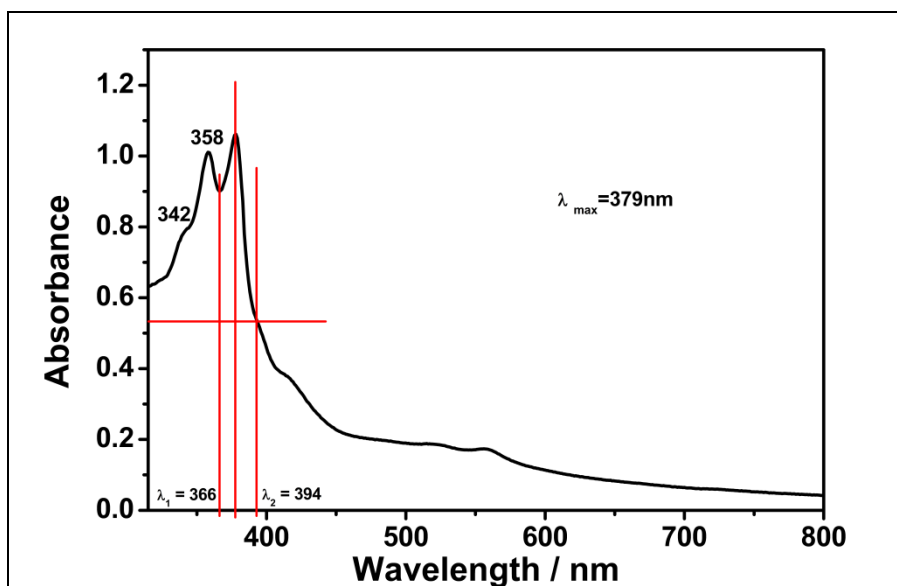


Figure 4.2: Absorption Spectrum of TANPI in NMP

$\Delta\bar{\nu}_{1/2}$ of selected absorption of TANPI in NMP

From Figure 4.2;

$$\lambda_1 = 366 \text{ nm}$$

$$366 \text{ nm} \times \frac{10^{-9} \text{ m}}{1 \text{ nm}} \times \frac{1 \text{ cm}}{10^{-2} \text{ m}} = 3.66 \times 10^{-5} \text{ cm}$$

$$\bar{\nu}_1 = \frac{1}{\lambda_1} = \frac{1}{3.66 \times 10^{-5} \text{ cm}} = 27322.40 \text{ cm}^{-1}$$

$$\lambda_2 = 394 \text{ nm}$$

$$394 \text{ nm} \times \frac{10^{-9} \text{ m}}{1 \text{ nm}} \times \frac{1 \text{ cm}}{10^{-2} \text{ m}} = 3.94 \times 10^{-5} \text{ cm}$$

$$\bar{\nu}_2 = \frac{1}{\lambda_2} = \frac{1}{3.94 \times 10^{-5} \text{ cm}} = 25380.71 \text{ cm}^{-1}$$

$$\Delta\bar{\nu}_{1/2} = \bar{\nu}_1 - \bar{\nu}_2 = 27322.40 \text{ cm}^{-1} - 25380.71 \text{ cm}^{-1} = 1941.769 \text{ cm}^{-1}$$

Similarly, for different solvents the half-width of TANPI were calculated and shown below in Table 4.4.

Table 4.4: Half-width of TANPI in different solvents

Solvents	$\lambda_{\max}(\text{nm})$	$\lambda_1(\text{nm})$	$\lambda_2(\text{nm})$	$\bar{\nu}_1(\text{cm}^{-1})$	$\bar{\nu}_2(\text{cm}^{-1})$	$\Delta\bar{\nu}_{1/2}(\text{cm}^{-1})$
DMSO	377	367	396	27247.79	25252.52	1995.27
NMP	379	366	395	27322.40	25380.71	1941.769
DMF	377	366	387	27322.40	25839.80	1482.60

4.1.4 Theoretical Radiative Lifetimes (τ_0)

The theoretical radiative lifetimes can be calculated by using following Eq. 4.4.

$$\tau_0 = \frac{3.5 \times 10^8}{\bar{\nu}_{\max}^2 \times \varepsilon_{\max} \times \Delta\bar{\nu}_{1/2}} \quad (\text{Eq.4.4})$$

τ_0 of TANPI in NMP

As shown in Figure 4.2,

$$\lambda_{\max} = 377 \text{ nm}$$

$$377 \text{ nm} \times \frac{10^{-9} \text{ m}}{1 \text{ nm}} \times \frac{100 \text{ cm}}{1 \text{ m}} = 3.77 \times 10^{-5} \text{ cm}$$

$$\Delta\bar{\nu}_{\max} = \frac{1}{3.77 \times 10^{-5} \text{ cm}} = 26525.198 \text{ cm}^{-1}$$

$$\bar{\nu}_{\max}^2 = (26525.198 \text{ cm}^{-1})^2 = 7.036 \times 10^8 \text{ cm}^{-2}$$

$$\Delta\bar{\nu}_{1/2} = 1941.769 \text{ cm}^{-1}$$

$$\tau_0 = \frac{3.5 \times 10^8}{7.036 \times 10^8 \times 41648.08 \times 1941.769} = 6.151 \times 10^{-9} \text{ s}$$

$$\tau_0 = 6.151 \times 10^{-9} \text{ s} \times \frac{1 \text{ ns}}{10^{-9} \text{ s}} = 6.151 \text{ ns}$$

Accordingly, all theoretical radiative lifetimes of TANPI were calculated (Table 4.5).

Table 4.5: In different solvents the Theoretical Radiative Lifetimes of TANPI

solvents	$\lambda_{\max}(\text{nm})$	$\epsilon_{\max} (\text{M}^{-1} \cdot \text{cm}^{-1})$	$\bar{\nu}_{\max}^2 (\text{cm}^{-2})$	$\Delta\bar{\nu}_{1/2} (\text{cm}^{-1})$	$\tau_0 (\text{ns})$
DMSO	379	31062.10	6.96×10^8	1995.27	8.11
NMP	379	41648.80	7.036×10^8	1941.769	6.15
DMF	378	33987.32	6.99×10^8	1482.60	9.94

4.1.5 Theoretical Fluorescence Lifetime (τ_f)

The Eq. 4.5 shown below was used for the calculation of theoretical fluorescence lifetime.

$$\tau_f = \tau_0 \cdot \Phi_f \quad (\text{Eq.4.5})$$

Theoretical Fluorescence Lifetime of TANPI in NMP

$$\tau_f = 6.151 \times 0.02 = 0.12 \text{ ns}$$

The Table 4.6 presents the calculated theoretical fluorescence lifetime of TANPI in various solvents.

Table 4.6: In different solvents Theoretical fluorescence lifetime

Solvents	$\tau_0 (\text{ns})$	Φ_f	$\tau_f (\text{ns})$
DMSO	8.11	0.01	0.81
NMP	6.15	0.02	0.12
DMF	9.94	0.01	0.81

4.1.6 Theoretical Fluorescence Rate Constant (k_f)

Turro's equation, Eq. 4.6, used to calculate the theoretical fluorescence rate constant, k_f for TANPI [33].

$$k_f = \frac{1}{\tau_0} \quad (\text{Eq.4.6})$$

k_f Calculation of TANPI in NMP

$$k_f = \frac{1}{6.151 \times 10^{-9}} = 1.63 \times 10^8 \text{ s}^{-1}$$

Table 4.7 shows the calculated theoretical fluorescence rate constants of TANPI in different solvents.

Table 4.7: Calculated theoretical fluorescence lifetime data of TANPI in different solvents

Solvents	τ_0 (s)	k_f (s^{-1})
DMSO	8.11×10^{-9}	1.23×10^8
NMP	6.15×10^{-9}	1.63×10^8
DMF	9.94×10^{-9}	1×10^8

4.1.7 Rate Constant of Radiationless Deactivation (k_d)

The k_d values of TANPI was calculated via Eq. 4.7 given below.

$$k_d = \left(\frac{k_f}{\Phi_f} \right) - k_f \quad (\text{Eq. 4.7})$$

k_d calculation of TANPI in NMP

$$k_d = \left(\frac{1.63 \times 10^8}{0.02} \right) - 1.63 \times 10^8 = 3.57 \times 10^9 \text{ s}^{-1}$$

Table 4.8: Radiationless deactivation rate constant of TANPI in different solvents

Solvents	k_f (s⁻¹)	Φ_f	k_d (s⁻¹)
DMSO	1.23×10^{-8}	0.01	1.21×10^9
NMP	1.63×10^{-8}	0.02	3.57×10^9
DMF	1×10^{-8}	0.01	9.9×10^9

4.1.8 Oscillator Strengths (f)

Electronic transition strength is expressed by dimensionless quantity oscillator strength. Oscillator strength was calculated by using Eq. 4.8 shown below.

$$f = 4.32 \times 10^{-9} \times \Delta\bar{\nu}_{1/2} \times \epsilon_{max} \quad (\text{Eq. 4.8})$$

Oscillator Strengths of TANPI in NMP

$$f = 4.32 \times 10^{-9} \times 1941.769 \times 41648.8 = 0.35$$

Oscillator strengths of TANPI were calculated in different solvents and Table 4.9 shows oscillator strength data.

Table 4.9: Oscillator strength data of TANPI in different solvents

Solvents	ϵ_{max} (M⁻¹.cm⁻¹)	$\Delta\bar{\nu}_{1/2}$ (cm⁻¹)	f
DMSO	31062.10	1995.27	0.27
NMP	41648.80	1941.769	0.35
DMF	33987.32	1482.60	0.22

4.1.9 Singlet Energy (E_s)

A chromophore needed minimum amount of energy for excitation from ground to excited state. This energy is called singlet energy. Turro's equation, Eq. 4.9, was used to calculate the singlet energy, E_s [33].

$$E_s = \frac{2.86 \times 10^5}{\lambda_{\max}} \quad (\text{Eq.4.9})$$

E_s of TANPI in NMP

$$\lambda_{\max} = 377 \text{ nm}$$

$$E_s = 377 \text{ nm} \times \frac{10 \text{ \AA}}{1 \text{ nm}} = 3770 \text{ \AA}$$

$$E_s = \frac{2.86 \times 10^5}{3770} = 75.86 \text{ kcal mol}^{-1}$$

Similarly, the singlet energies were calculated for TANPI in different solvents and listed in Table 4.10.

Table 4.10: Singlet energy of TANPI in different solvents

Solvents	λ_{\max}(nm)	E_s (kcal.mol⁻¹)
DMSO	379	75.46
NMP	379	75.86
DMF	378	75.66

4.1.10 Optical Band Gap Energy (E_g)

Optical band gap energies of TANPI were calculated in different solvents by using Eq. 4.10 shown below.

$$E_g = \frac{1240 \text{ eV nm}}{\lambda} \quad (\text{Eq. 4.10})$$

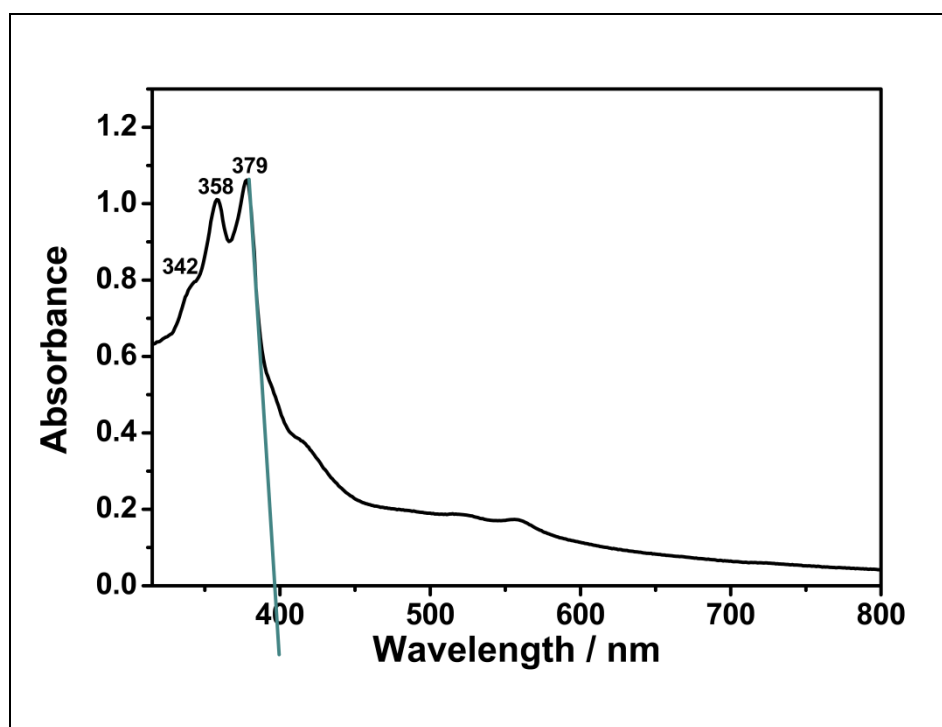


Figure 4.3: Absorption Spectrum of TANPI in NMP

Band gap energy of TANPI in NMP

$$E_g = \frac{1240 \text{ eV nm}}{396 \text{ nm}} = 3.13 \text{ eV}$$

With the similar method, the band gap energies of TANPI were calculated for other solvents and shown in Table 4.11.

Table 4.11: Band gap energy of TANPI in different solvents

Solvents	λ (nm)	E_g (eV)
DMSO	404	3.07
NMP	396	3.13
DMF	396	3.13

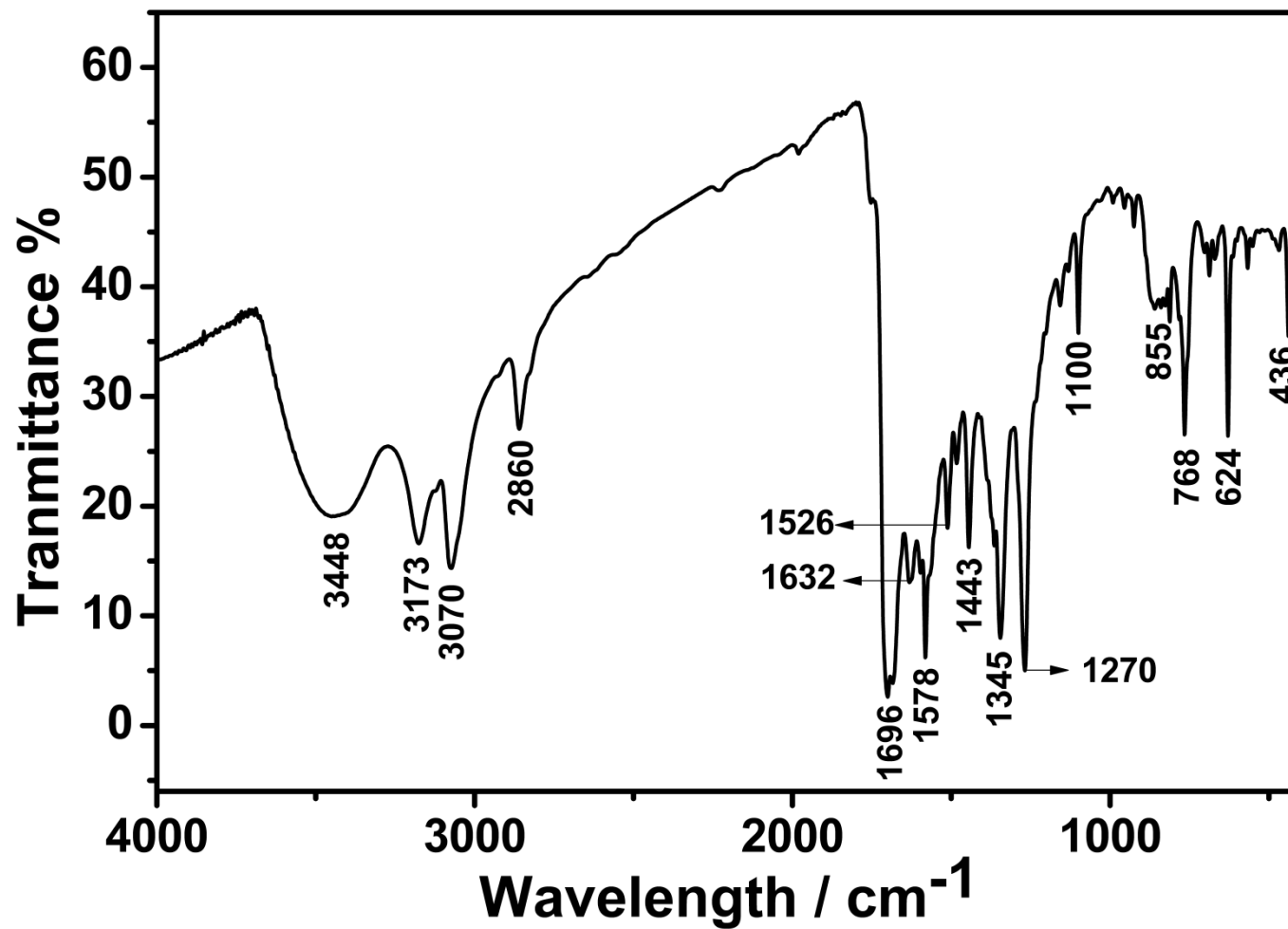


Figure 4.4: FT-IR Spectrum of TANPI

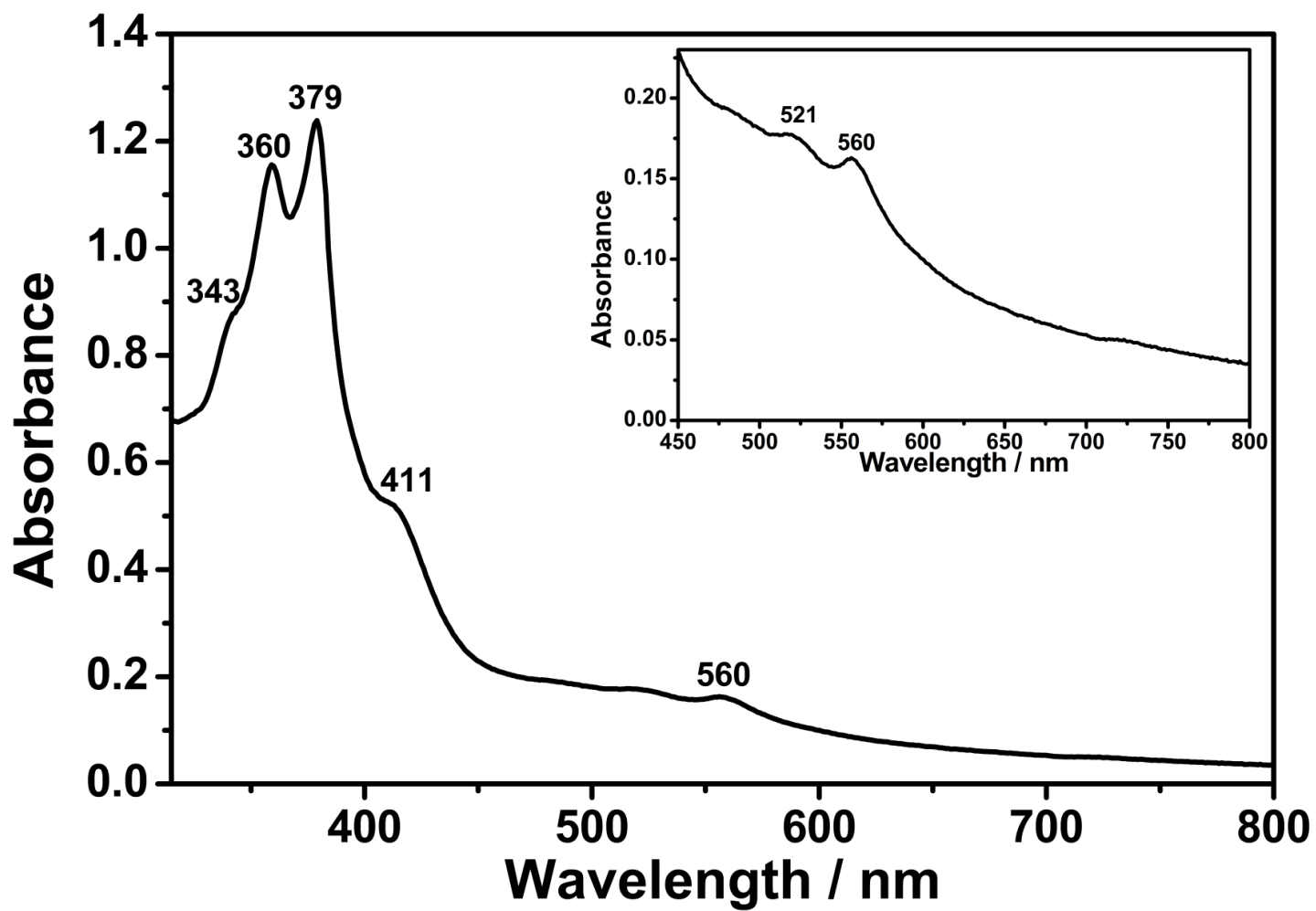


Figure 4.5: Absorption Spectrum of TANPI in DMSO ($C = 1 \times 10^{-5}$ M, Inset: Enlarged Spectrum, 450-800 nm)

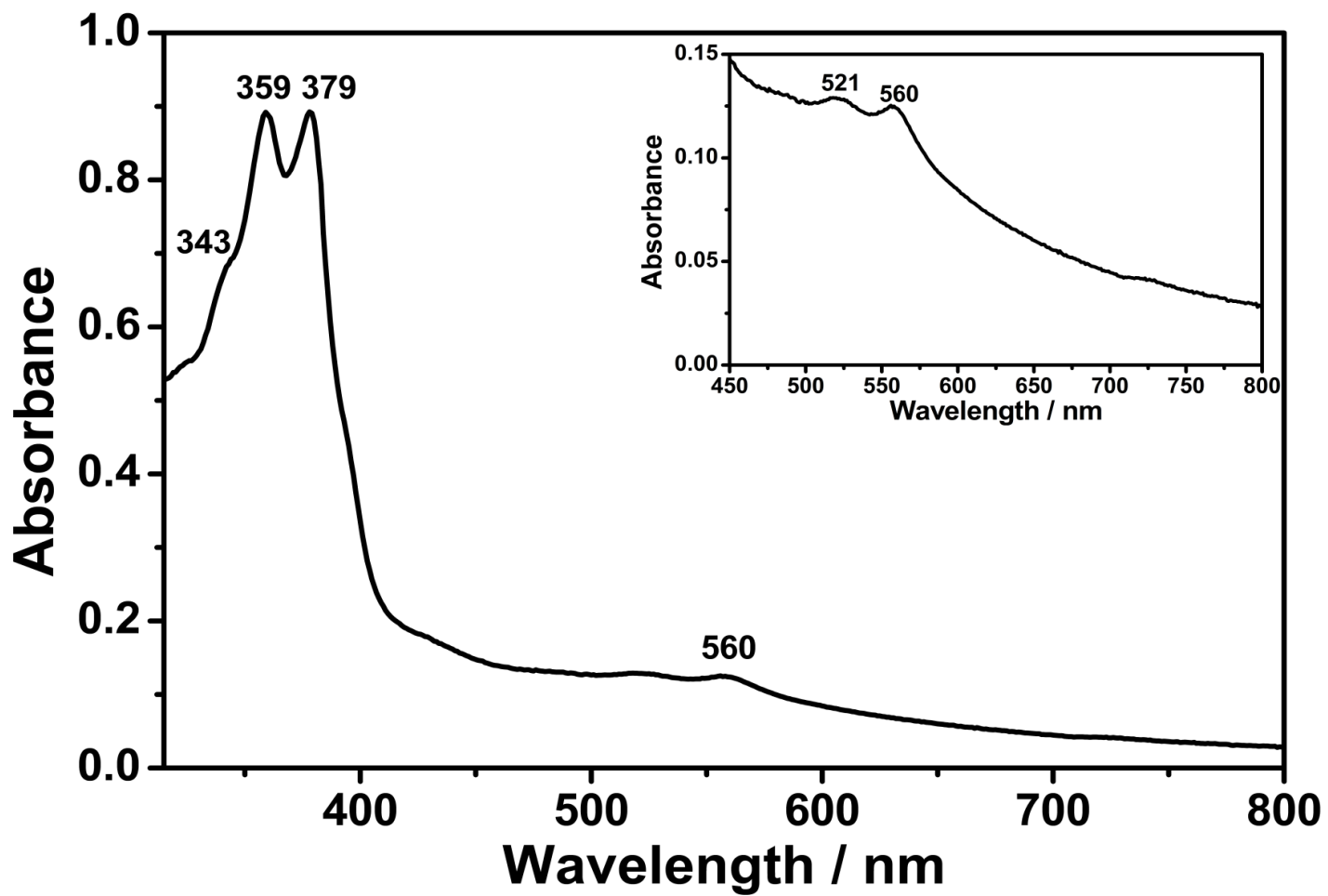


Figure 4.6: Absorption Spectrum of TANPI in DMSO (Microfiltered, Inset: Enlarged Spectrum, 450-800 nm)

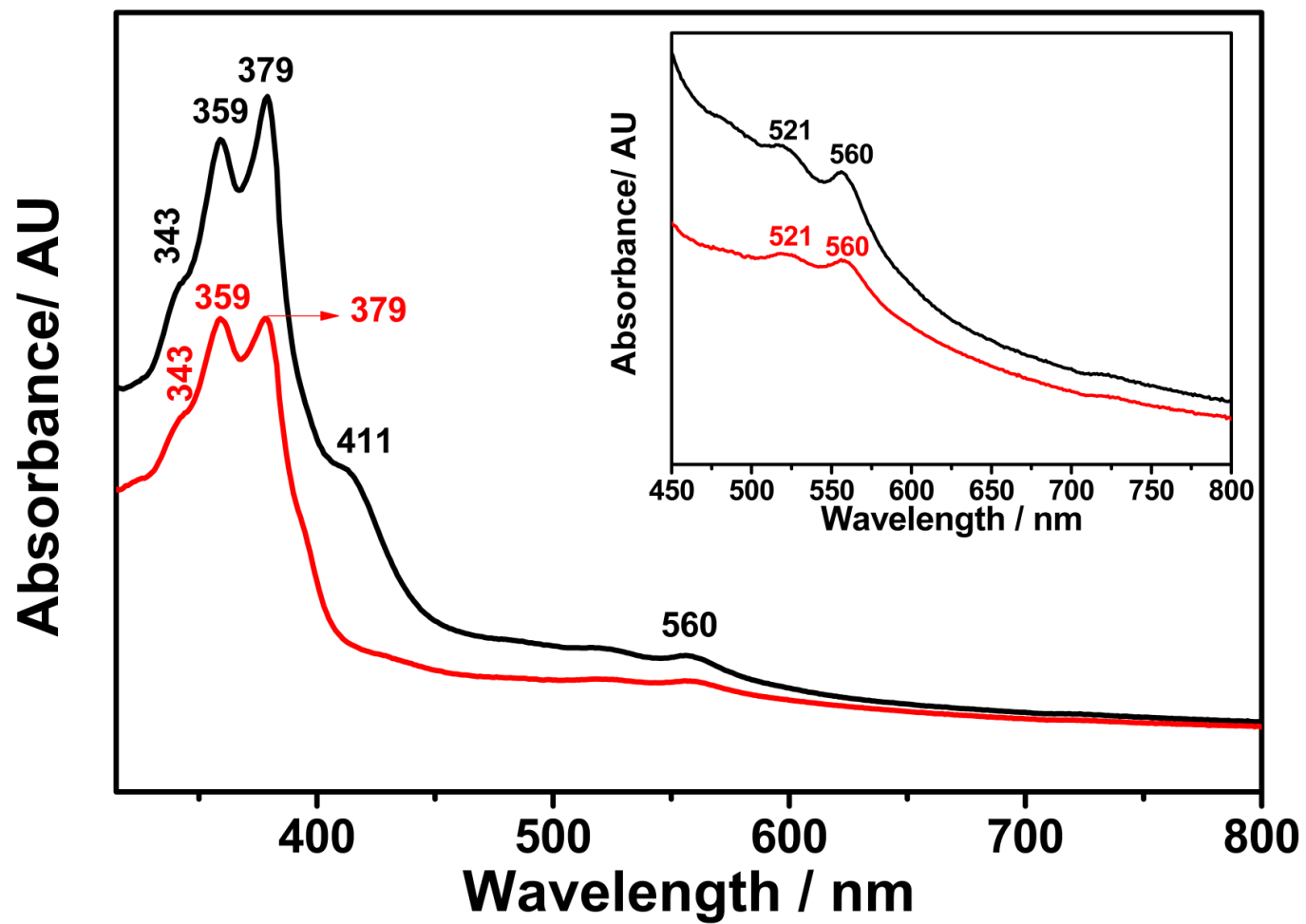


Figure 4.7: Absorption Spectrum of TANPI in DMSO (—: $C = 1 \times 10^{-5} \text{ M}$; —: Microfiltered; Inset: Enlarged Spectrum, 450-800 nm)

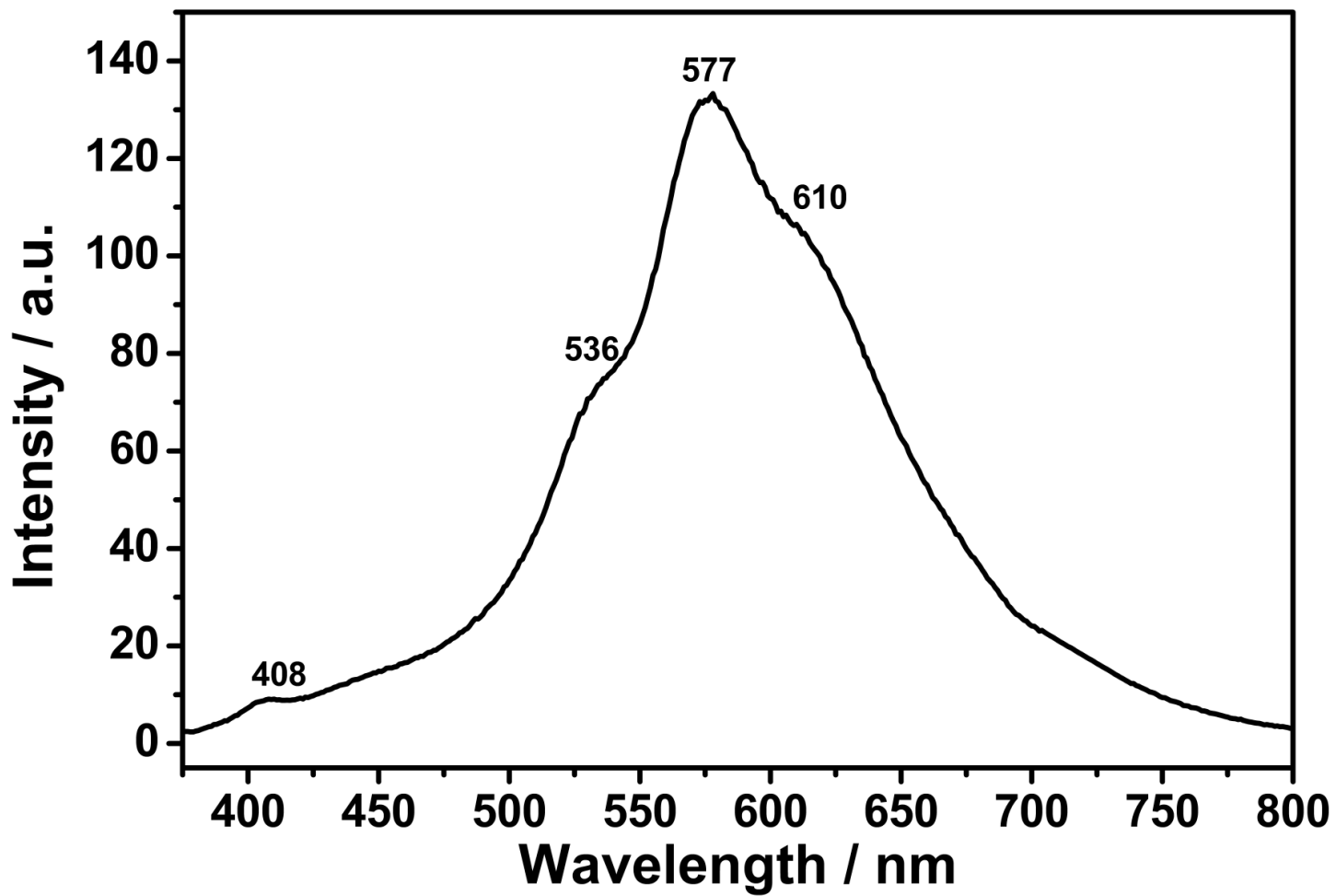


Figure 4.8: Emission Spectrum of TANPI in DMSO ($C = 1 \times 10^{-5}$ M; $\lambda_{\text{exc}} = 360$ nm)

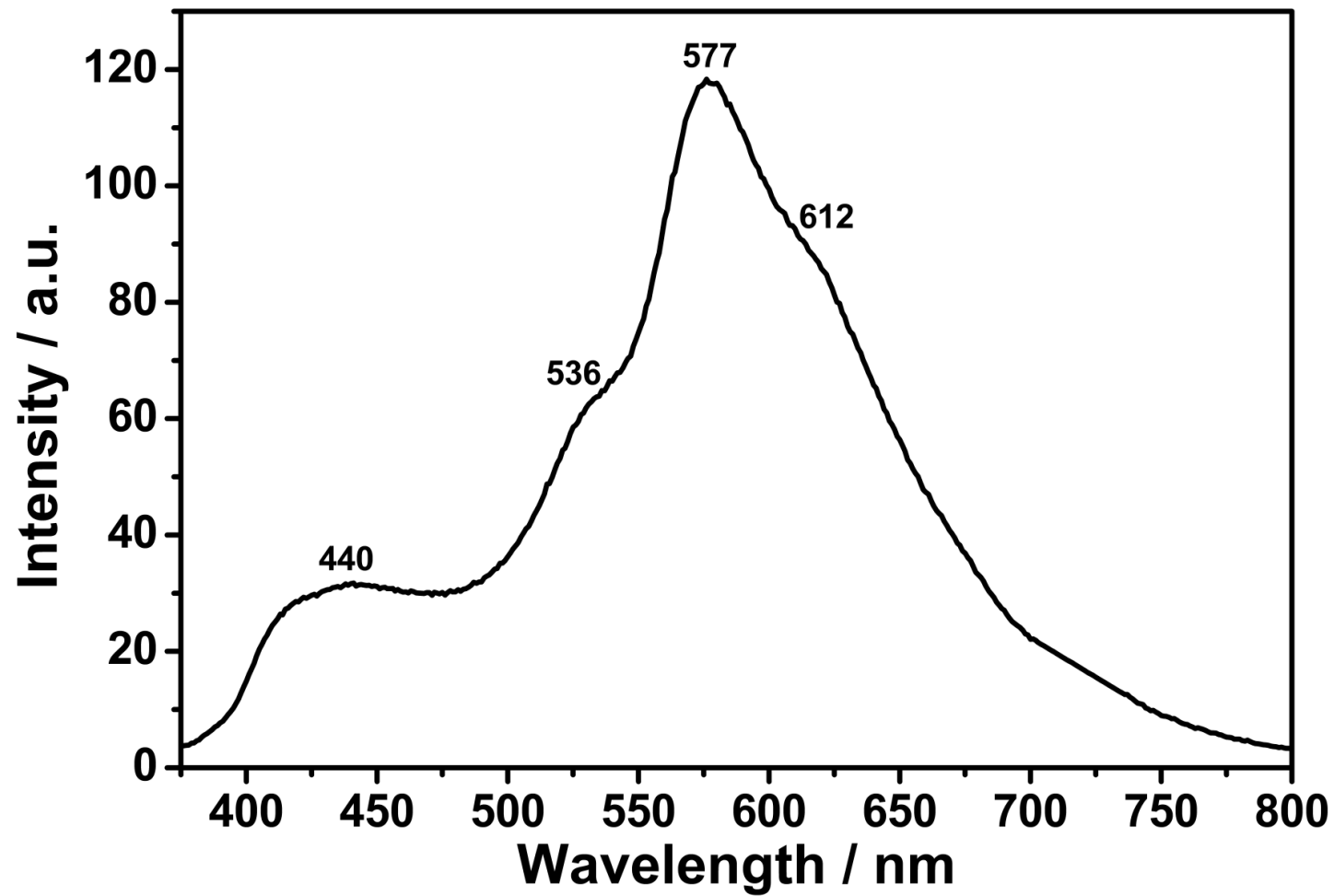


Figure 4.9: Emission Spectrum of TANPI in DMSO (Microfiltered; $\lambda_{\text{exc}} = 360$ nm)

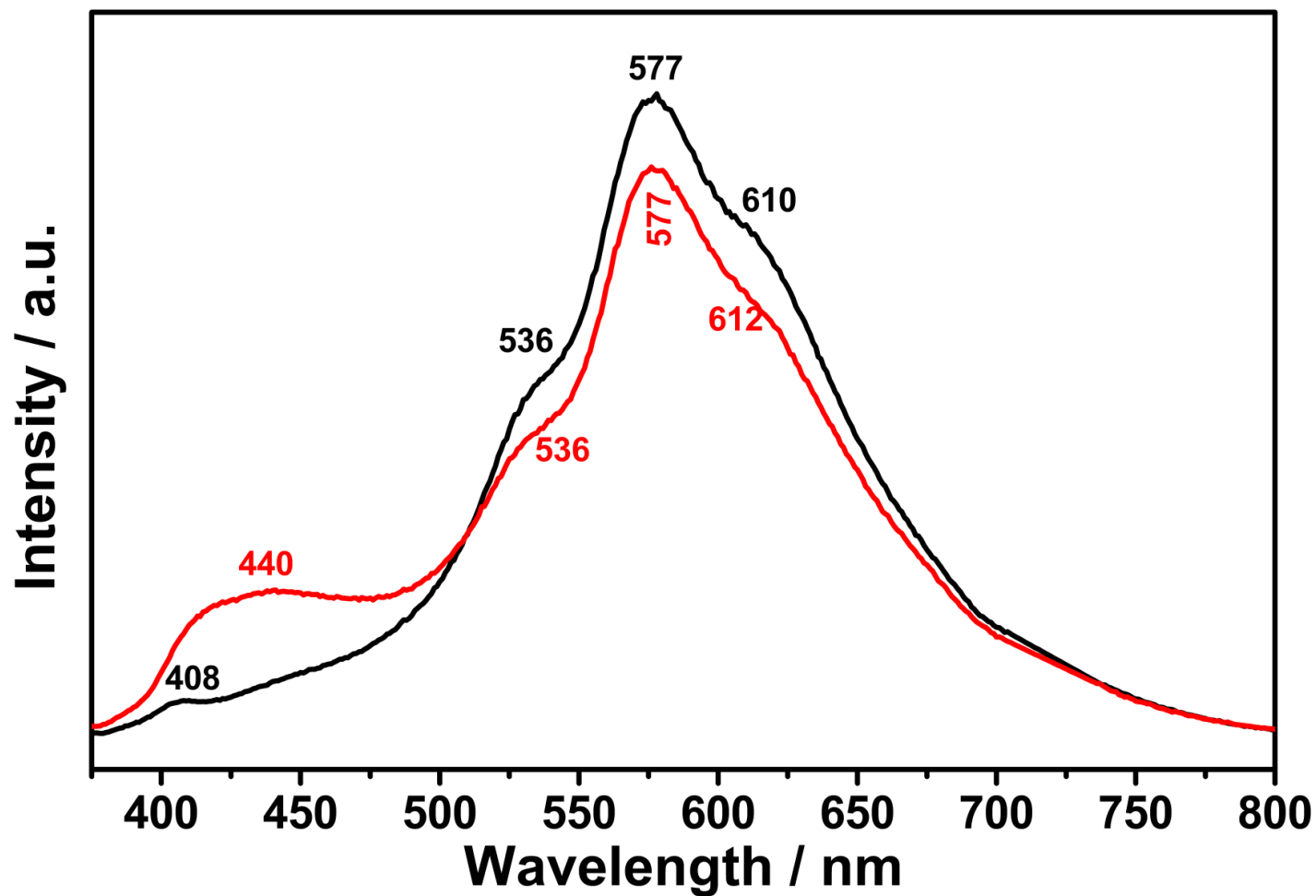


Figure 4.10: Emission Spectrum of TANPI in DMSO (—: $C = 1 \times 10^{-5} \text{ M}$; - - : Microfiltered; $\lambda_{\text{exc}} = 360 \text{ nm}$)

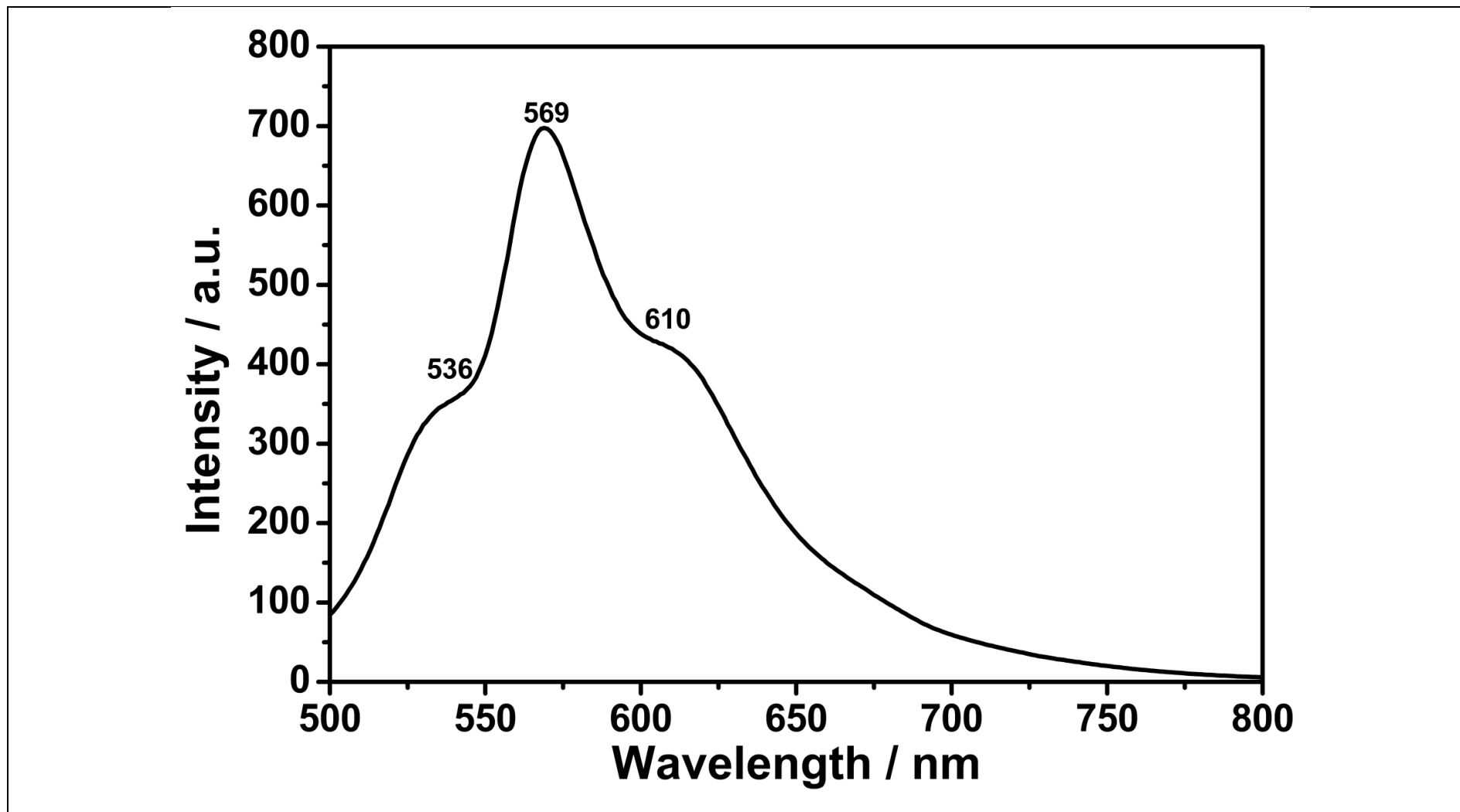


Figure 4.11: Emission Spectrum of TANPI in DMSO ($C = 1 \times 10^{-5}$ M; $\lambda_{exc} = 485$ nm)

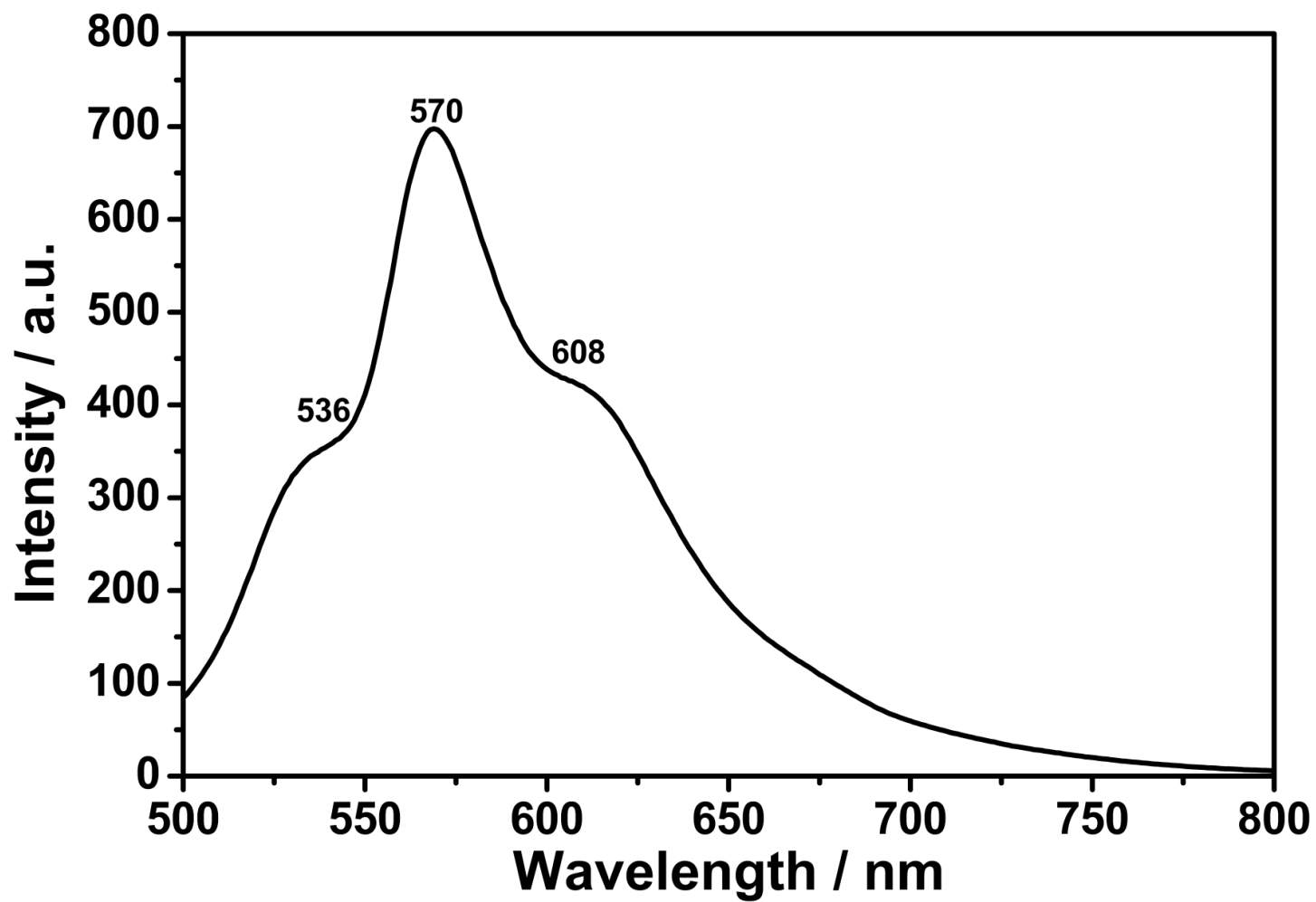


Figure 4.12: Emission Spectrum of TANPI in DMSO (Microfiltered; $\lambda_{\text{exc}} = 485 \text{ nm}$)

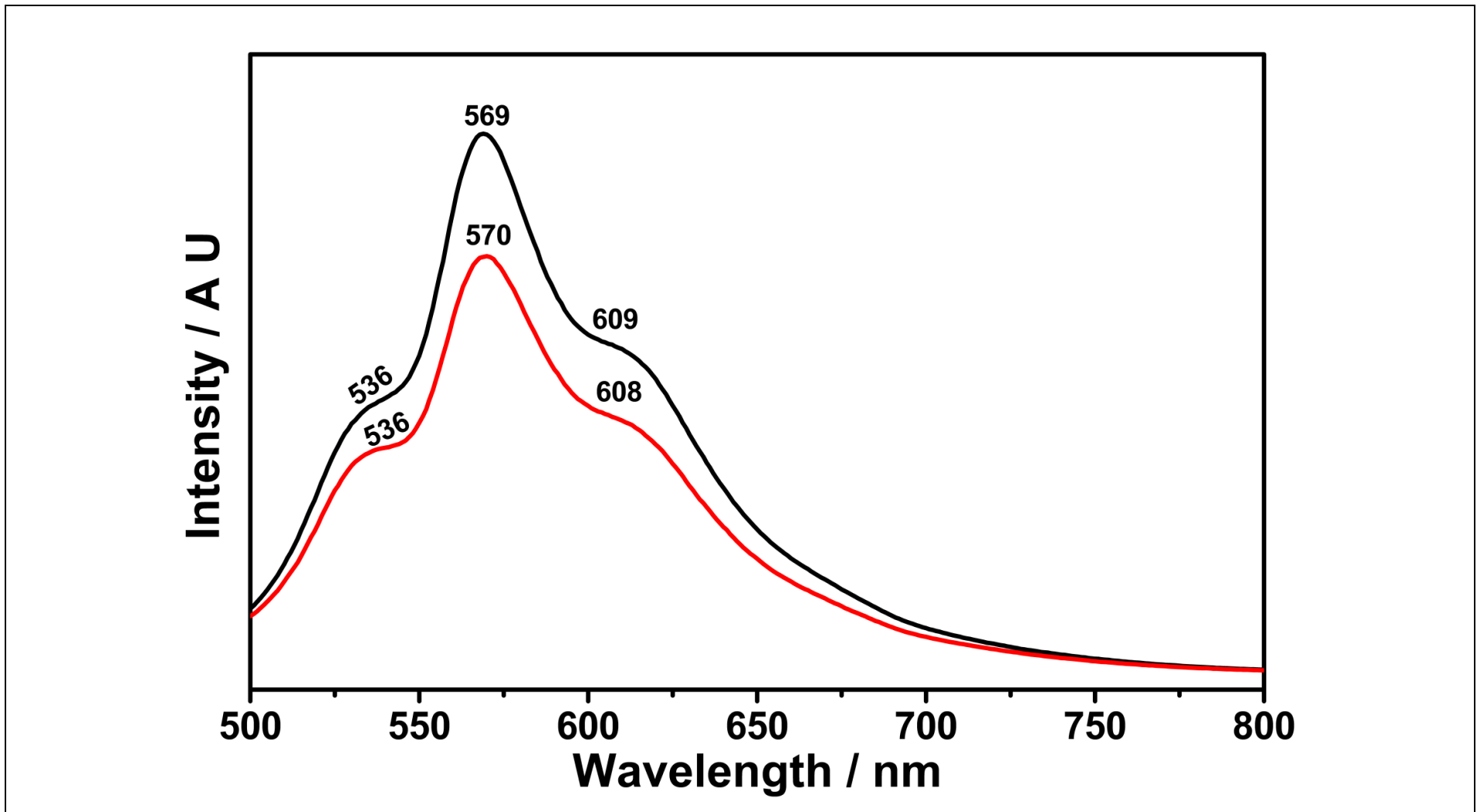


Figure 4.13: Emission Spectrum of TANPI in DMSO (—: $C = 1 \times 10^{-5}$ M; —: Microfiltered ; $\lambda_{exc} = 485$ nm)

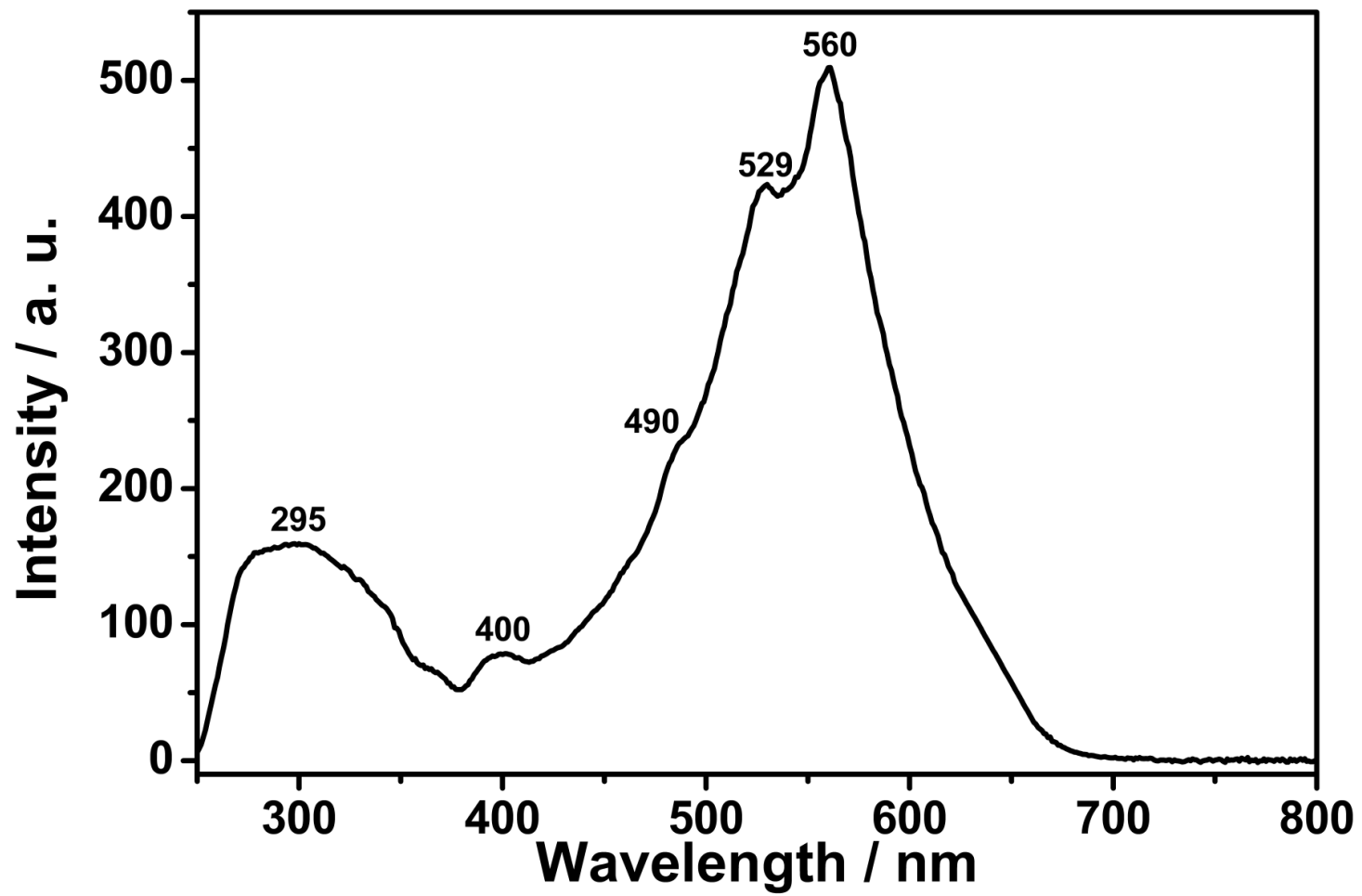


Figure 4.14: Excitation Spectrum of TANPI in DMSO ($C = 1 \times 10^{-5}$ M; $\lambda_{\text{emis}} = 650$ nm)

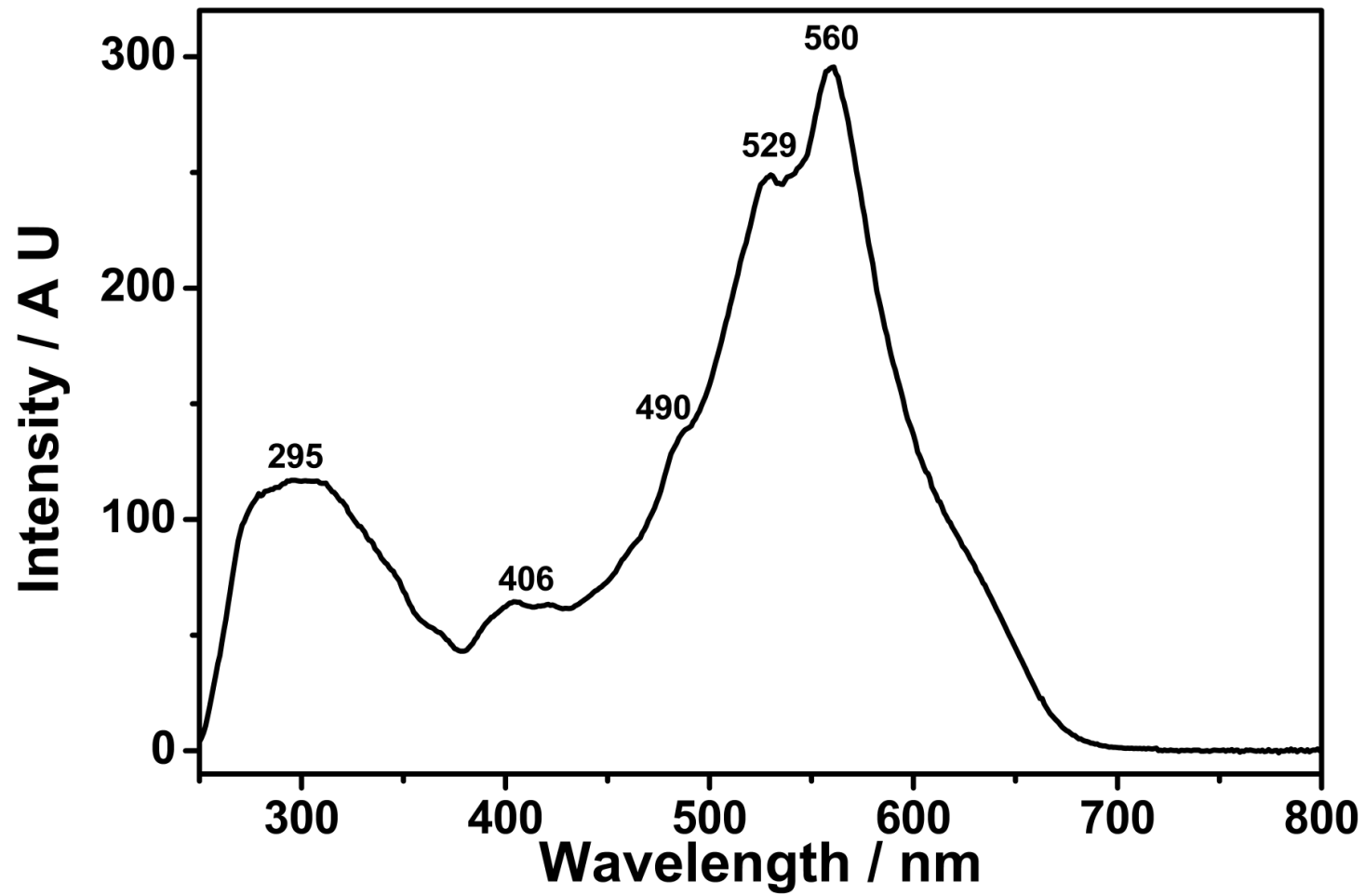


Figure 4.15: Excitation Spectrum of TANPI in DMSO (Microfiltered; $\lambda_{\text{emis}} = 650 \text{ nm}$)

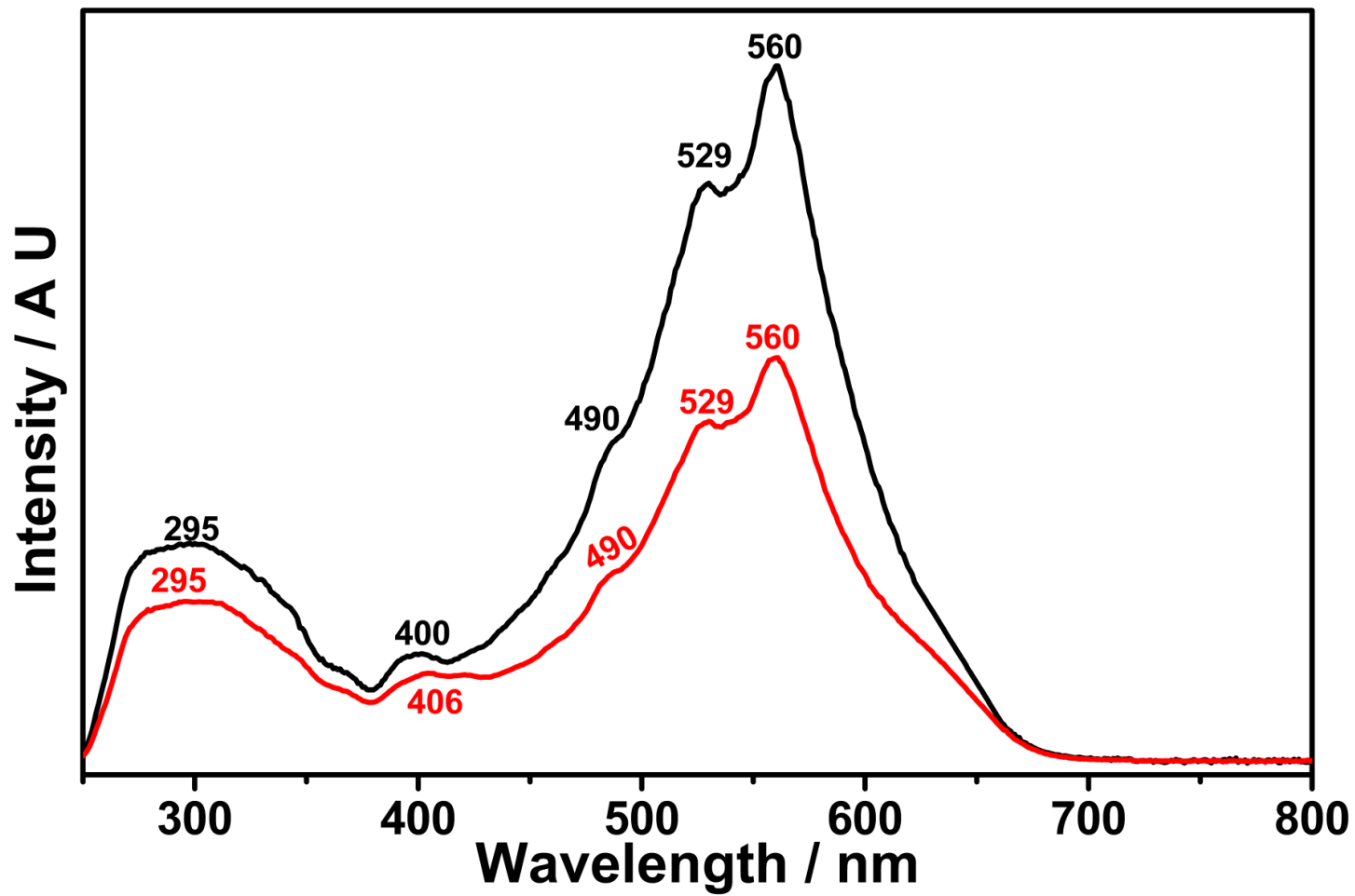


Figure 4.16: Excitation Spectrum of TANPI in DMSO (—: $C = 1 \times 10^{-5} \text{ M}$; —: Microfiltered; $\lambda_{\text{emis}} = 650 \text{ nm}$)

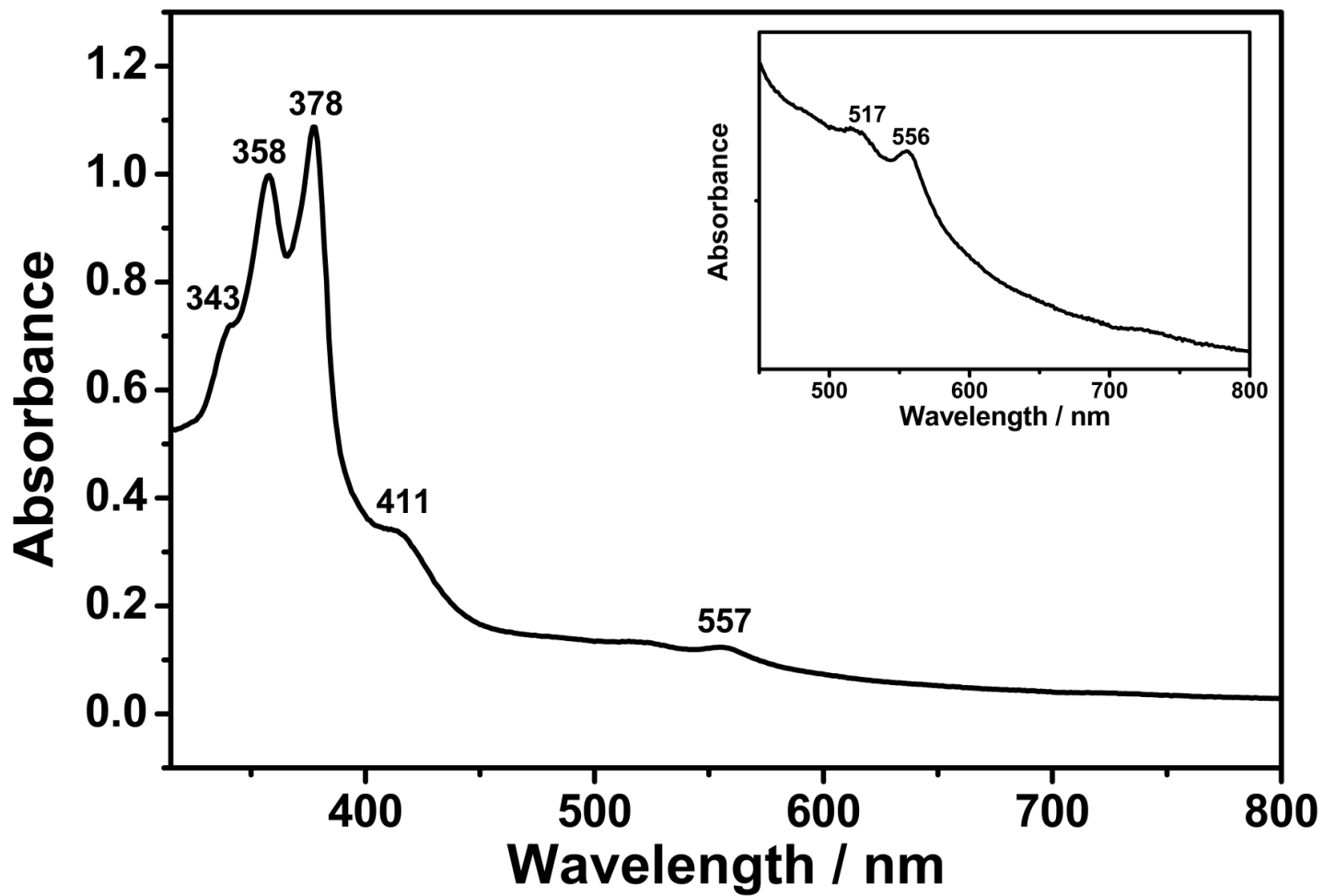


Figure 4.17: Absorption Spectrum of TANPI in DMF ($C = 1 \times 10^{-5}$ M, Inset: Enlarged Spectrum, 450-800 nm)

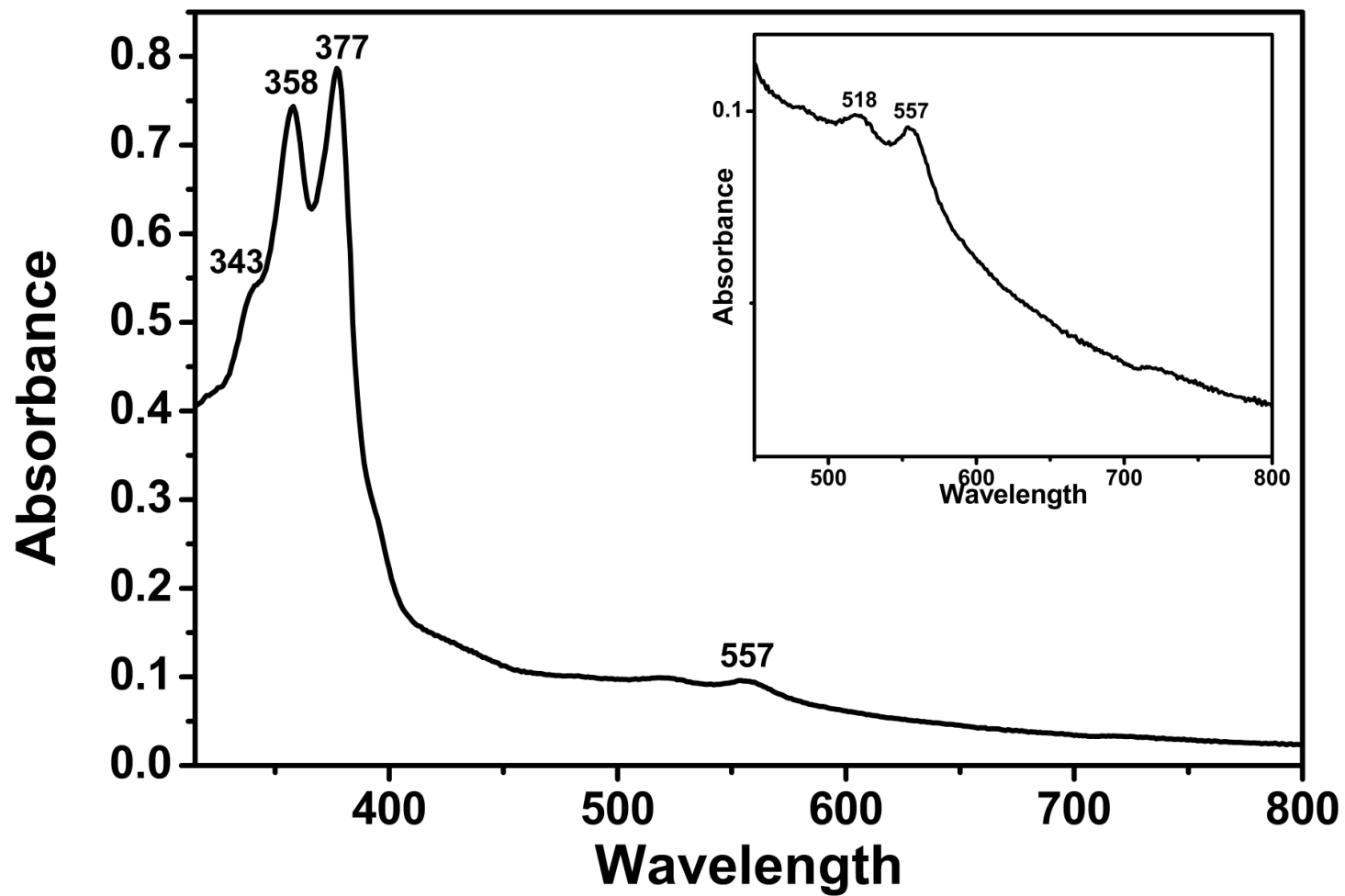


Figure 4.18: Absorption Spectrum of TANPI in DMF (Microfiltered; Inset: Enlarged Spectrum; 450-800 nm)

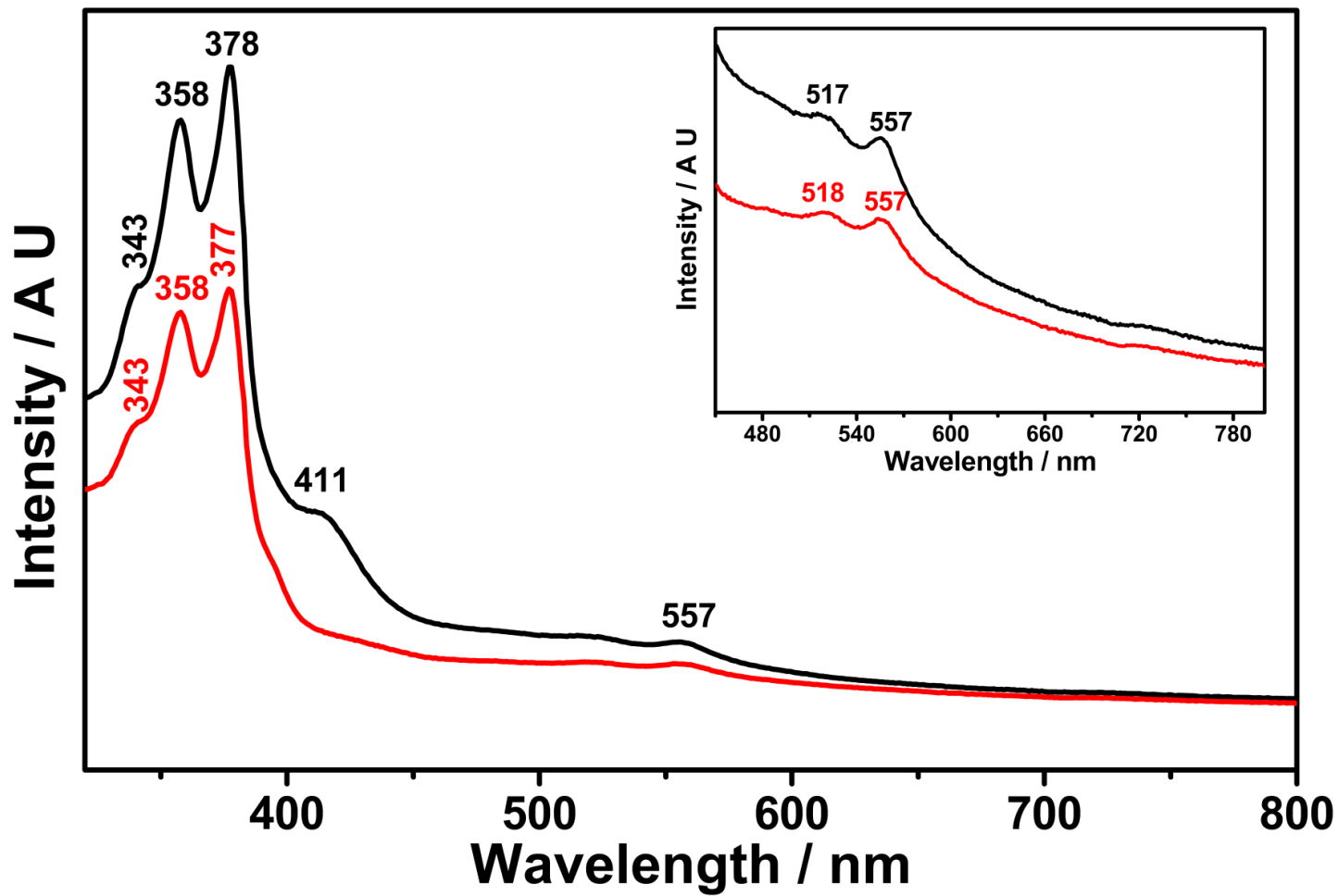


Figure 4.19: Absorption Spectrum of TANPI in DMF (—: $C = 1 \times 10^{-5} \text{ M}$; —: Microfiltered ; Inset: Enlarged Spectrum, 450-800 nm)

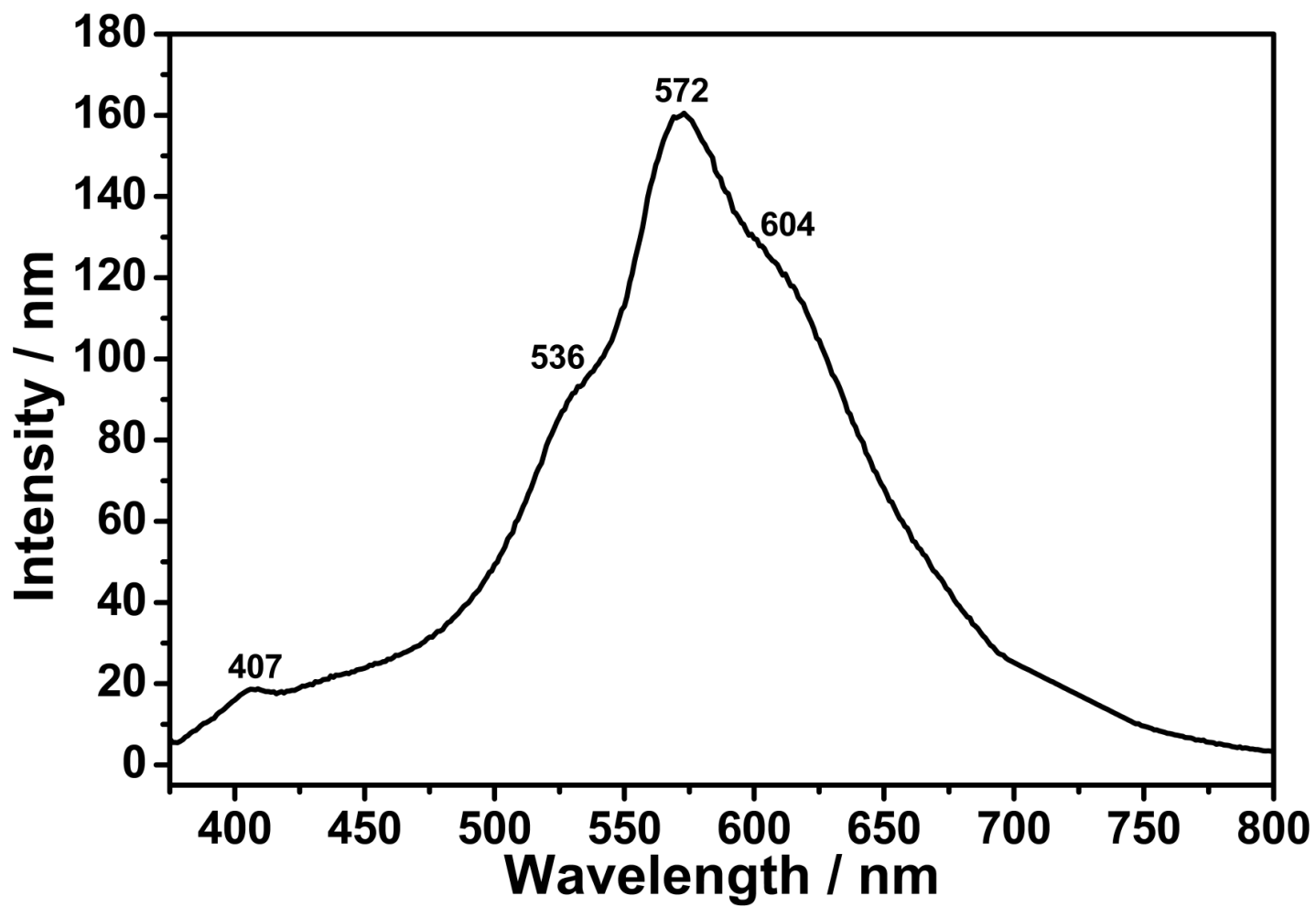


Figure 4.20: Emission Spectrum of TANPI in DMF ($C = 1 \times 10^{-5} \text{ M}$; $\lambda_{\text{exc}} = 360 \text{ nm}$)

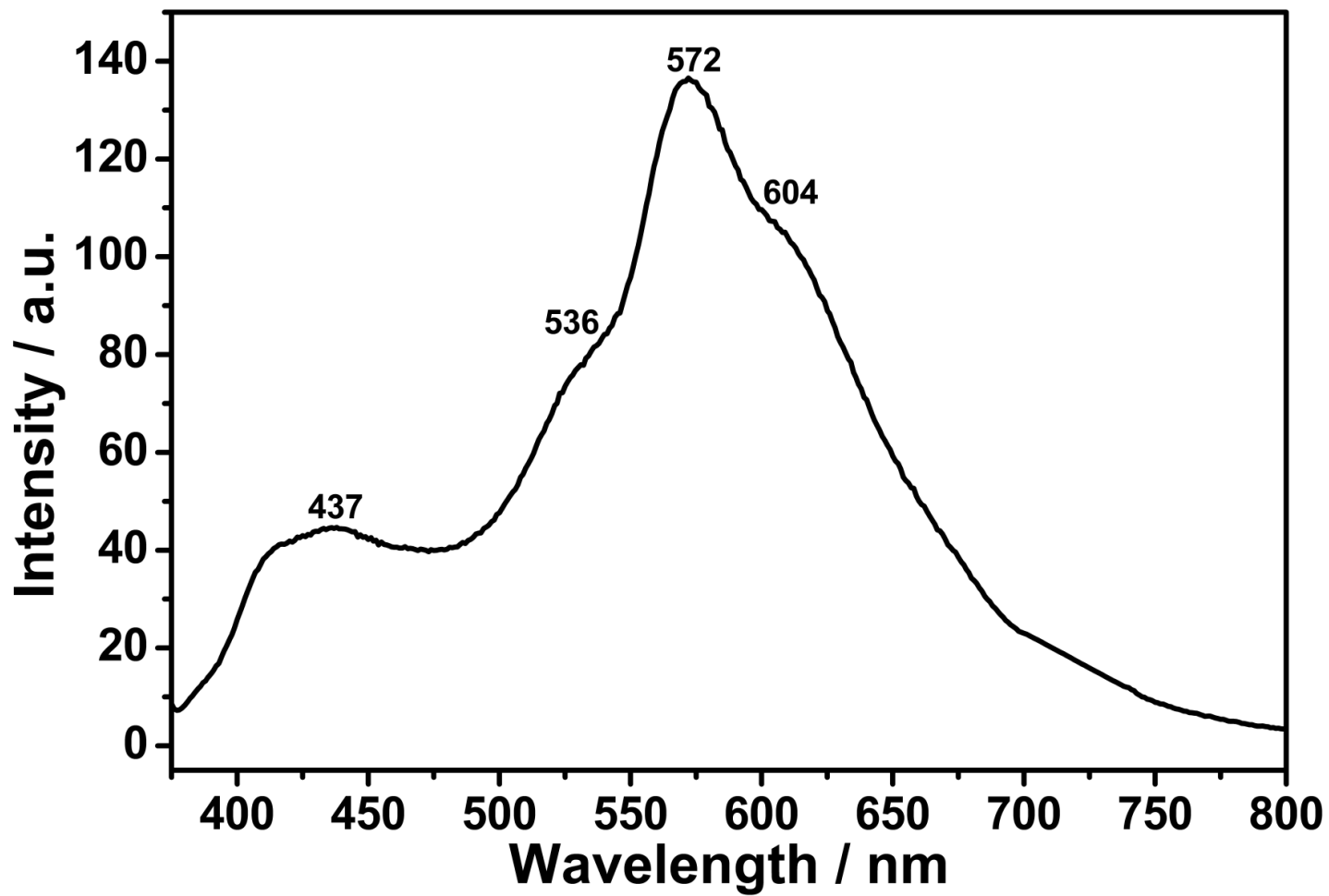


Figure 4.21: Emission Spectrum of TANPI in DMF (Microfiltered; $\lambda_{\text{exc}} = 360$ nm)

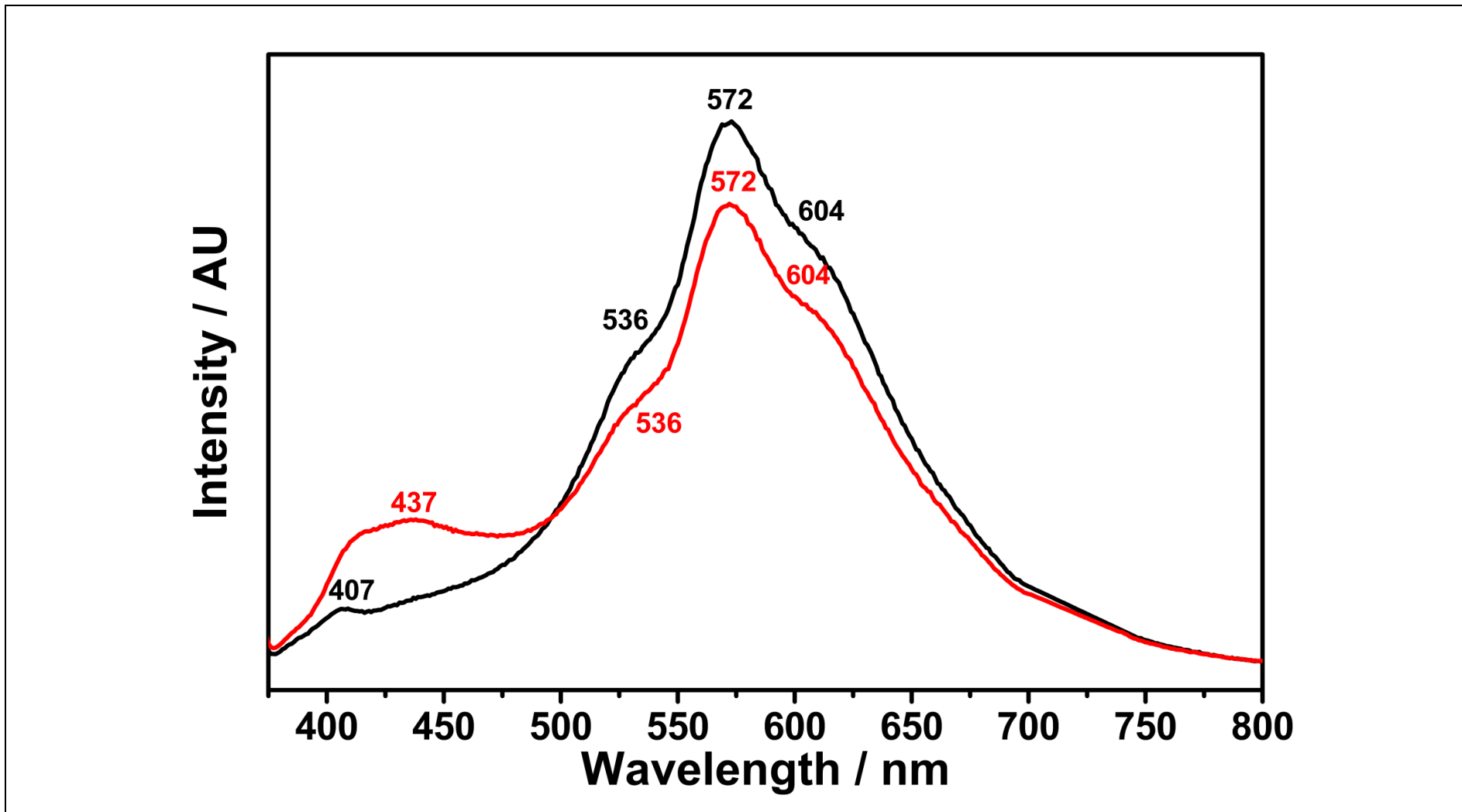


Figure 4.22: Emission Spectrum of TANPI in DMF (—: $C = 1 \times 10^{-5}$ M; —: Microfiltered; $\lambda_{\text{exc}} = 360$ nm)

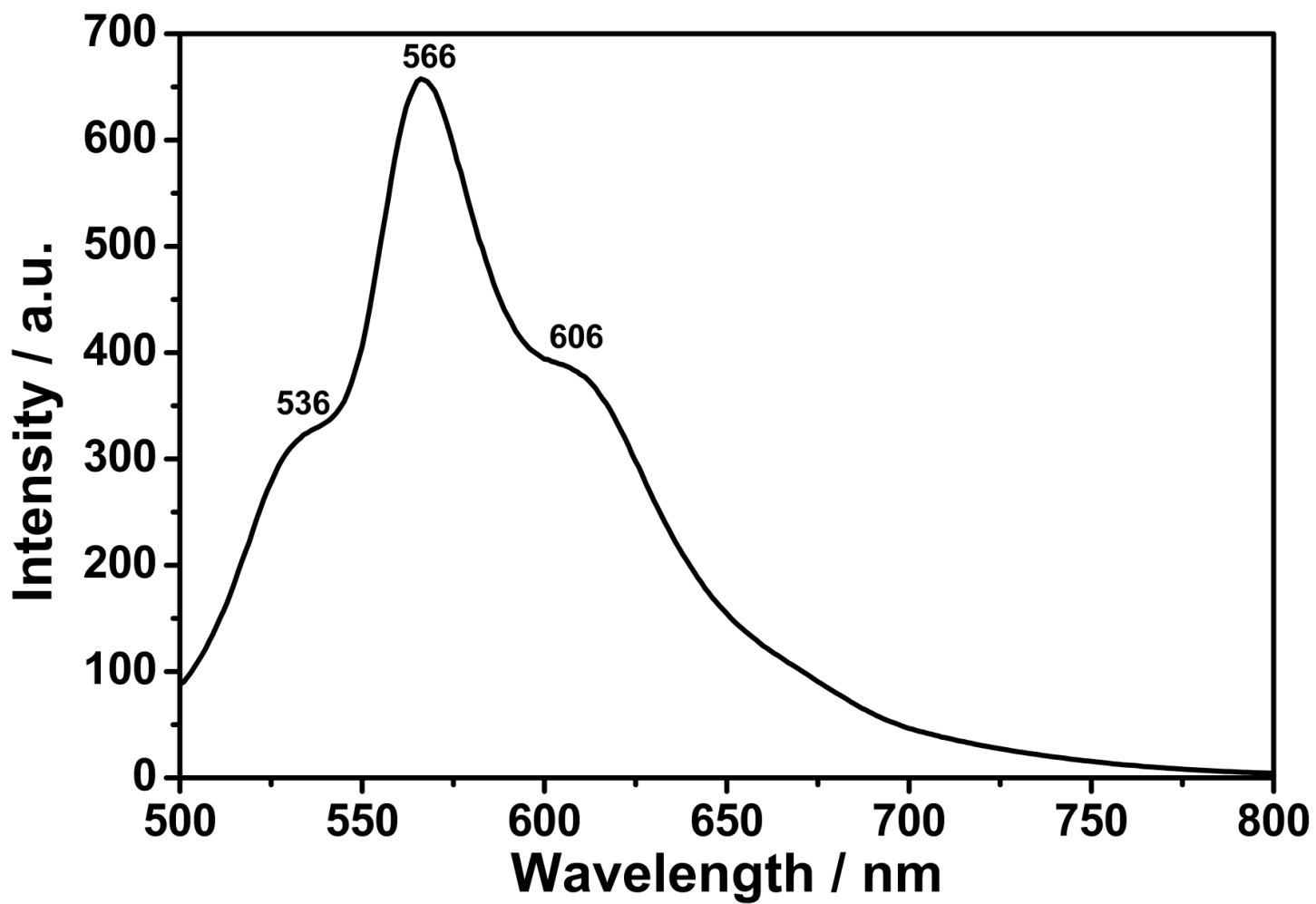


Figure 4.23: Emission Spectrum of TANPI in DMF ($C = 1 \times 10^{-5}$ M ; $\lambda_{\text{exc}} = 485$ nm)

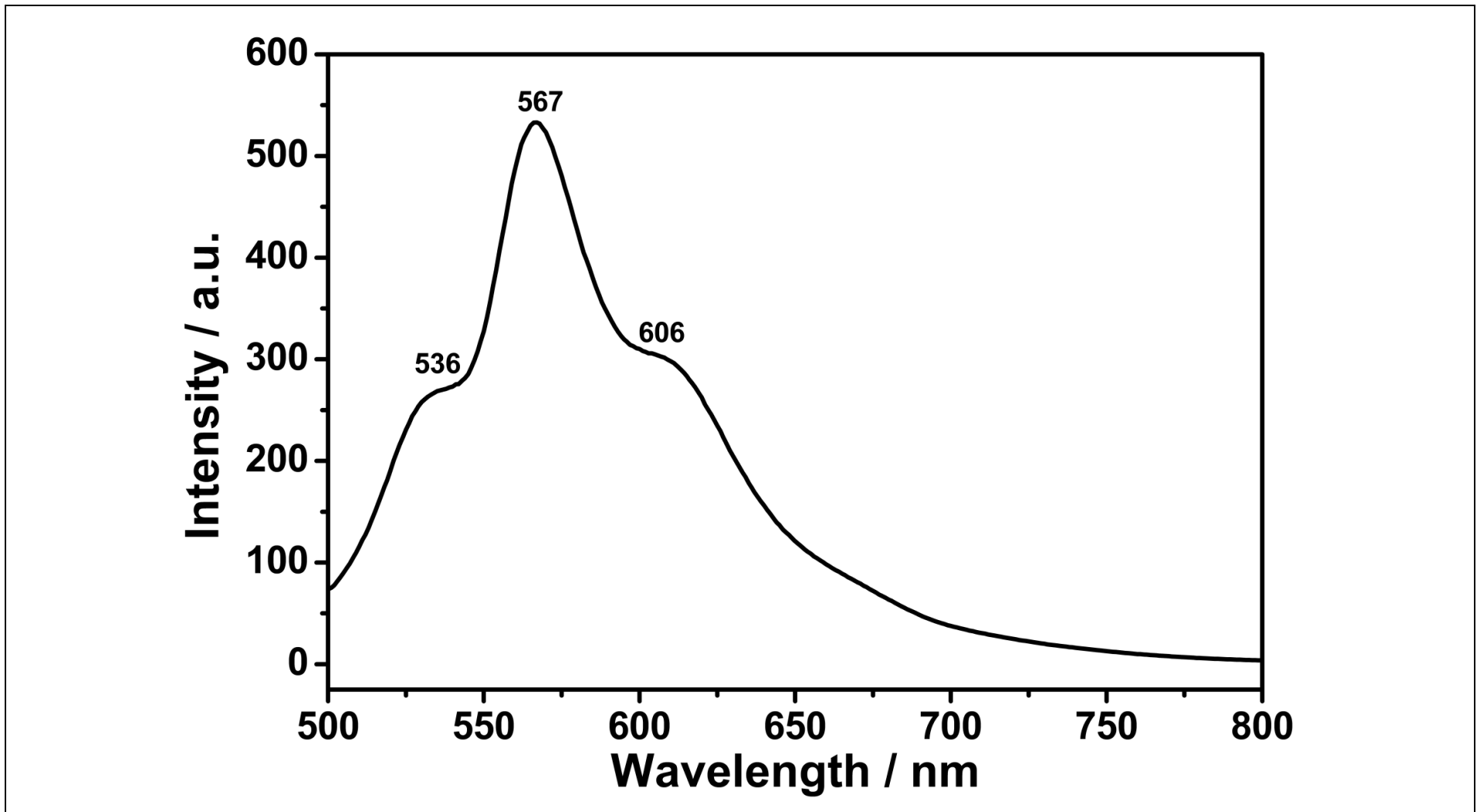


Figure 4.24: Emission Spectrum of TANPI in DMF (Microfiltered; $\lambda_{\text{exc}} = 485 \text{ nm}$)

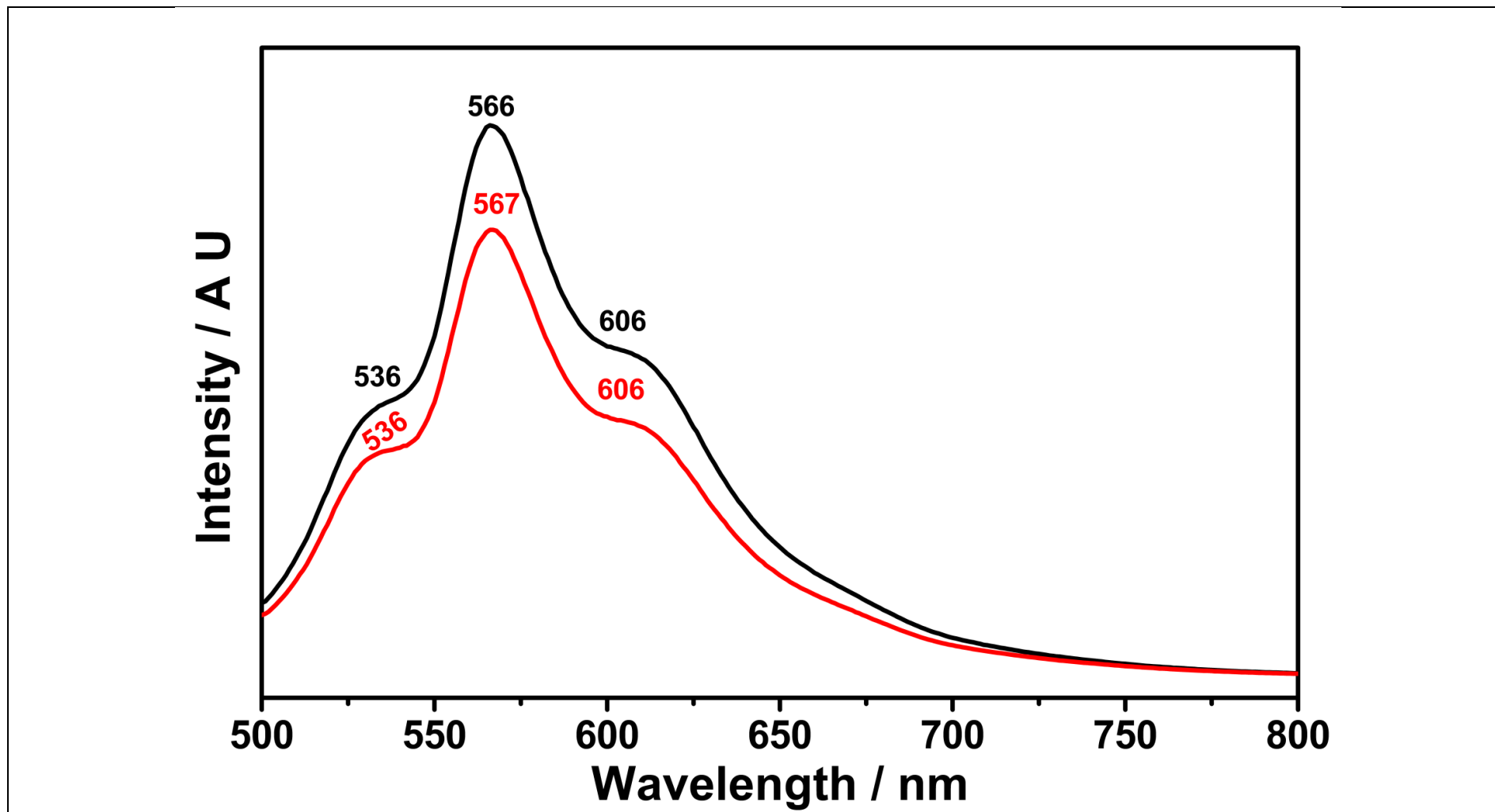


Figure 4.25: Emission Spectrum of TANDI in DMF (— : $C = 1 \times 10^{-5} \text{ M}$; — : Microfiltered; $\lambda_{\text{exc}} = 485 \text{ nm}$)

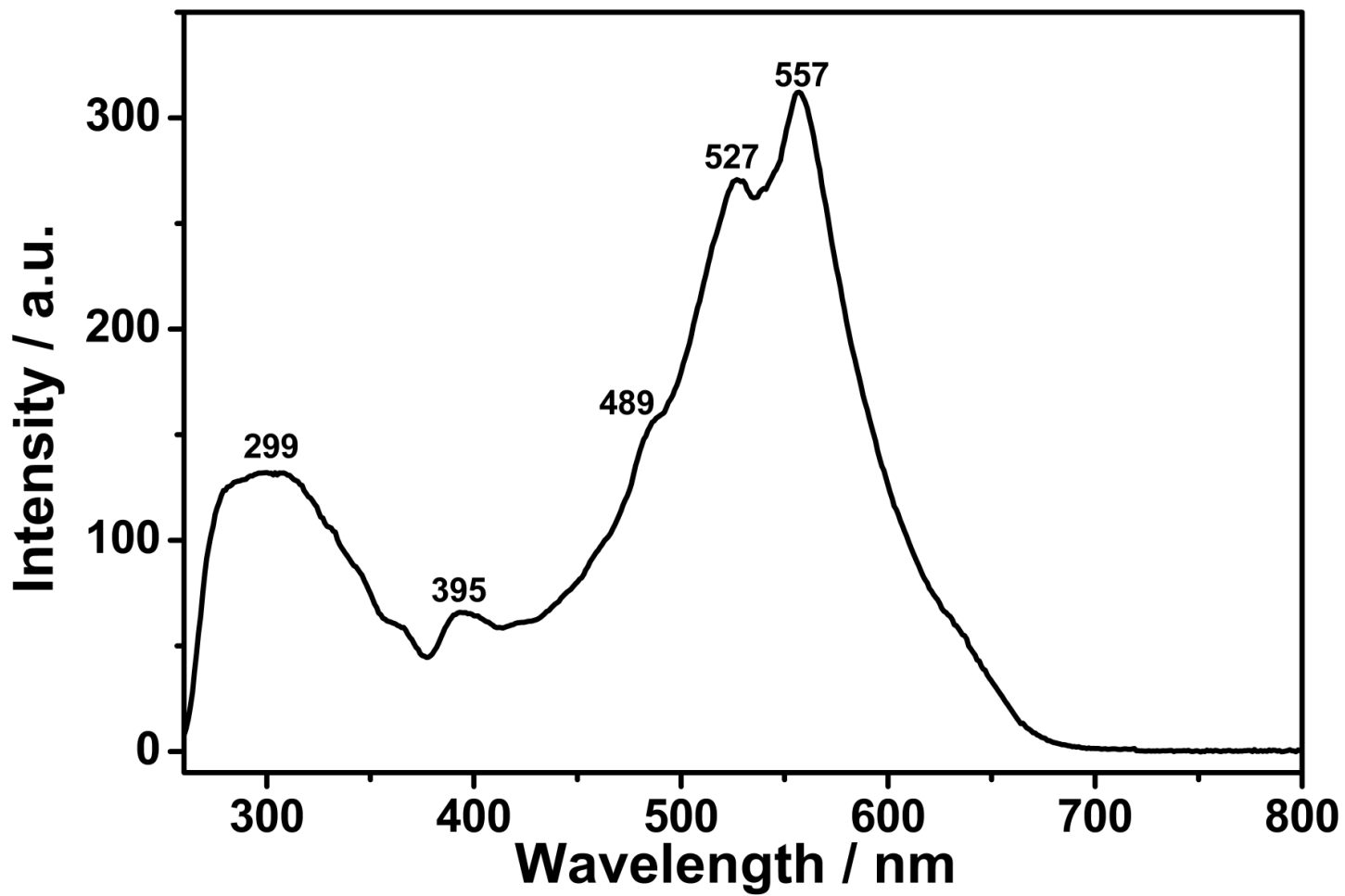


Figure 4.26: Excitation Spectrum of TANPI in DMF ($C = 1 \times 10^{-5}$ M; $\lambda_{\text{emis}} = 650$ nm)

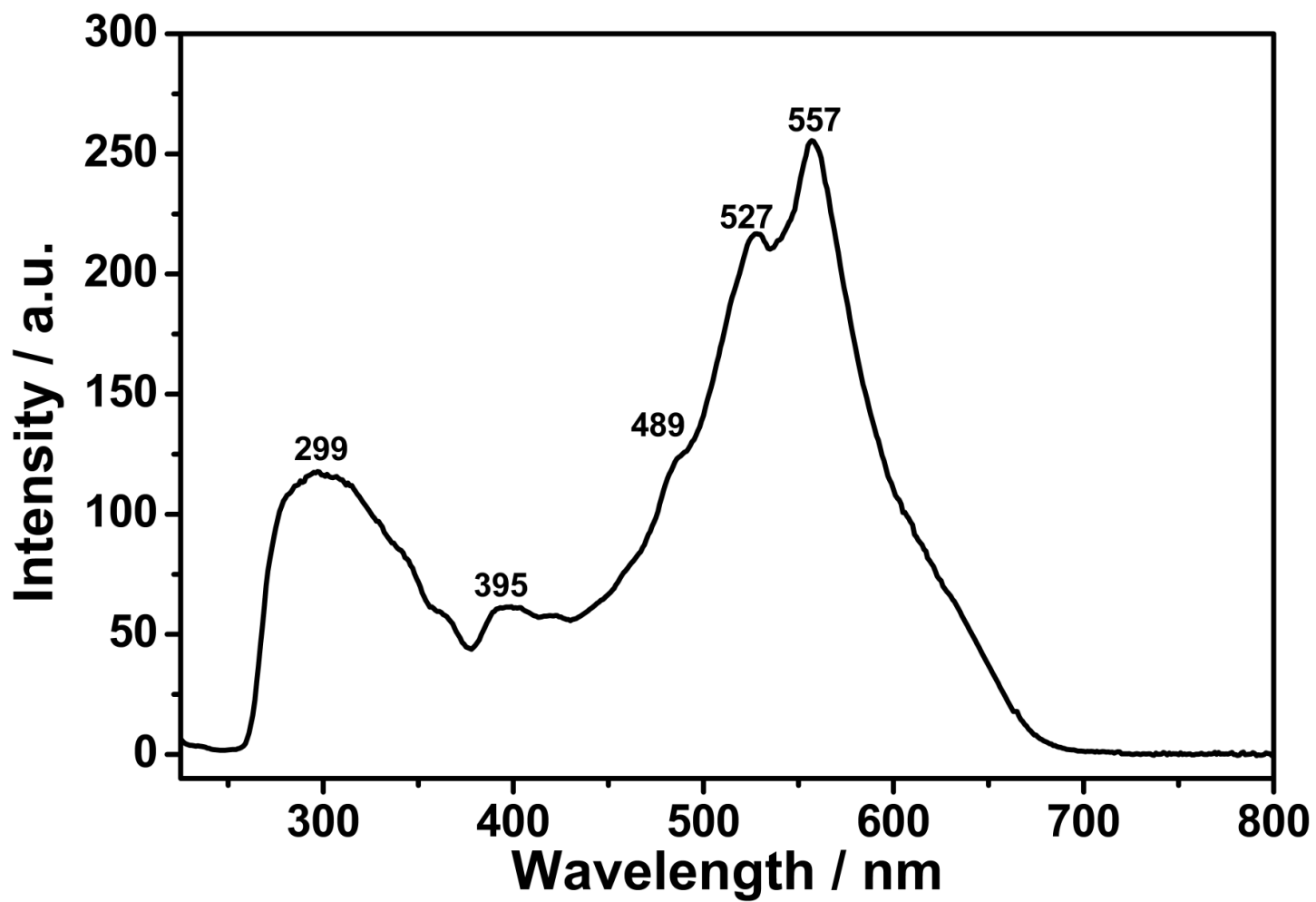


Figure 4.27: Excitation Spectrum of TANPI in DMF (Microfiltered; $\lambda_{\text{emis}} = 650 \text{ nm}$)

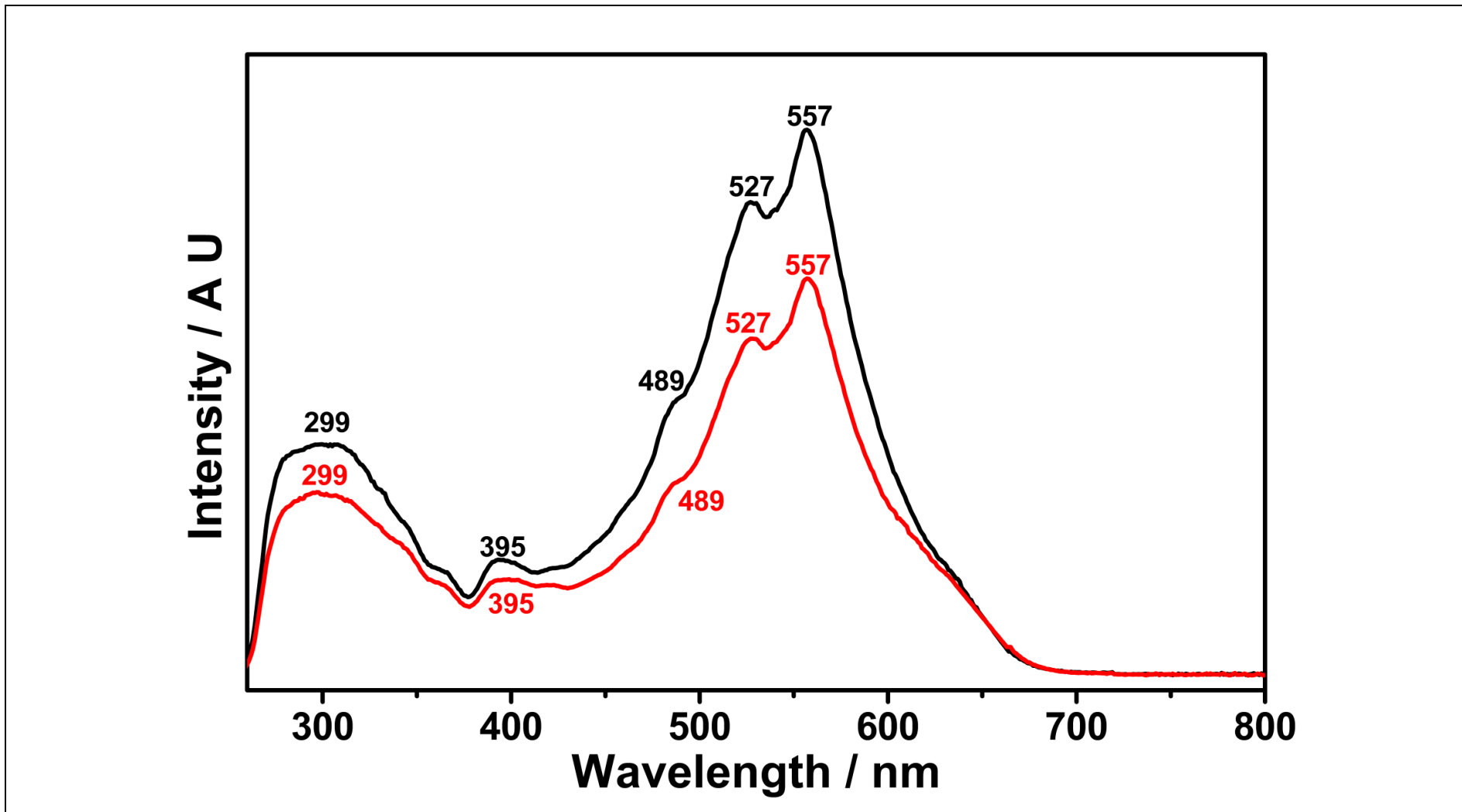


Figure 4.28: Excitation Spectrum of TANPI in DMF (—: $C = 1 \times 10^{-5}$ M; —: Microfiltered; $\lambda_{\text{emis}} = 650$ nm)

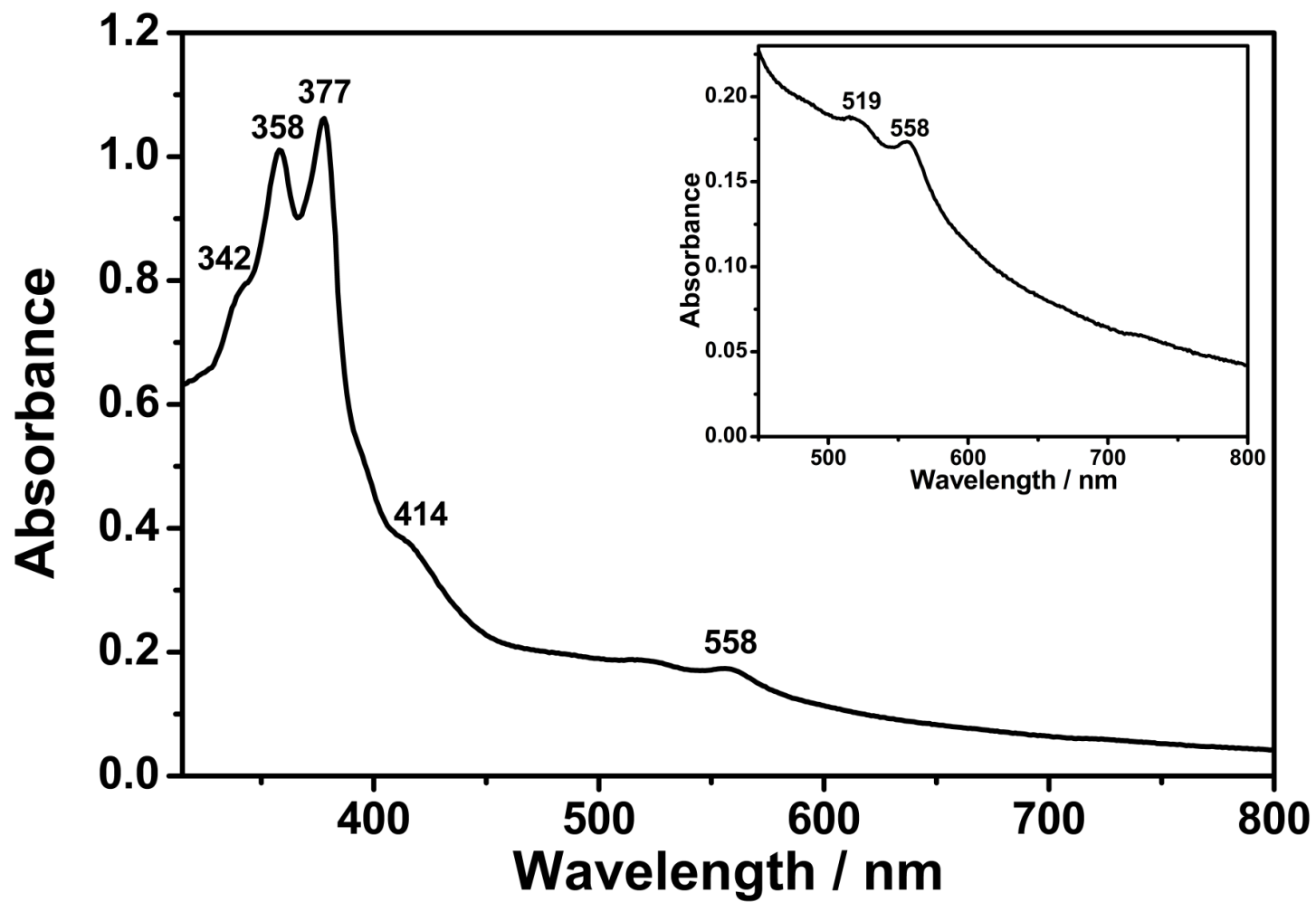


Figure 4.29: Absorption Spectrum of TANPI in NMP ($C = 1 \times 10^{-5}$ M, Inset: Enlarged Spectrum, 450-800 nm)

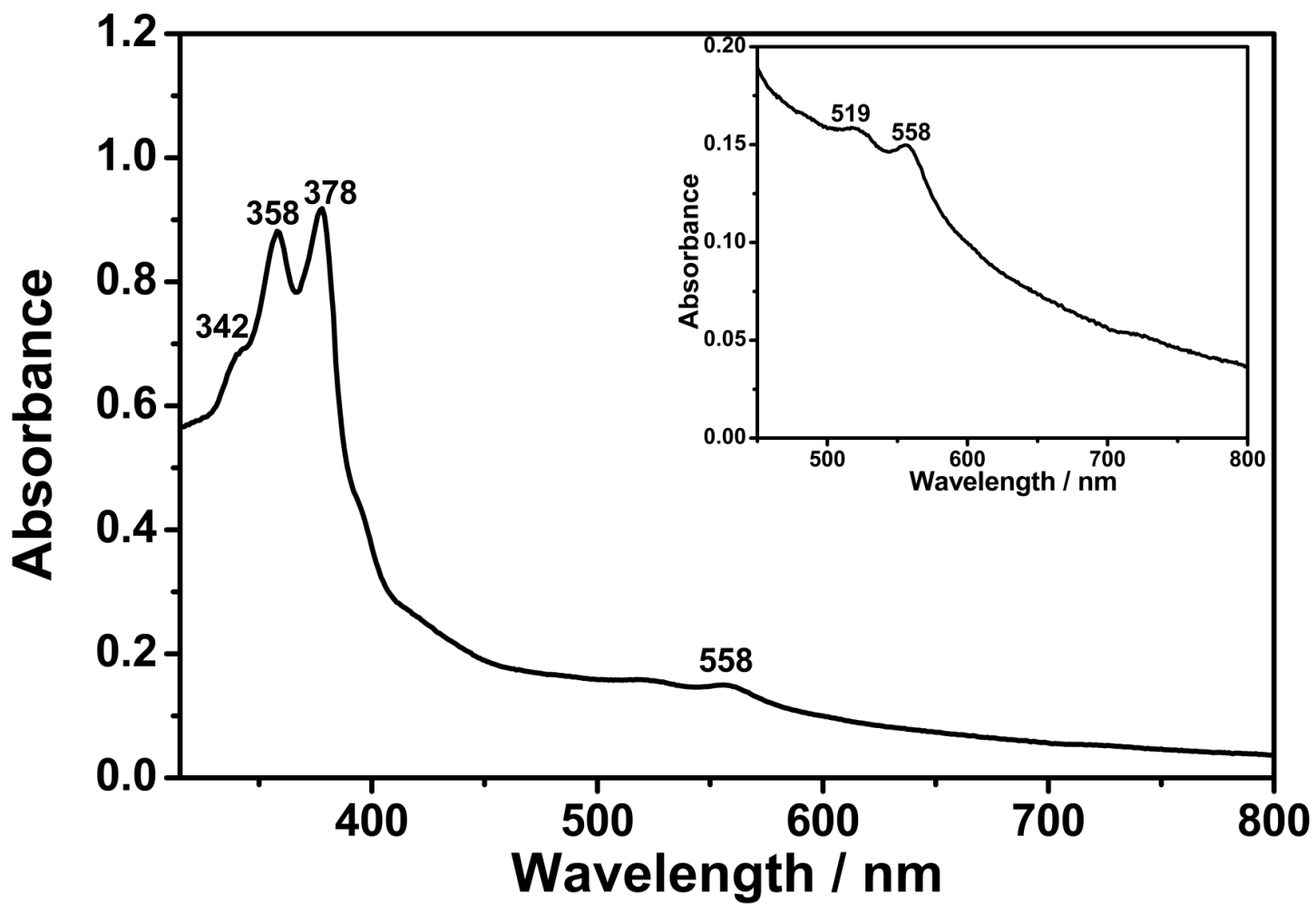


Figure 4.30: Absorption Spectrum of TANPI in NMP (Microfiltered ; Inset: Enlarged Spectrum, 450-800 nm)

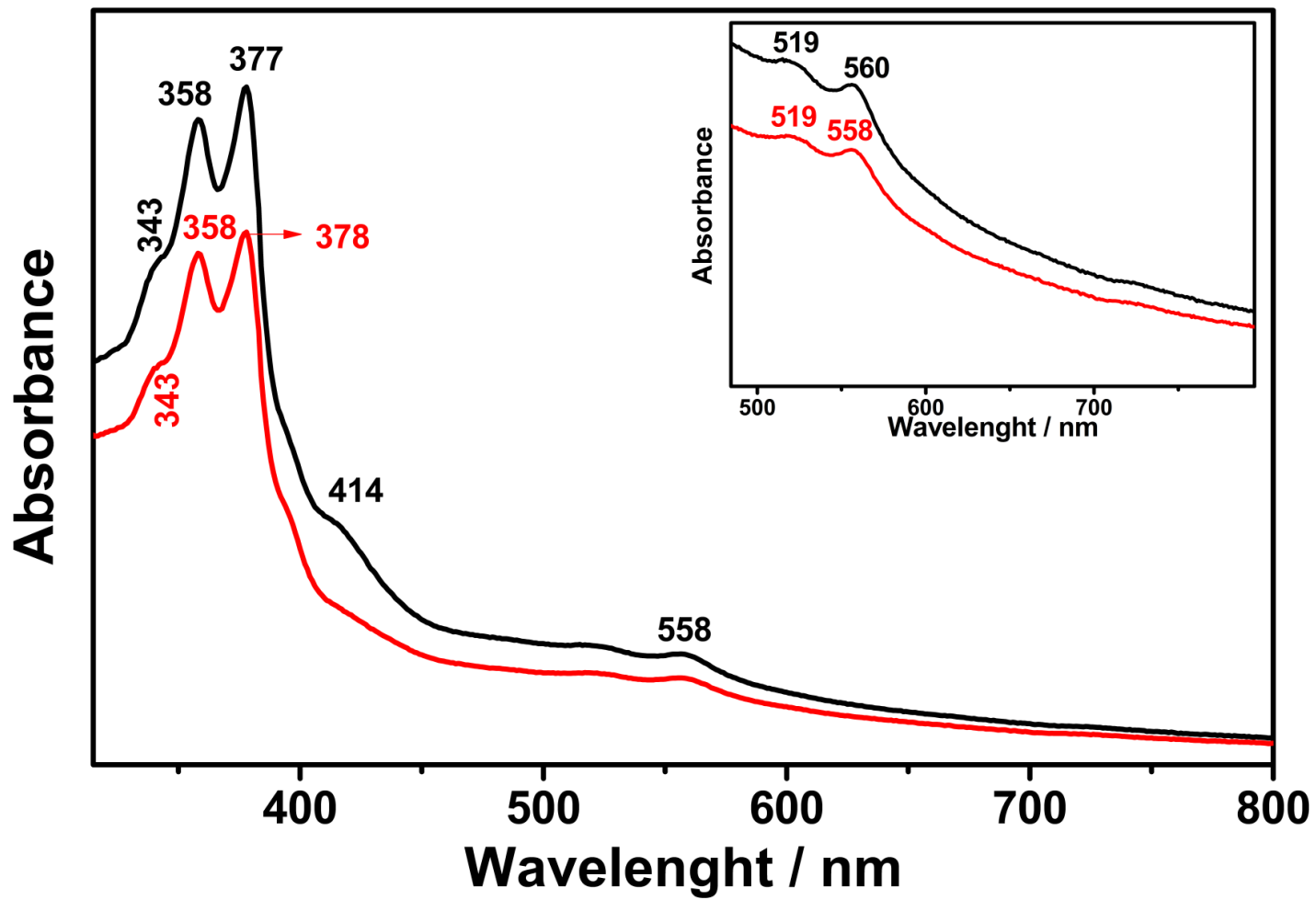


Figure 4.31: Absorption spectrum of TANPI in NMP (—: $C = 1 \times 10^{-5} \text{ M}$; —: Microfiltered ; Inset : Enlarged spectra 450-800 nm)

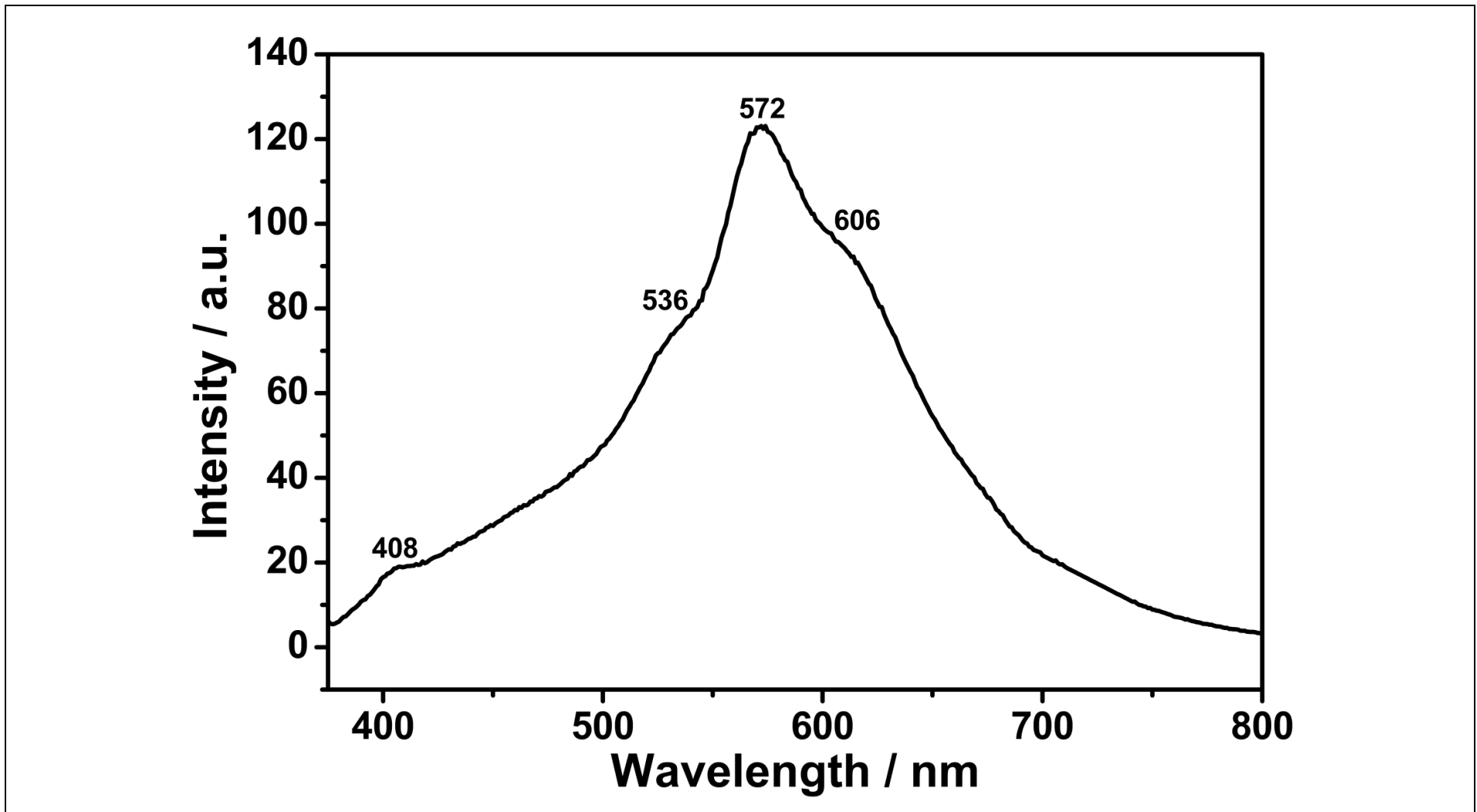


Figure 4.32: Emission Spectrum of TANPI in NMP ($C = 1 \times 10^{-5} \text{ M}$; $\lambda_{\text{exc}} = 360 \text{ nm}$)

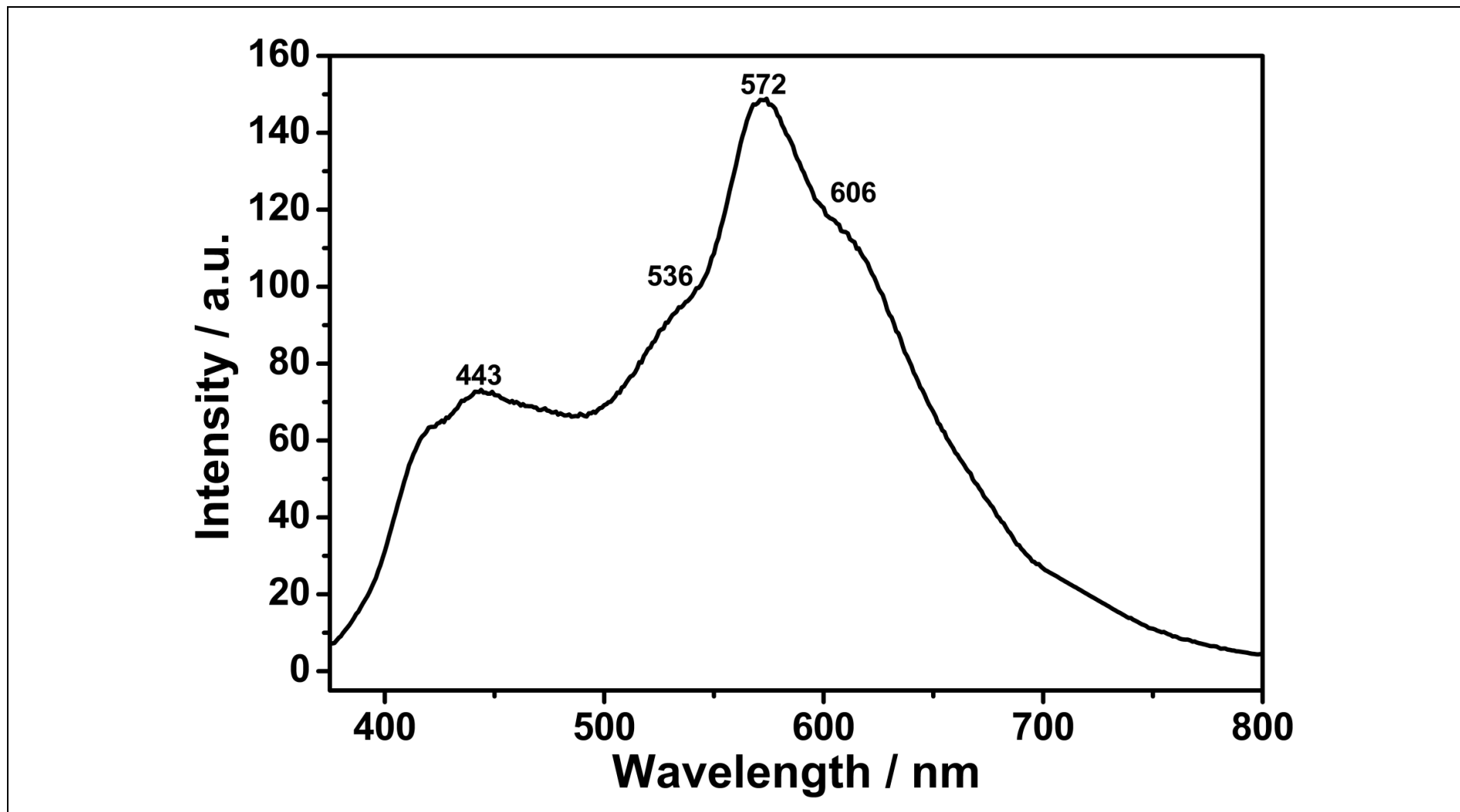


Figure 4.33: Emission Spectrum of TANPI in NMP (Microfiltered; $\lambda_{\text{exc}} = 360$ nm)

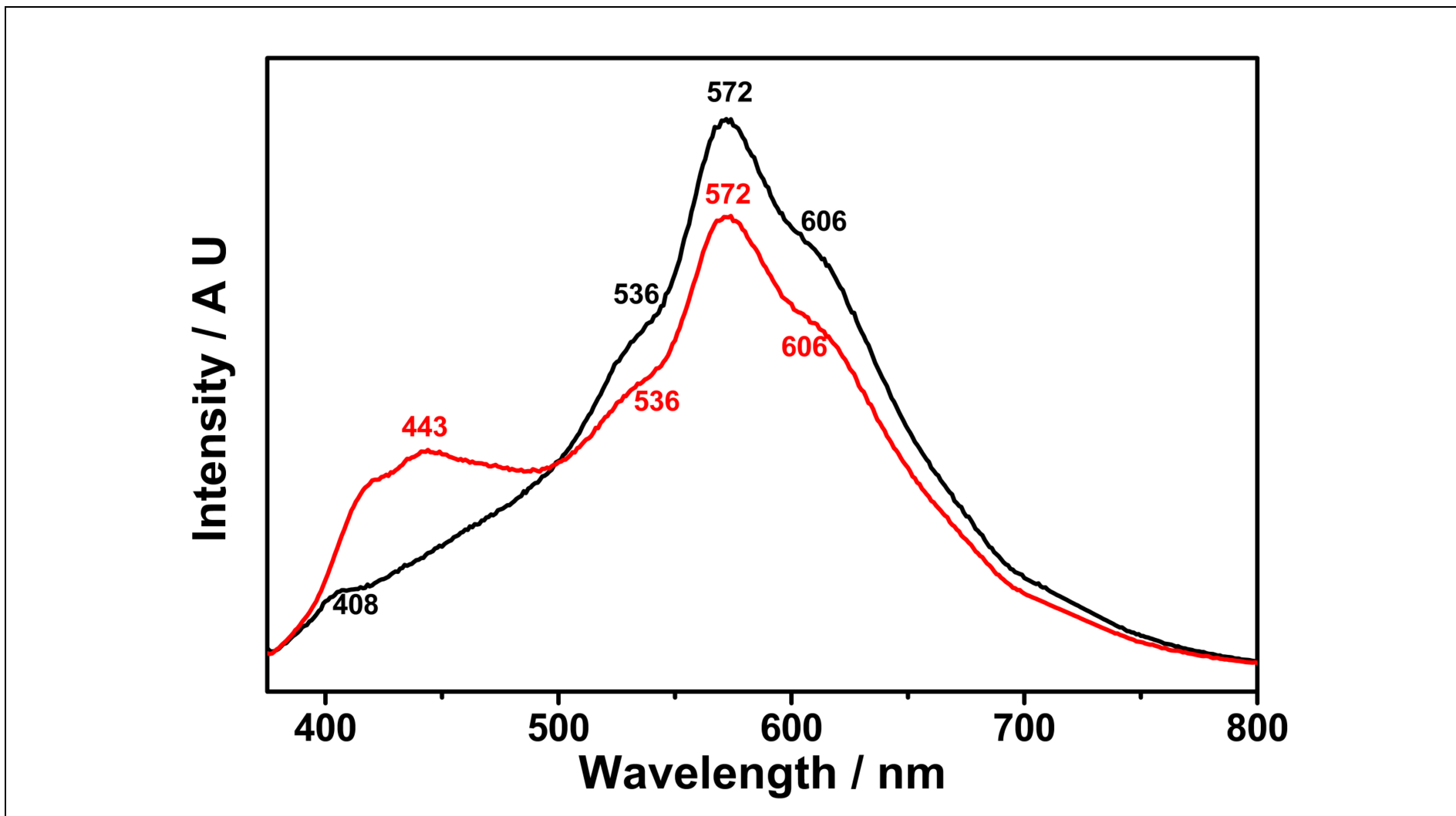


Figure 4.34: Emission spectrum of TANPI in NMP (— : $C = 1 \times 10^{-5} \text{ M}$; — : Microfiltered; $\lambda_{\text{exc}} = 360 \text{ nm}$)

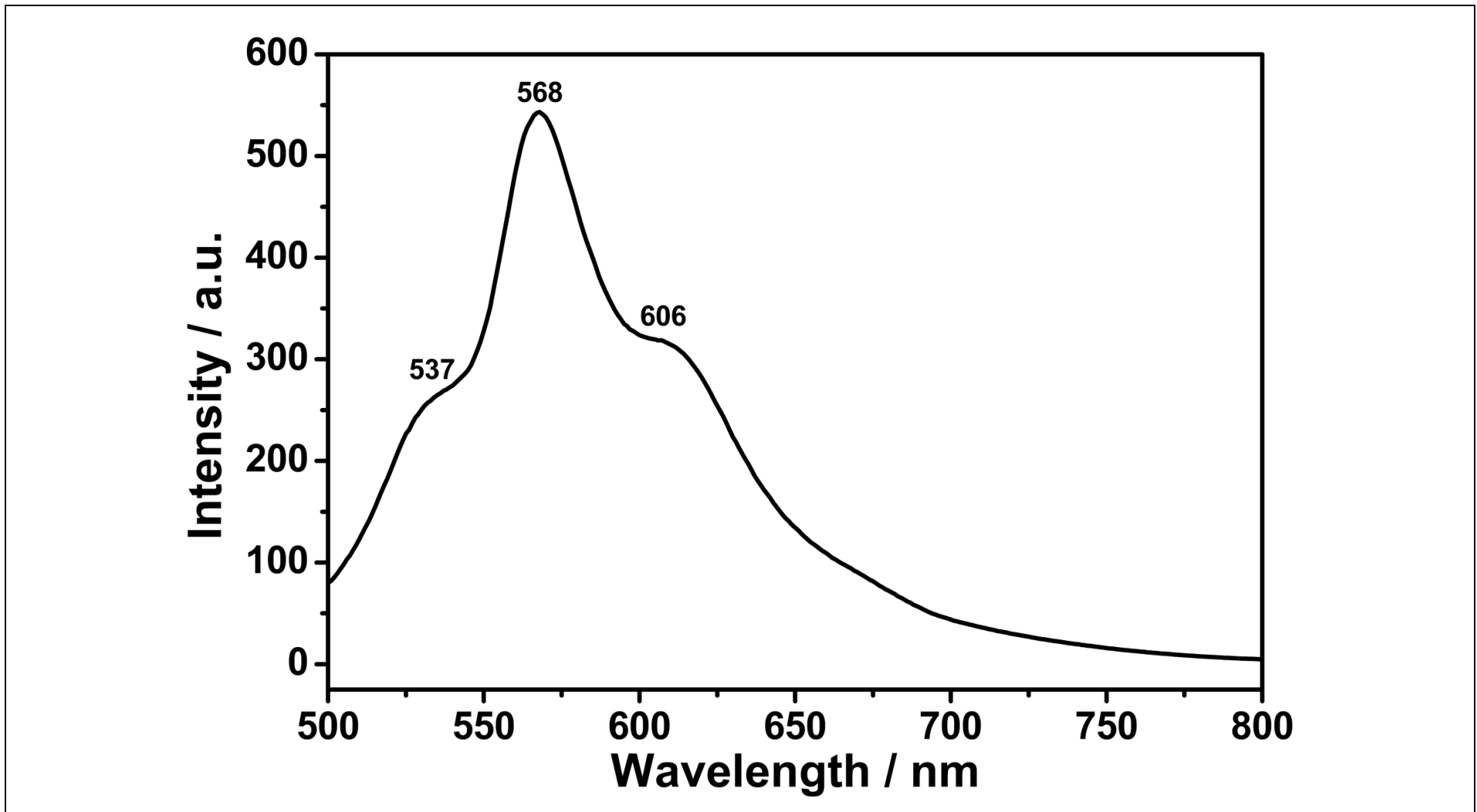


Figure 4.35: Emission Spectrum of TANPI in NMP ($C = 1 \times 10^{-5}$ M; $\lambda_{\text{exc}} = 485$ nm)

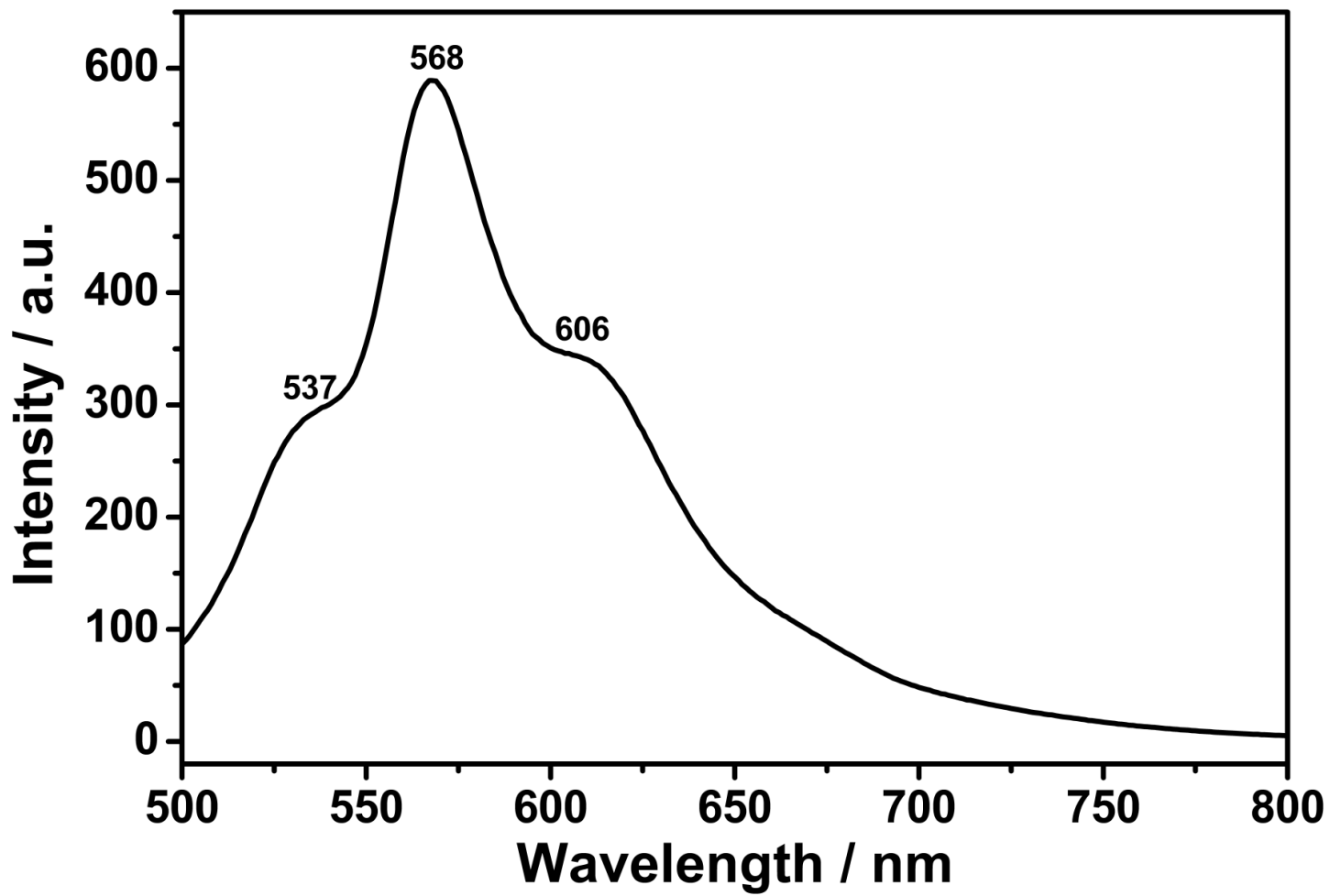


Figure 4.36: Emission Spectrum of TANPI in NMP (Microfiltered; $\lambda_{exc} = 485$ nm)

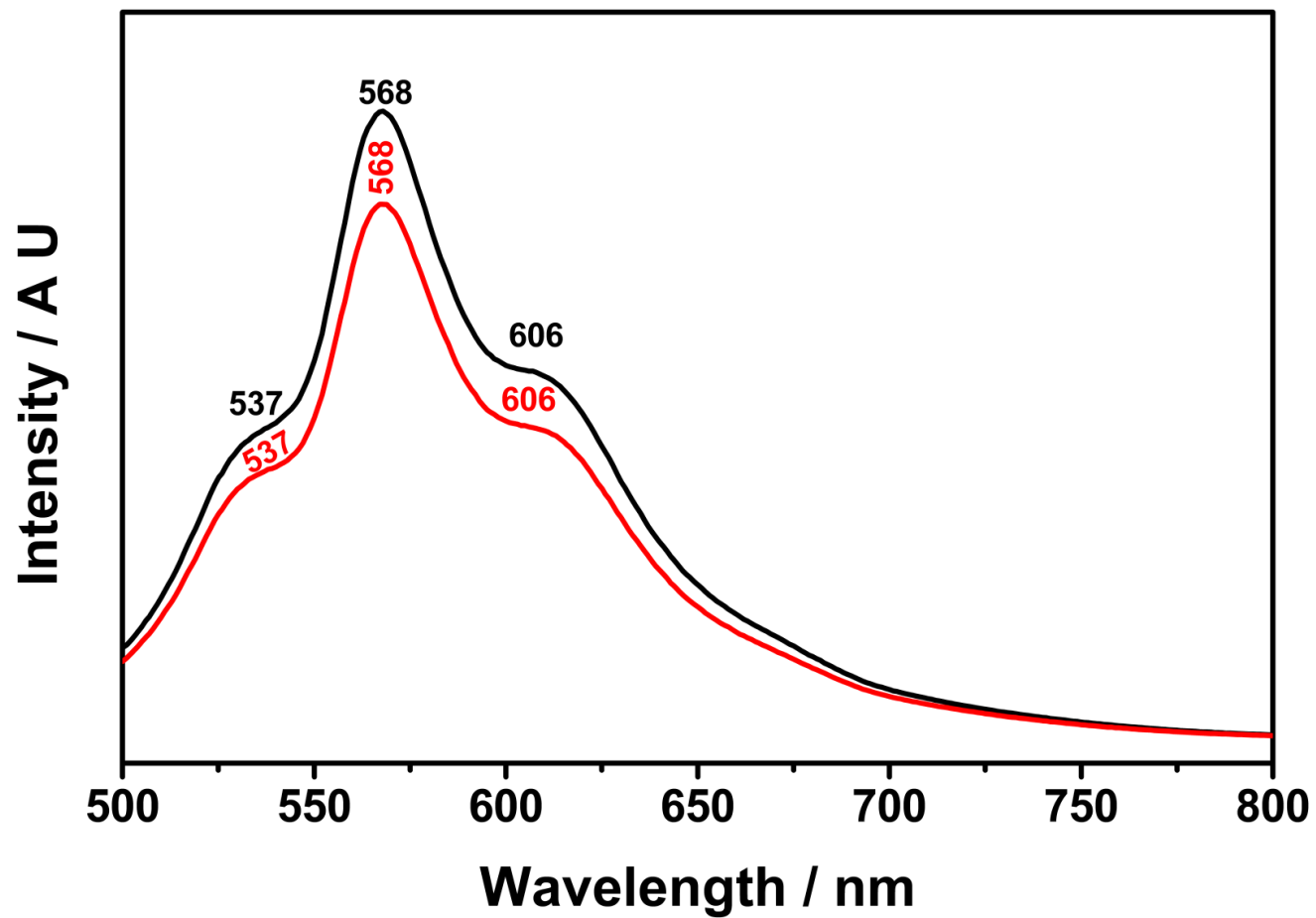


Figure 4.37: Emission Spectrum of TANPI in NMP (—: $C = 1 \times 10^{-5}$ M; —: Microfiltered; $\lambda_{\text{exc}} = 485$ nm)

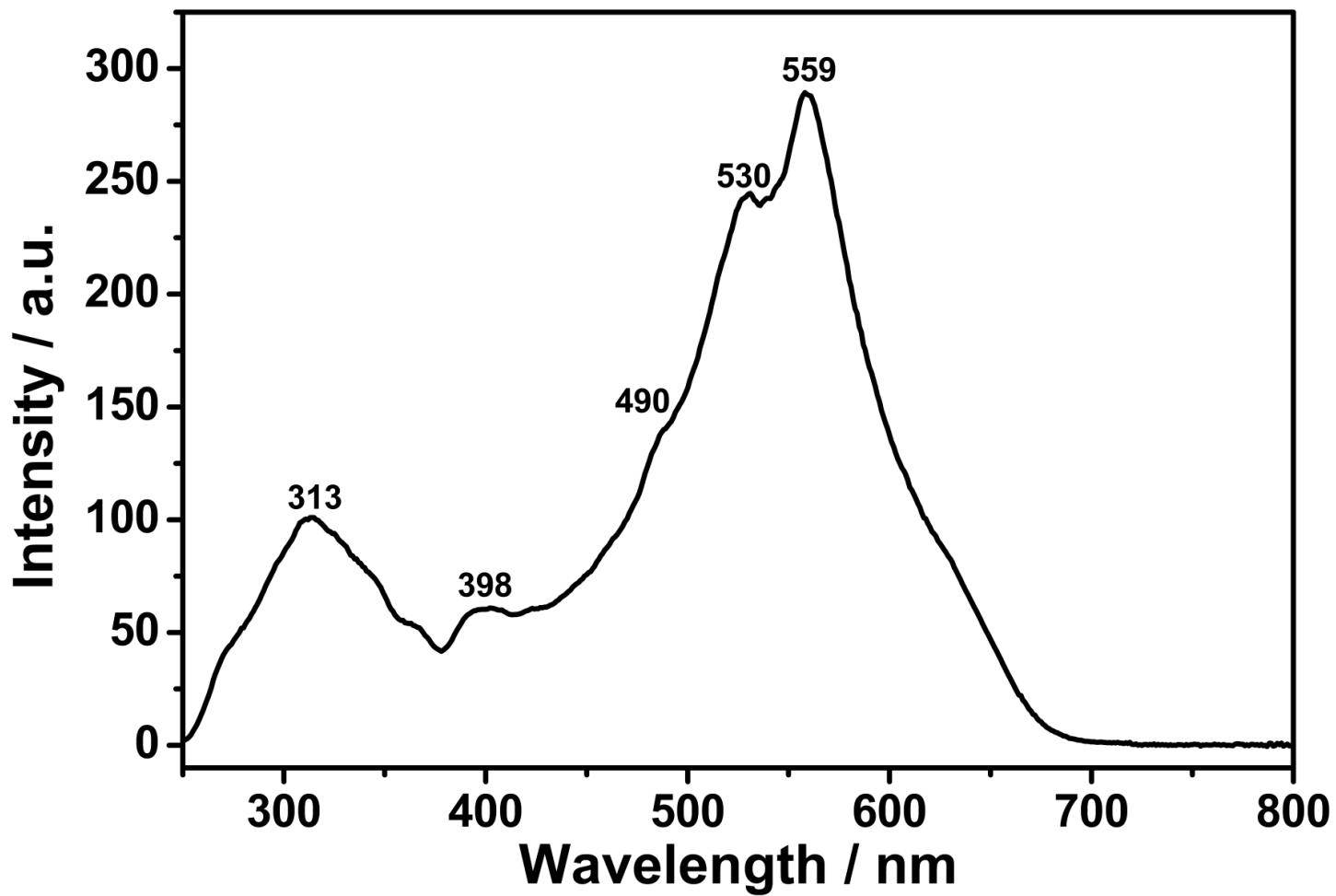


Figure 4.38: Excitation Spectrum of TANPI in NMP ($C = 1 \times 10^{-5}$ M; $\lambda_{\text{emis}} = 650$ nm)

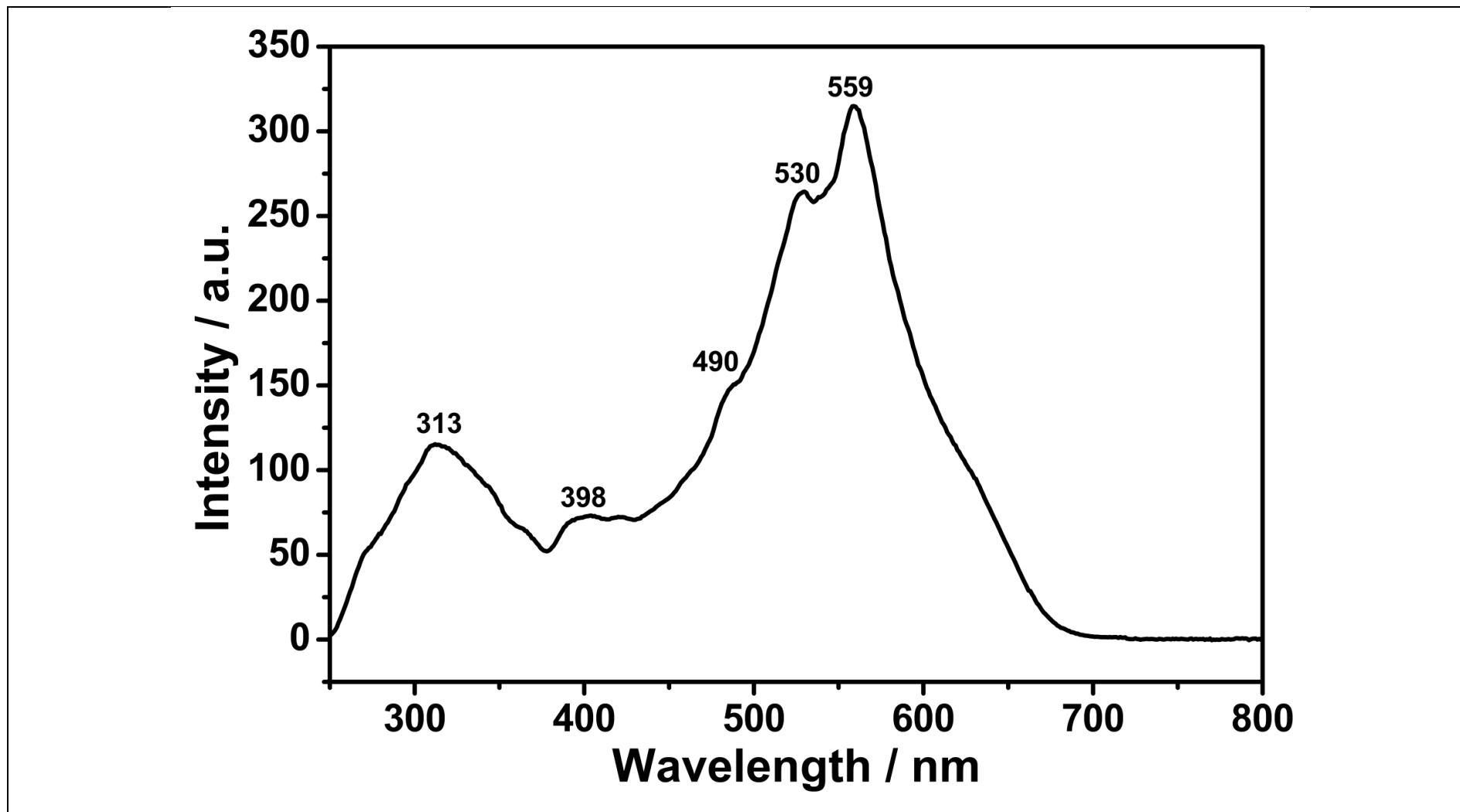


Figure 4.39: Excitation Spectrum of TANPI in NMP (Microfiltered; $\lambda_{\text{emis}} = 650 \text{ nm}$)

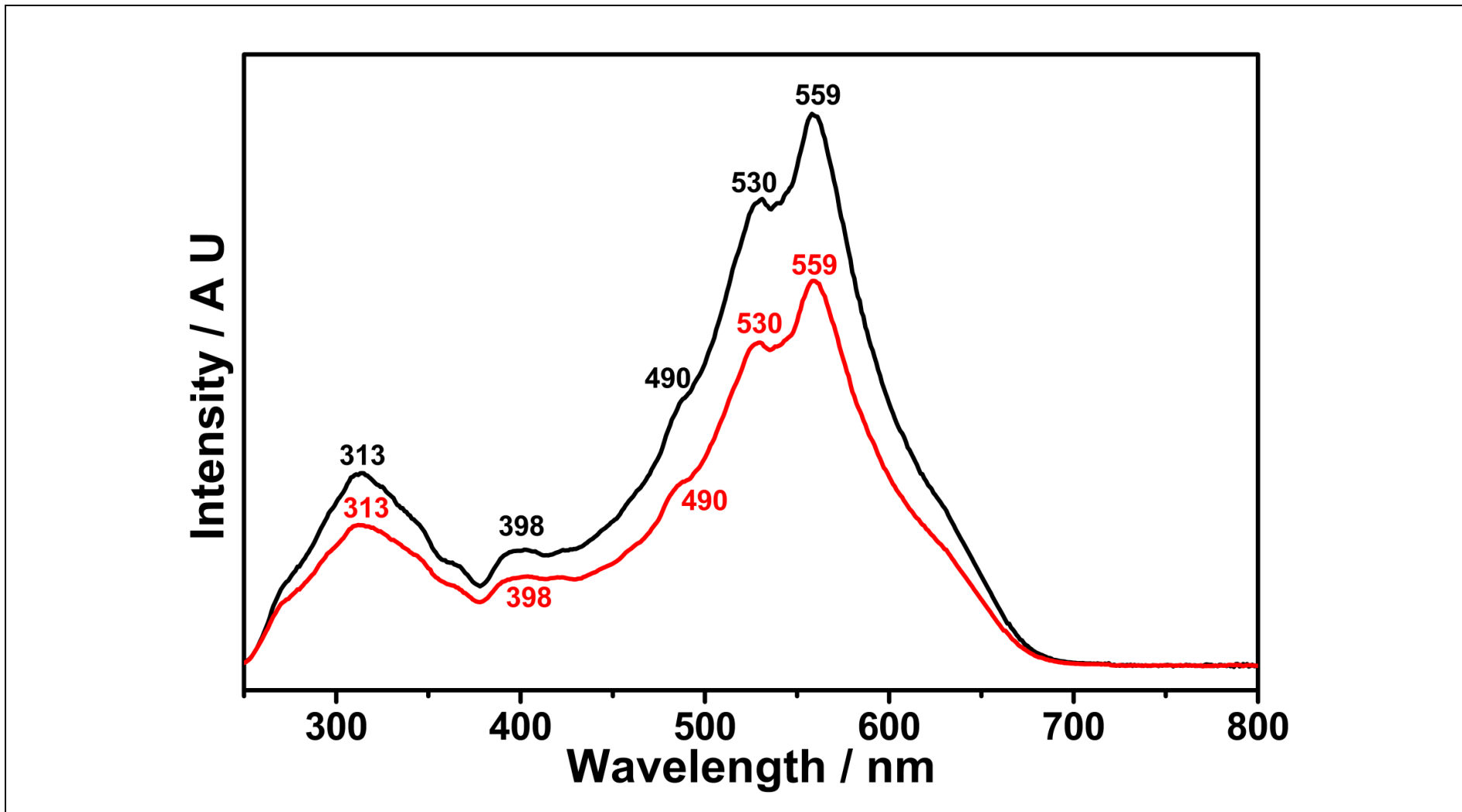


Figure 4.40: Excitation Spectrum of TANPI in NMP (—: $C = 1 \times 10^{-5} \text{ M}$; —: Microfiltered; $\lambda_{\text{emis}} = 650 \text{ nm}$)

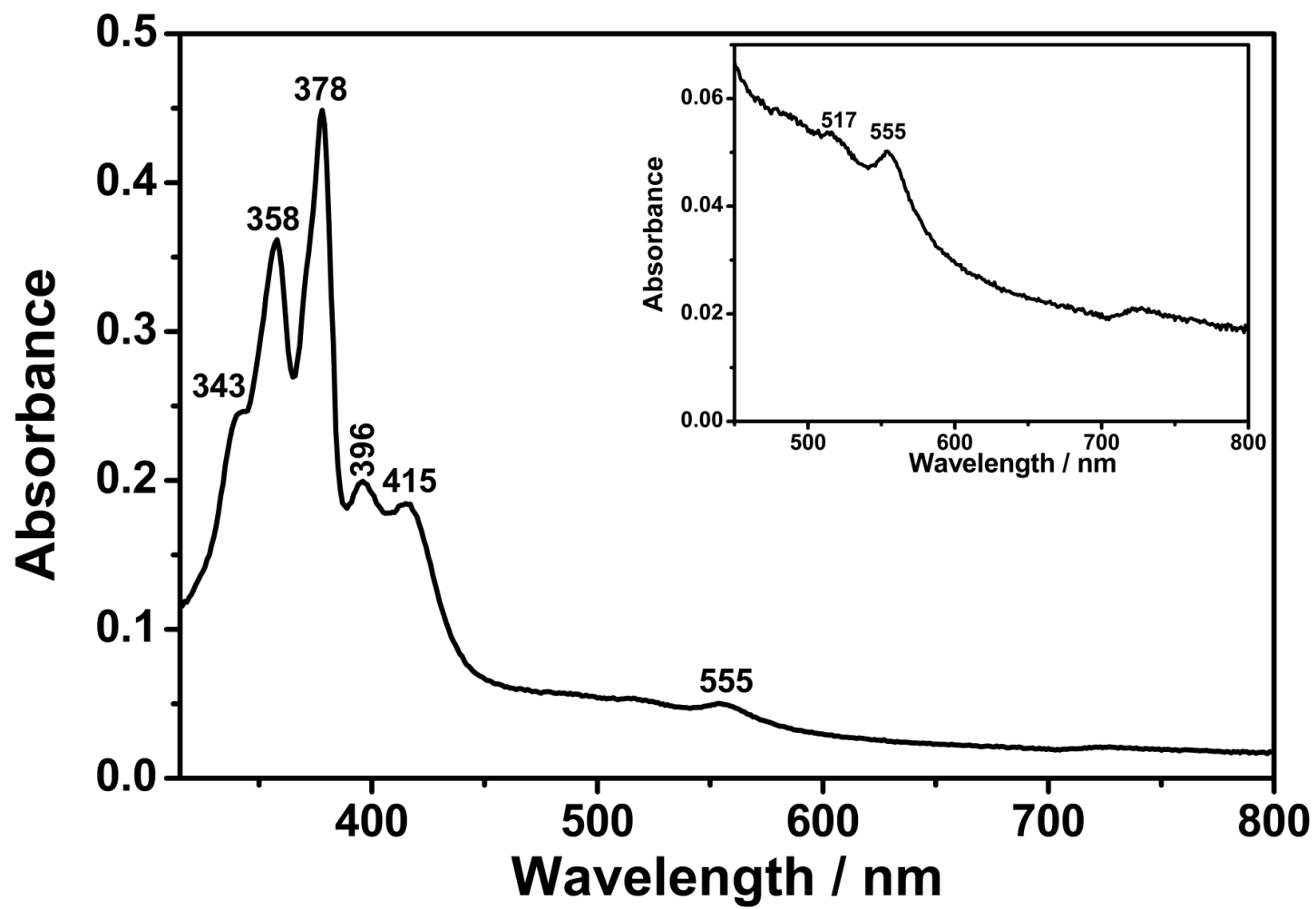


Figure 4.41: Absorption Spectrum of TANPI in TCE ($C = 1 \times 10^{-5}$ M, Inset: Enlarged Spectrum, 450-800 nm)

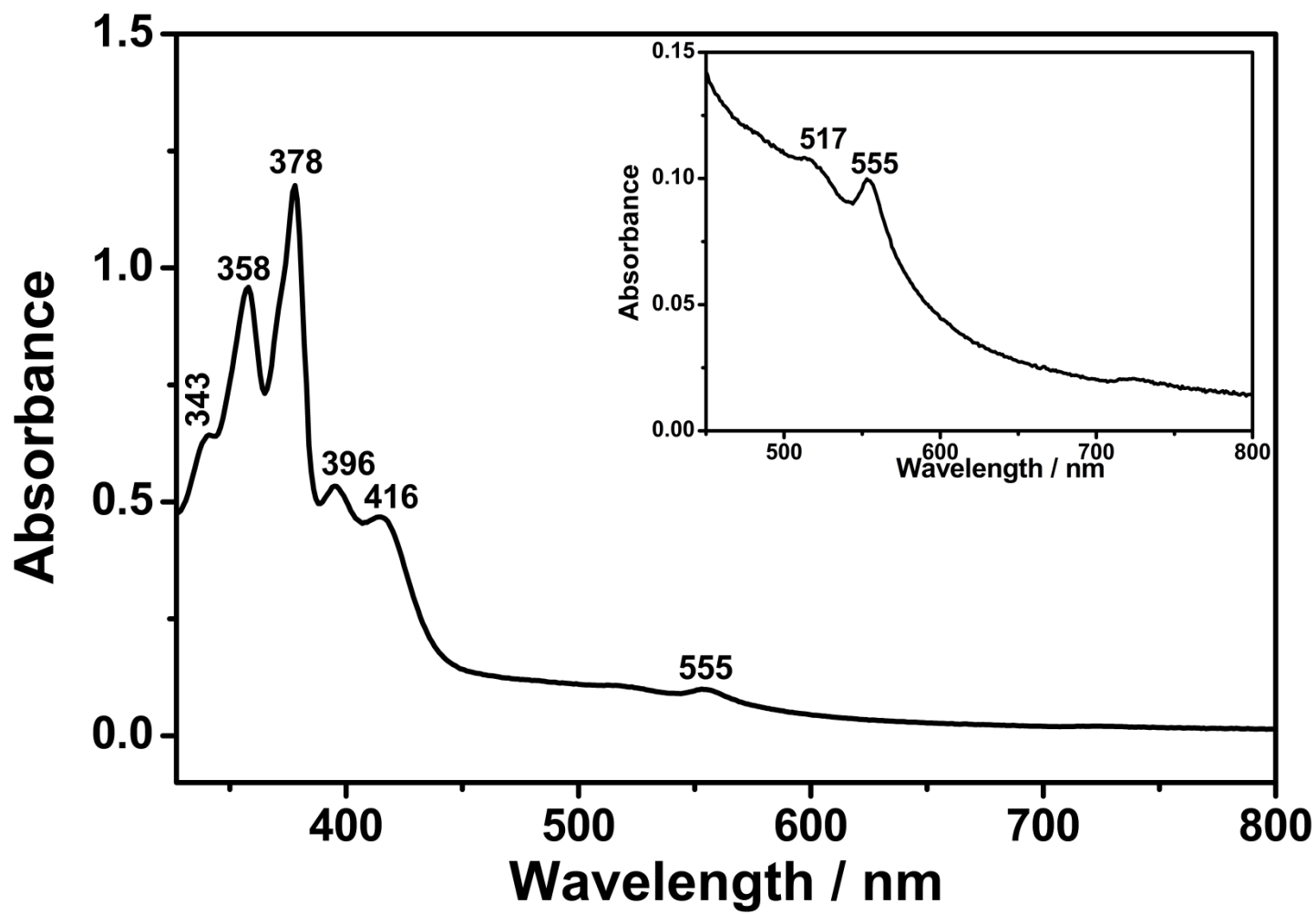


Figure 4.42: Absorption Spectrum of TANPI in TCE (Microfiltered, Inset: Enlarged Spectrum, 450-800 nm)

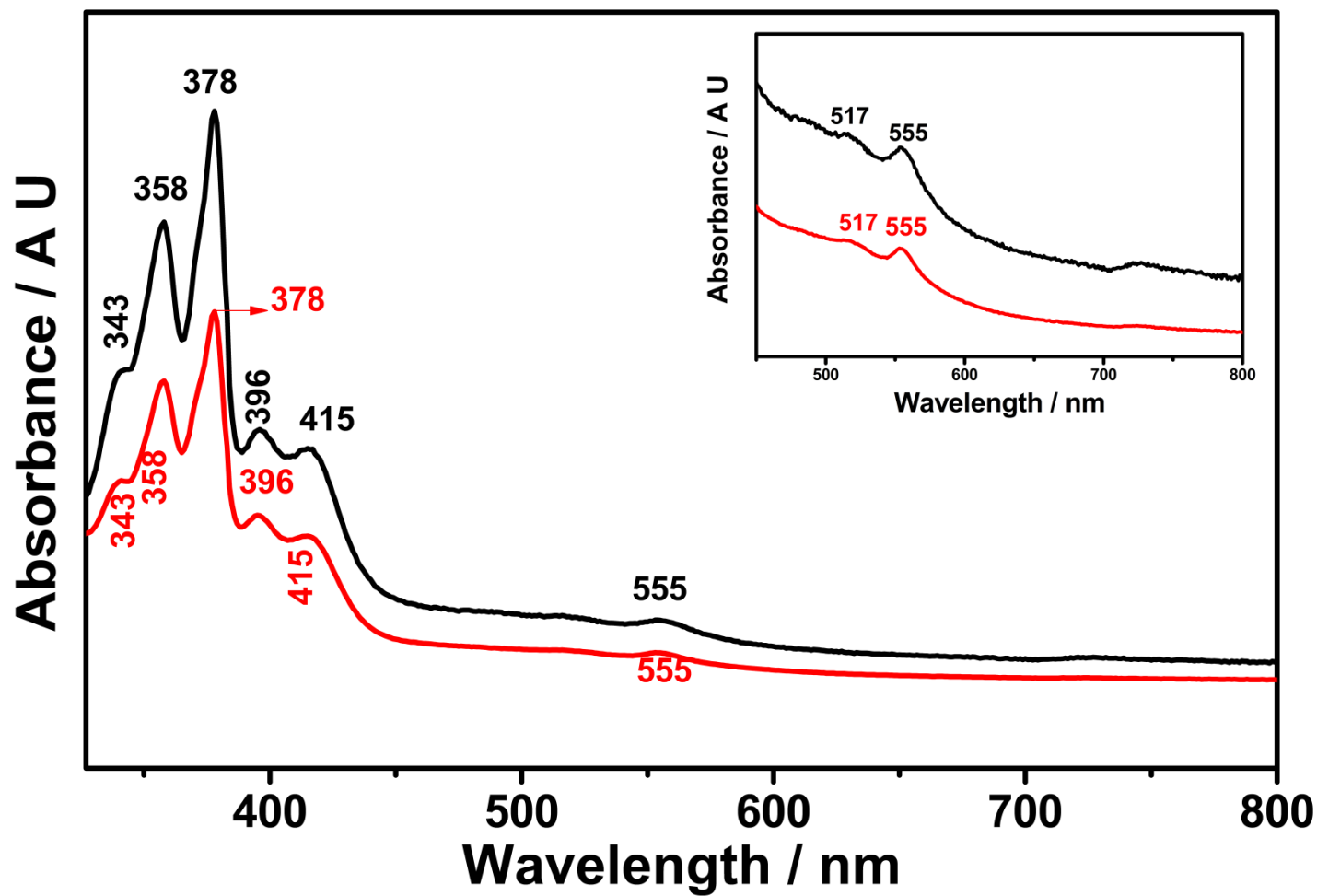


Figure 4.43: Absorption Spectrum of TANPI in TCE (—: $C = 1 \times 10^{-5} \text{ M}$; —: Microfiltered; Inset: Enlarged Spectrum, 450-800 nm)

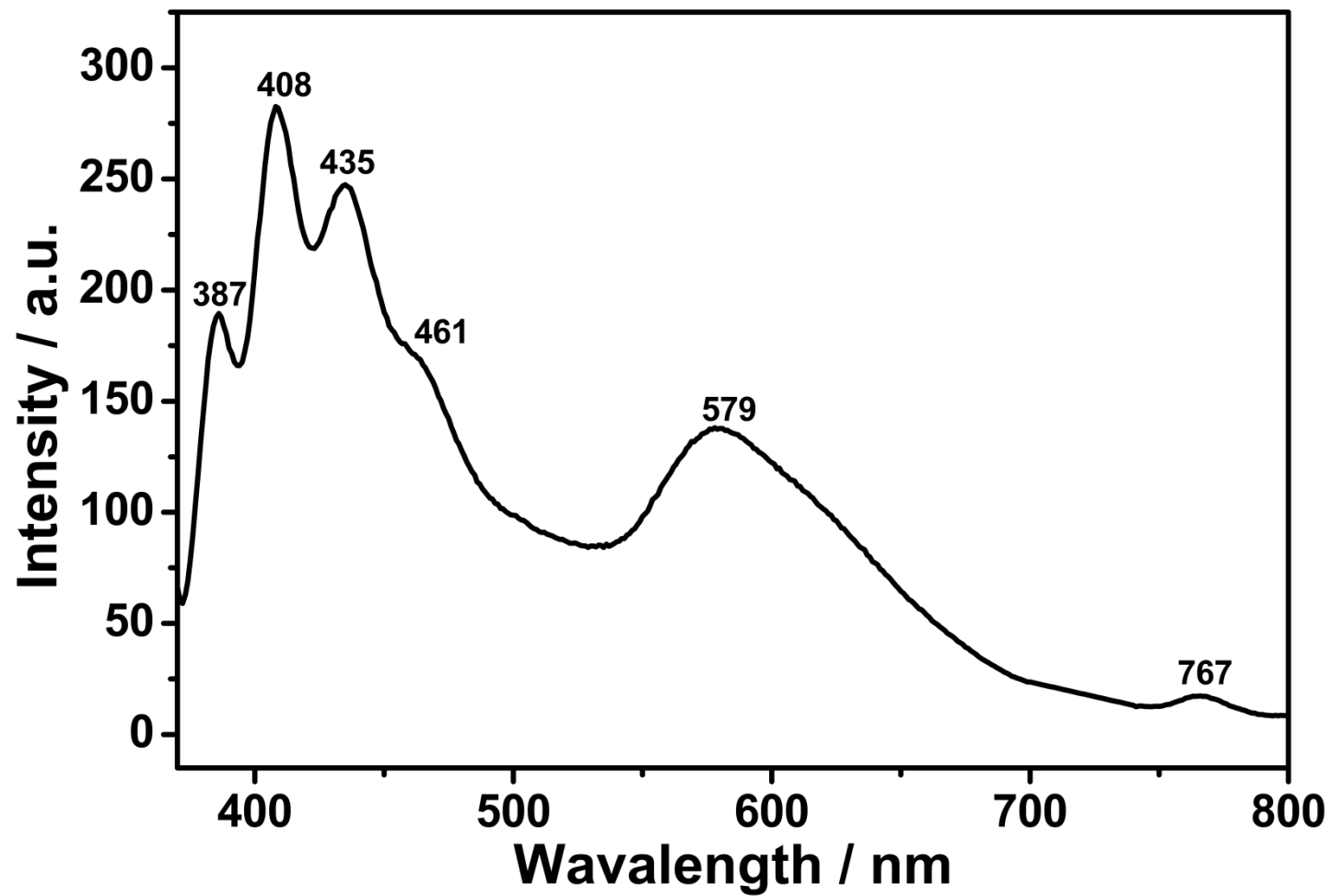


Figure 4.44: Emission Spectrum of TANPI in TCE ($C = 1 \times 10^{-5} \text{ M}$; $\lambda_{\text{exc}} = 360 \text{ nm}$)

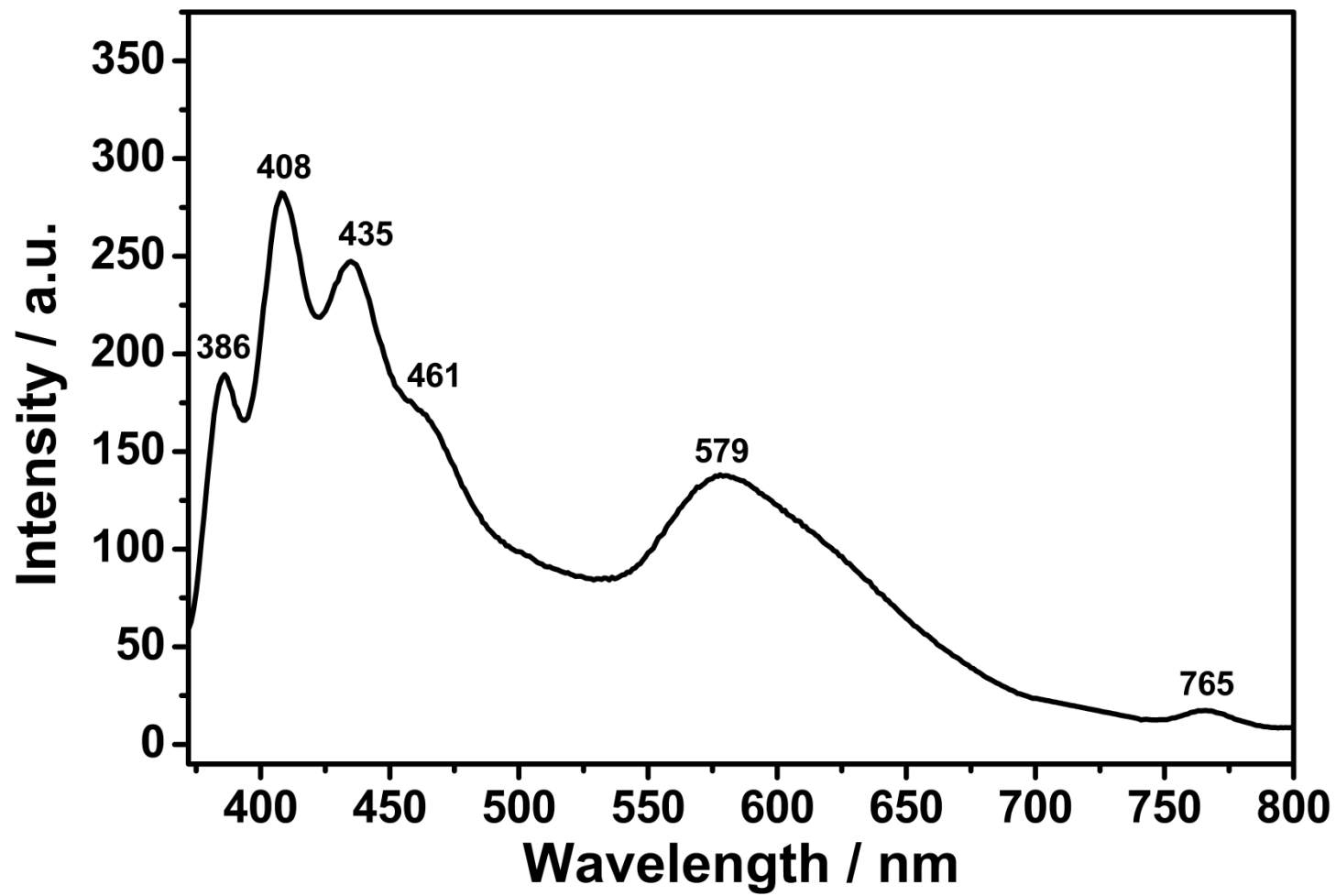


Figure 4.45: Emission Spectrum of TANPI in TCE (Microfiltered; $\lambda_{exc} = 360$ nm)

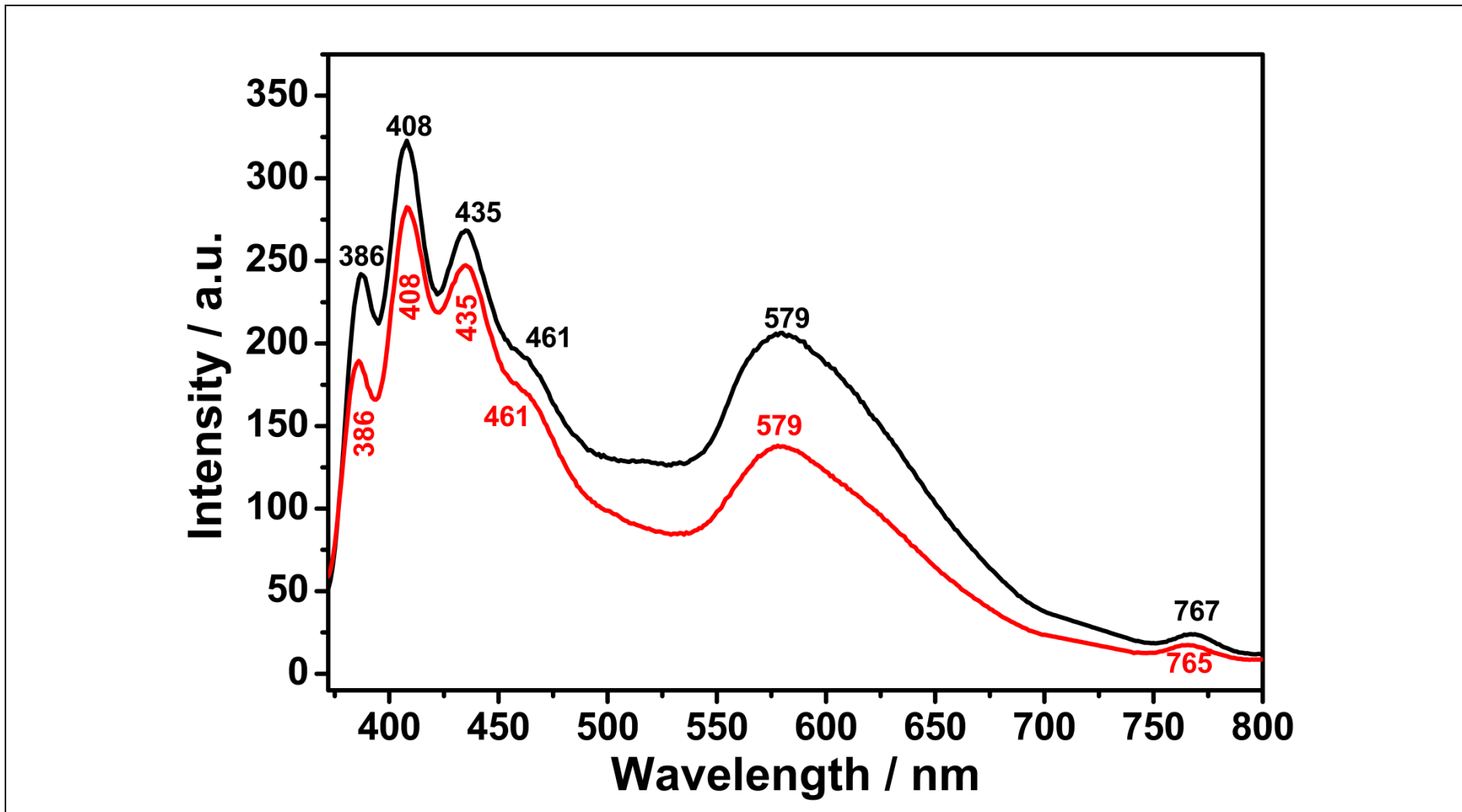


Figure 4.46: Emission Spectrum of TANPI in TCE (—: $C = 1 \times 10^{-5}$ M; —: Microfiltered; $\lambda_{\text{exc}} = 360$ nm)

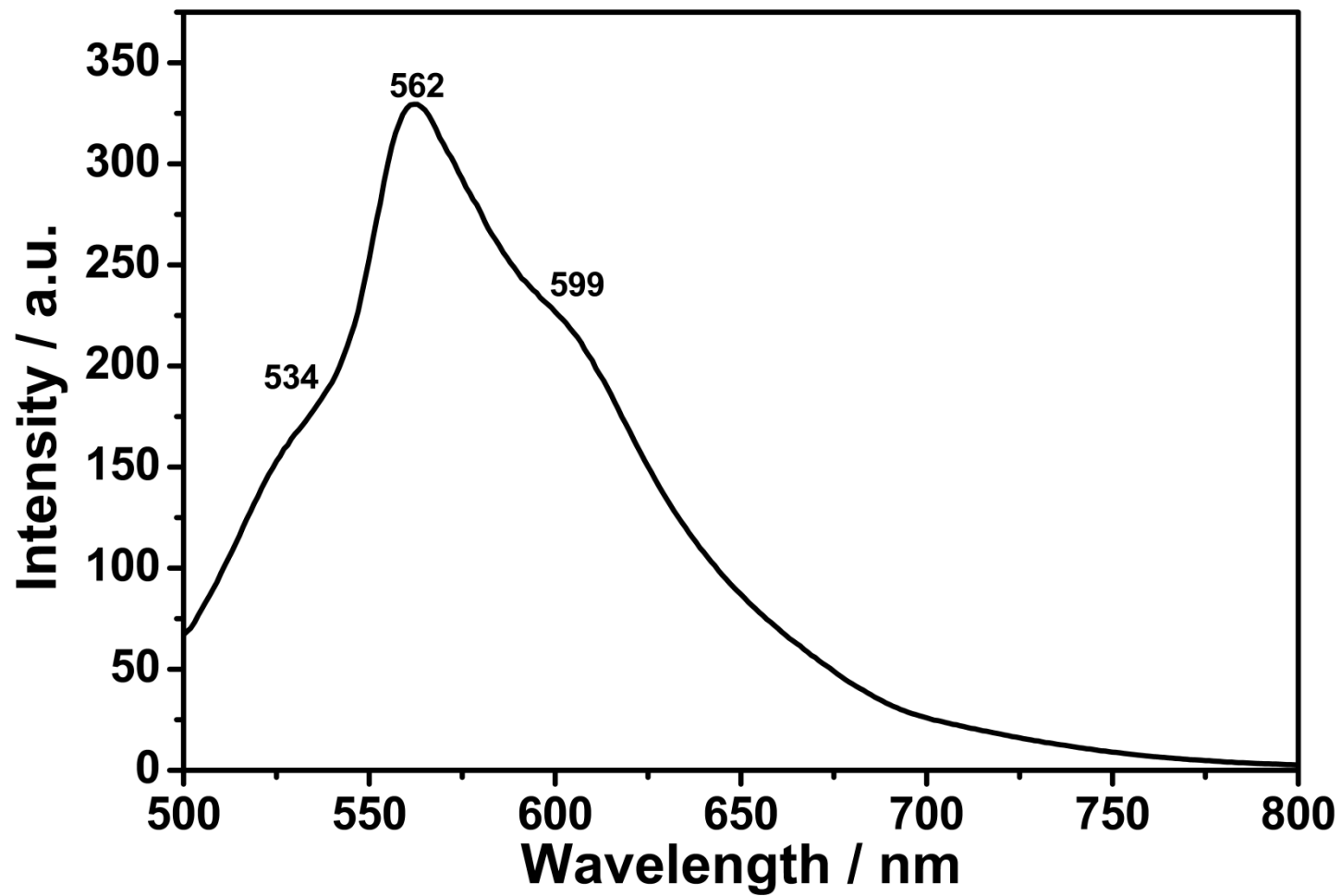


Figure 4.47: Emission Spectrum of TANPI in TCE ($C = 1 \times 10^{-5}$ M; $\lambda_{\text{exc}} = 485$ nm)

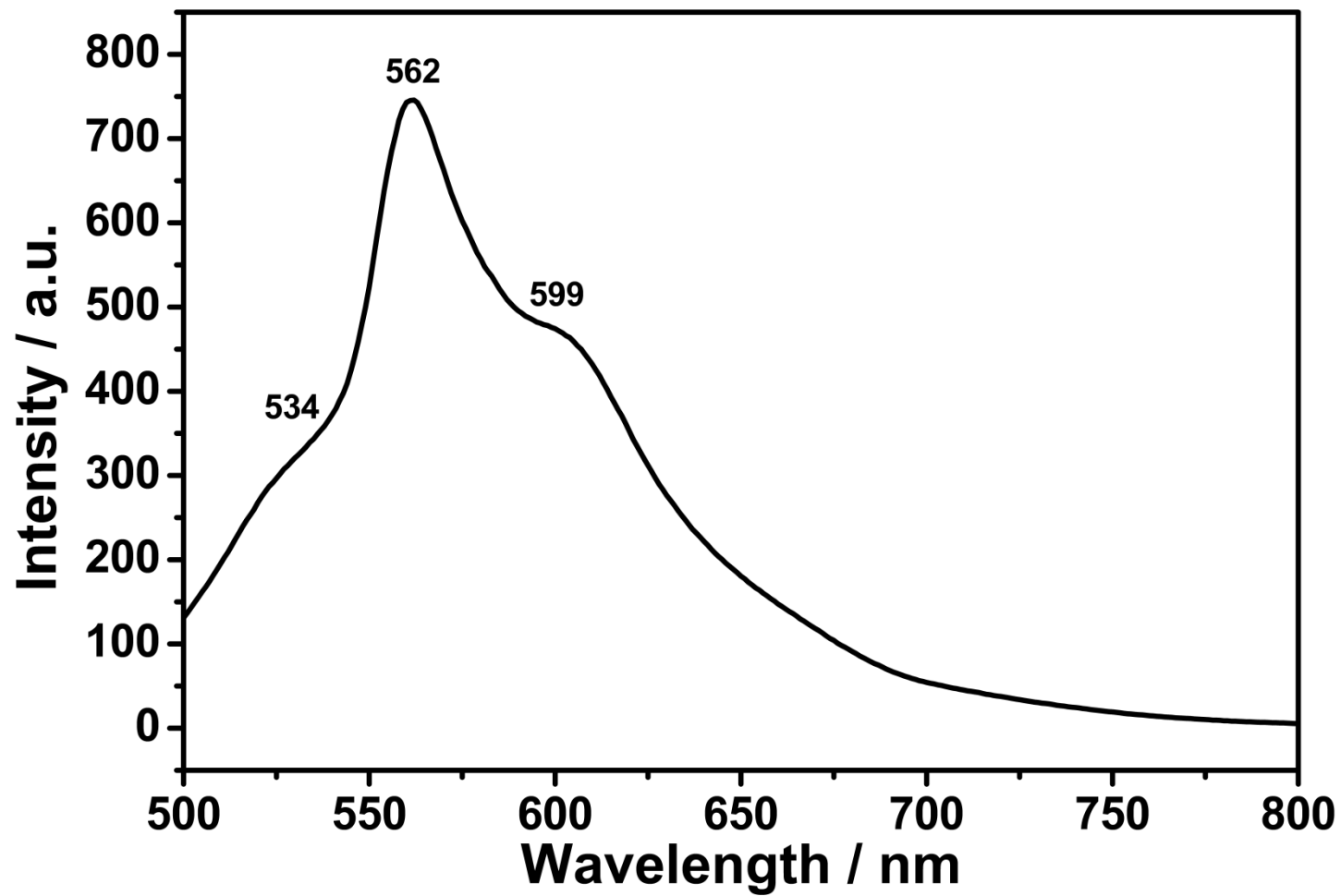


Figure 4.48: Emission Spectrum of TANPI in TCE (Microfiltered; $\lambda_{\text{exc}} = 485 \text{ nm}$)

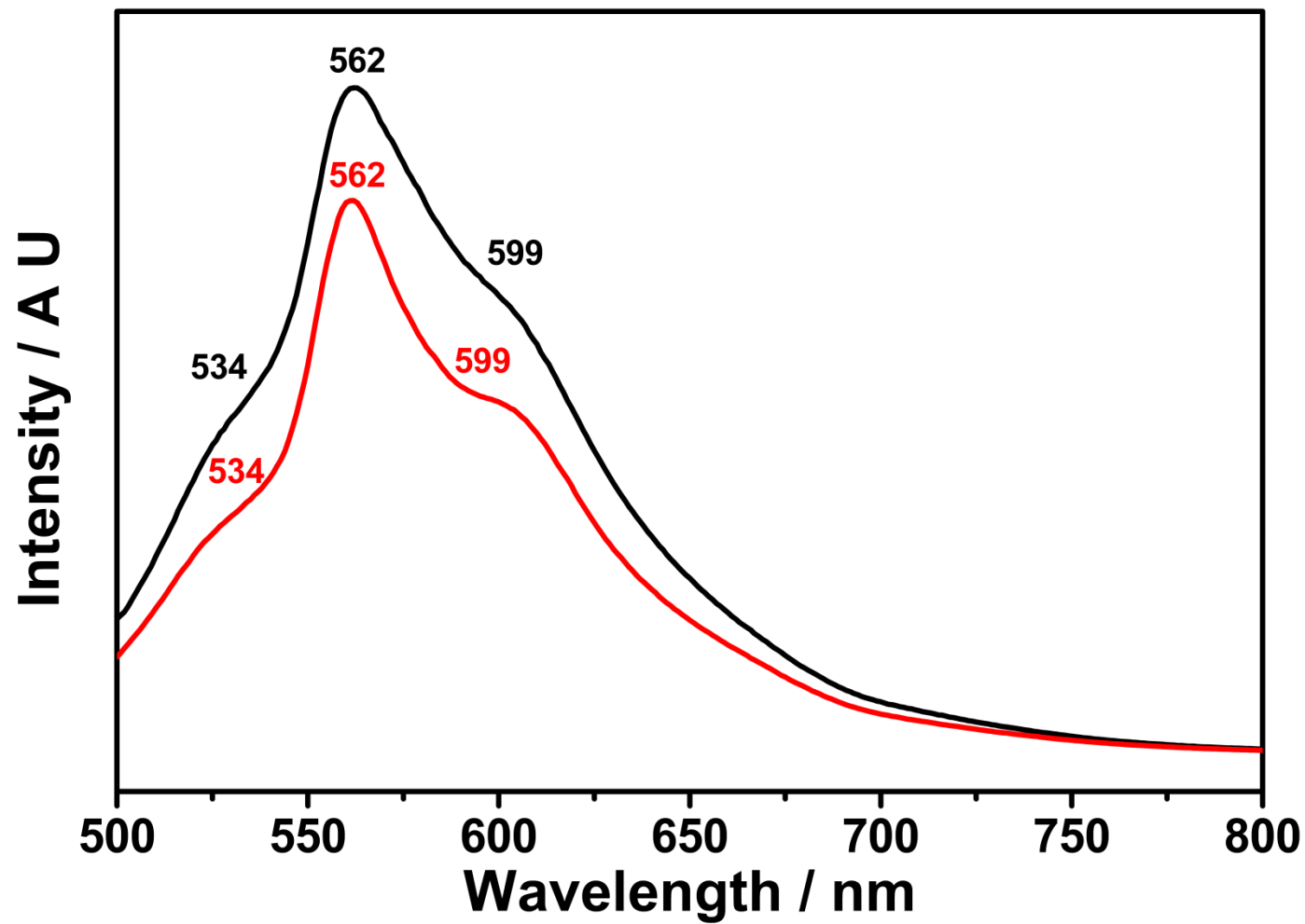


Figure 4.49: Emission Spectrum of TANPI in TCE (— : $C = 1 \times 10^{-5}$ M; — : Microfiltered; $\lambda_{\text{exc}} = 485$ nm)

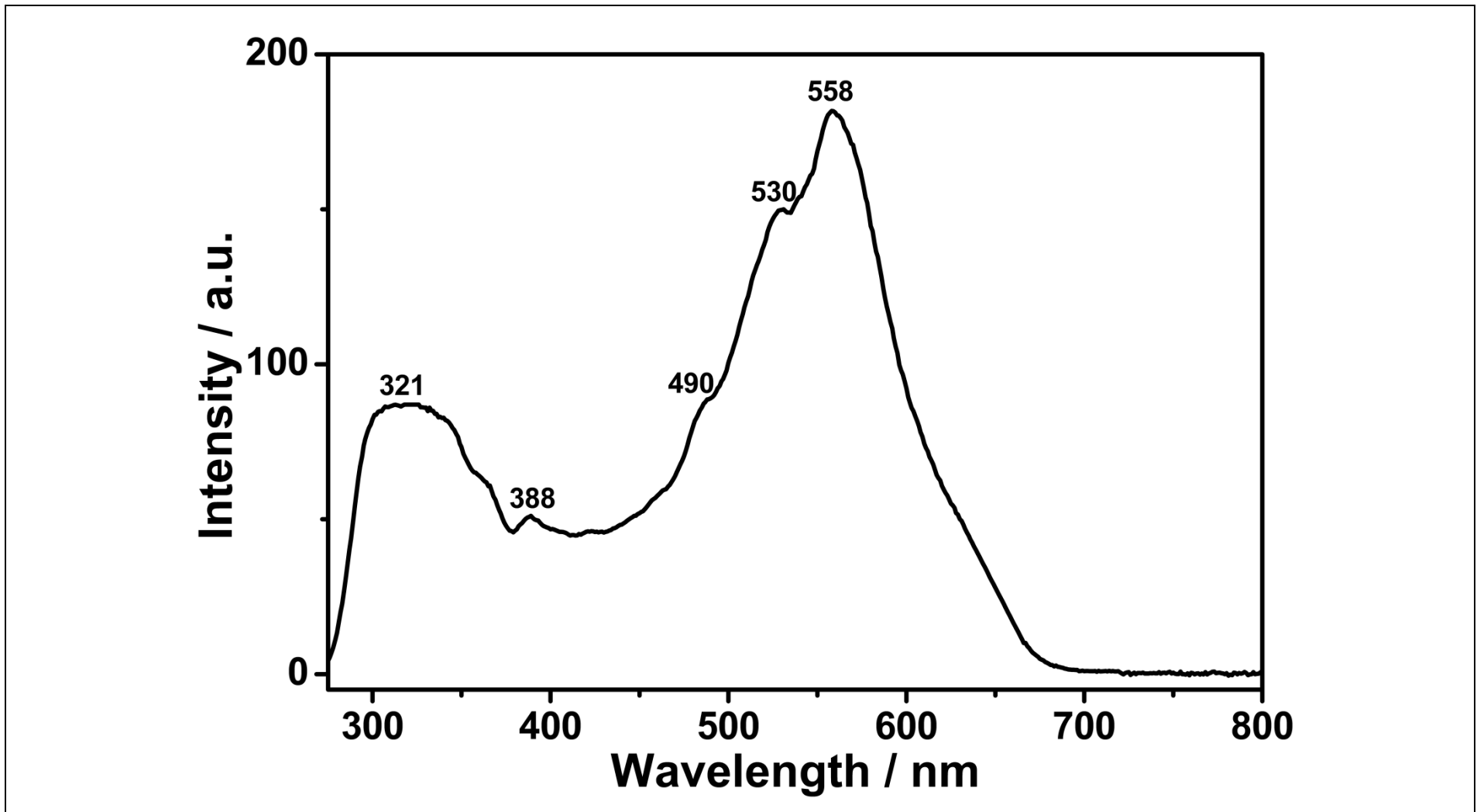


Figure 4.50: Excitation Spectrum of TANPI in TCE ($C = 1 \times 10^{-5} \text{ M}$; $\lambda_{\text{emis}} = 650 \text{ nm}$)

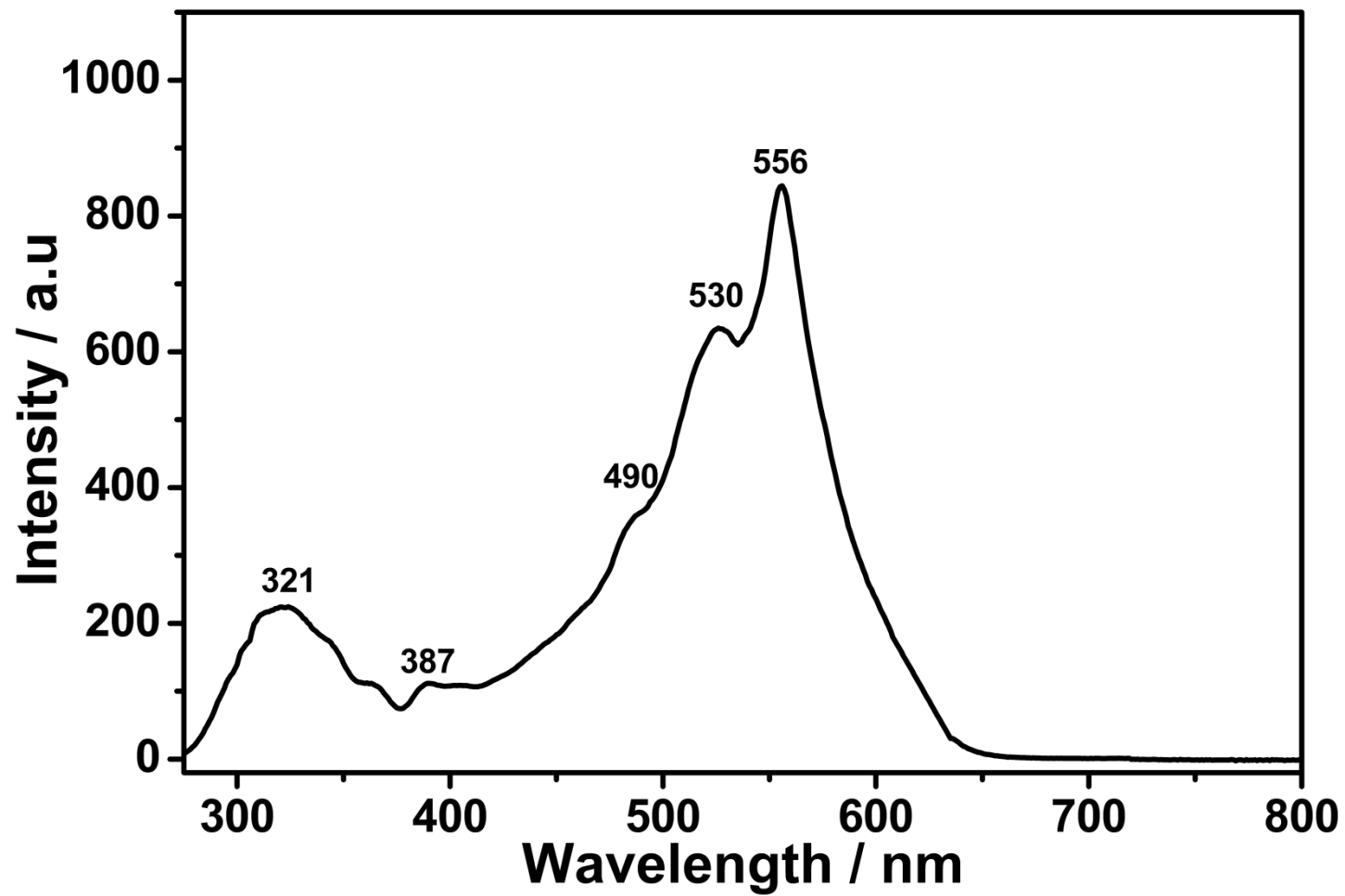


Figure 4.51: Excitation Spectrum of TANPI in TCE (Microfiltered; $\lambda_{\text{emis}} = 650 \text{ nm}$)

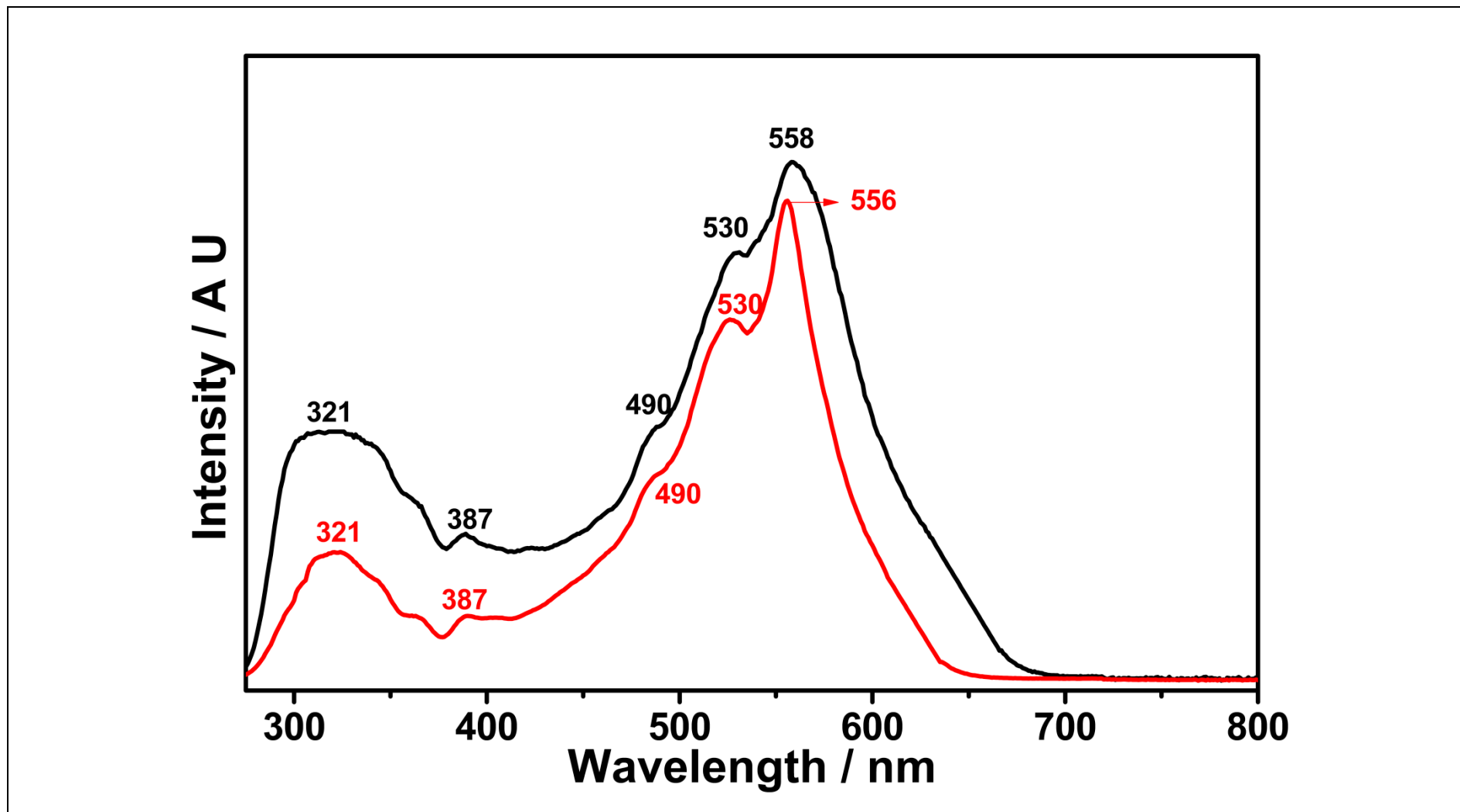


Figure 4.52: Excitation Spectrum of TANPI in TCE (—: $C = 1 \times 10^{-5} \text{ M}$; —: Microfiltered; $\lambda_{\text{emis}} = 650 \text{ nm}$)

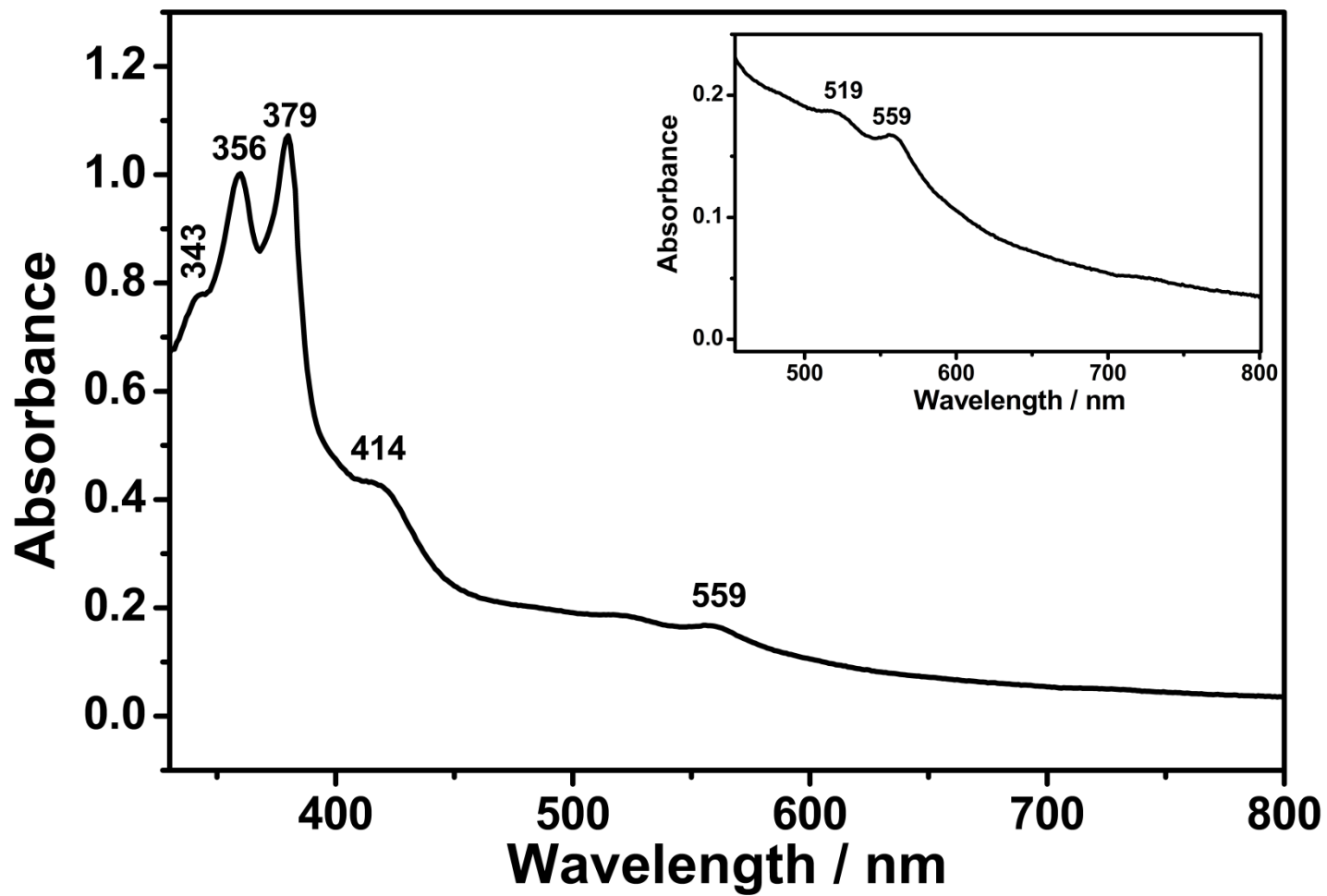


Figure 4.53: Absorption Spectrum of TANPI in Pyridine ($C = 1 \times 10^{-5}$ M, Inset: Enlarged Spectrum, 450-800 nm)

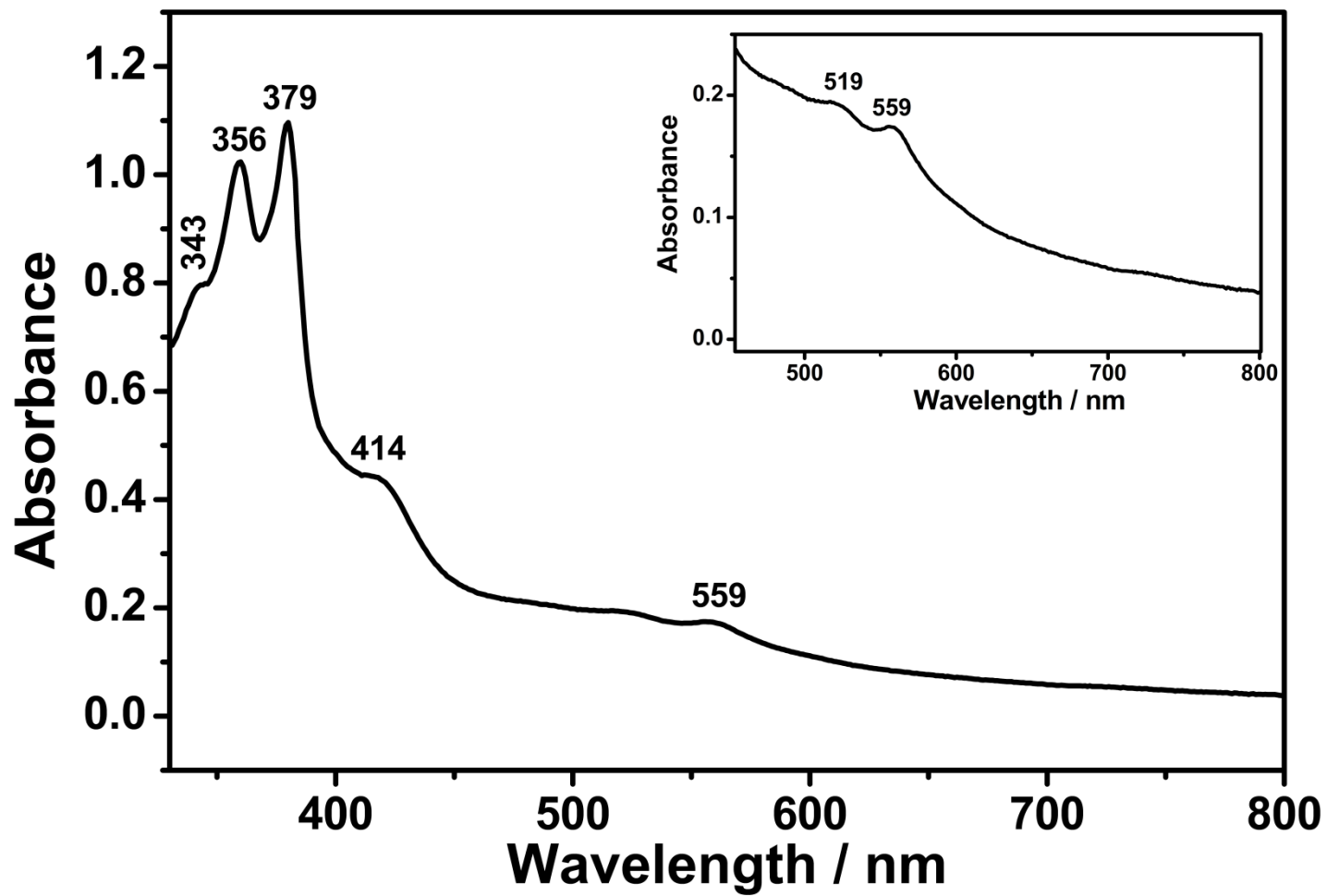


Figure 4.54: Absorption Spectrum of TANPI in Pyridine (Microfiltered, Inset: Enlarged spectrum, 450-800 nm)

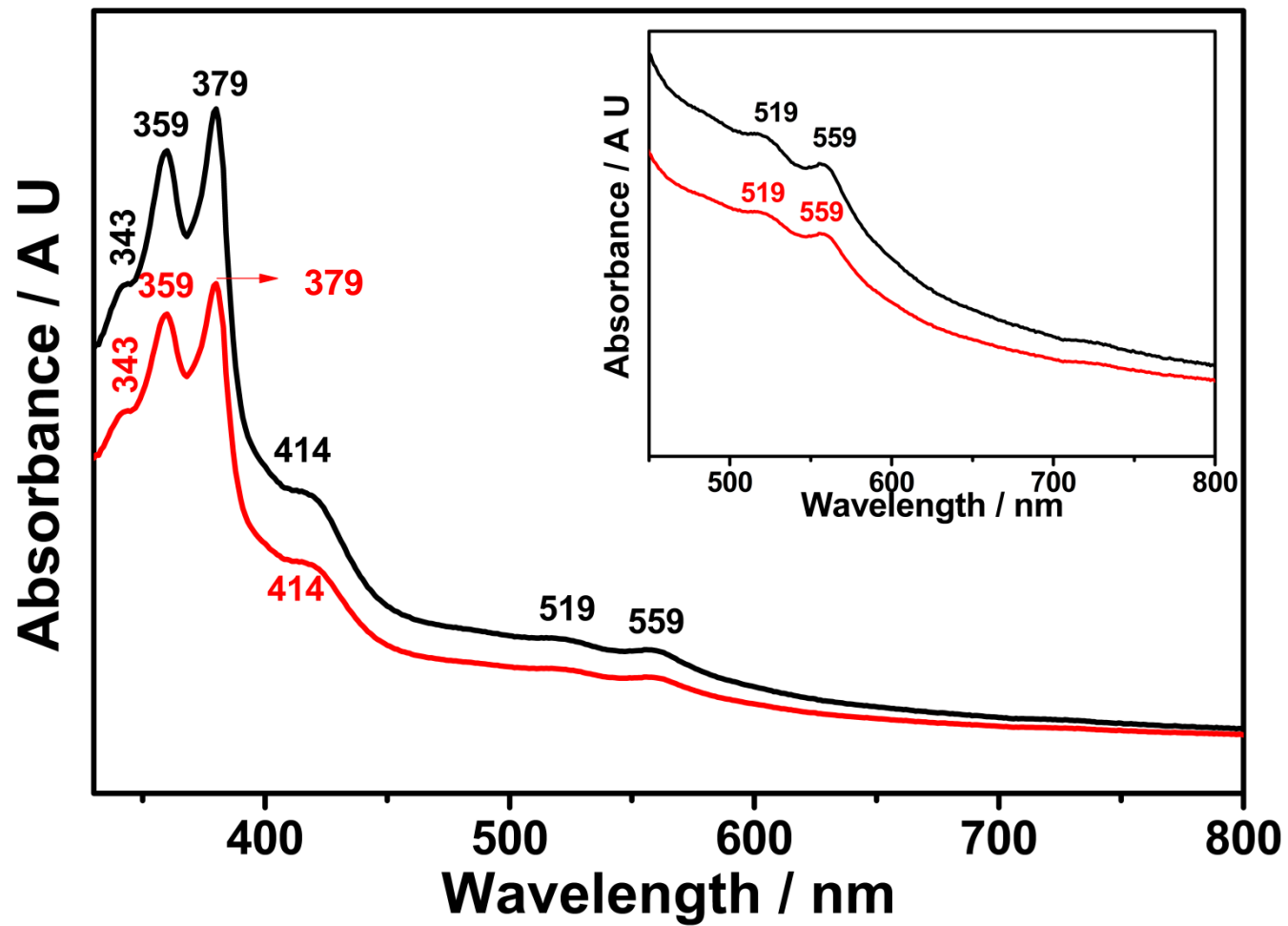


Figure 4.55: Absorption Spectrum of TANPI in Pyridine (—: $C = 1 \times 10^{-5} \text{ M}$; —: Microfiltered; Inset: Enlarged spectrum, 450-800 nm)

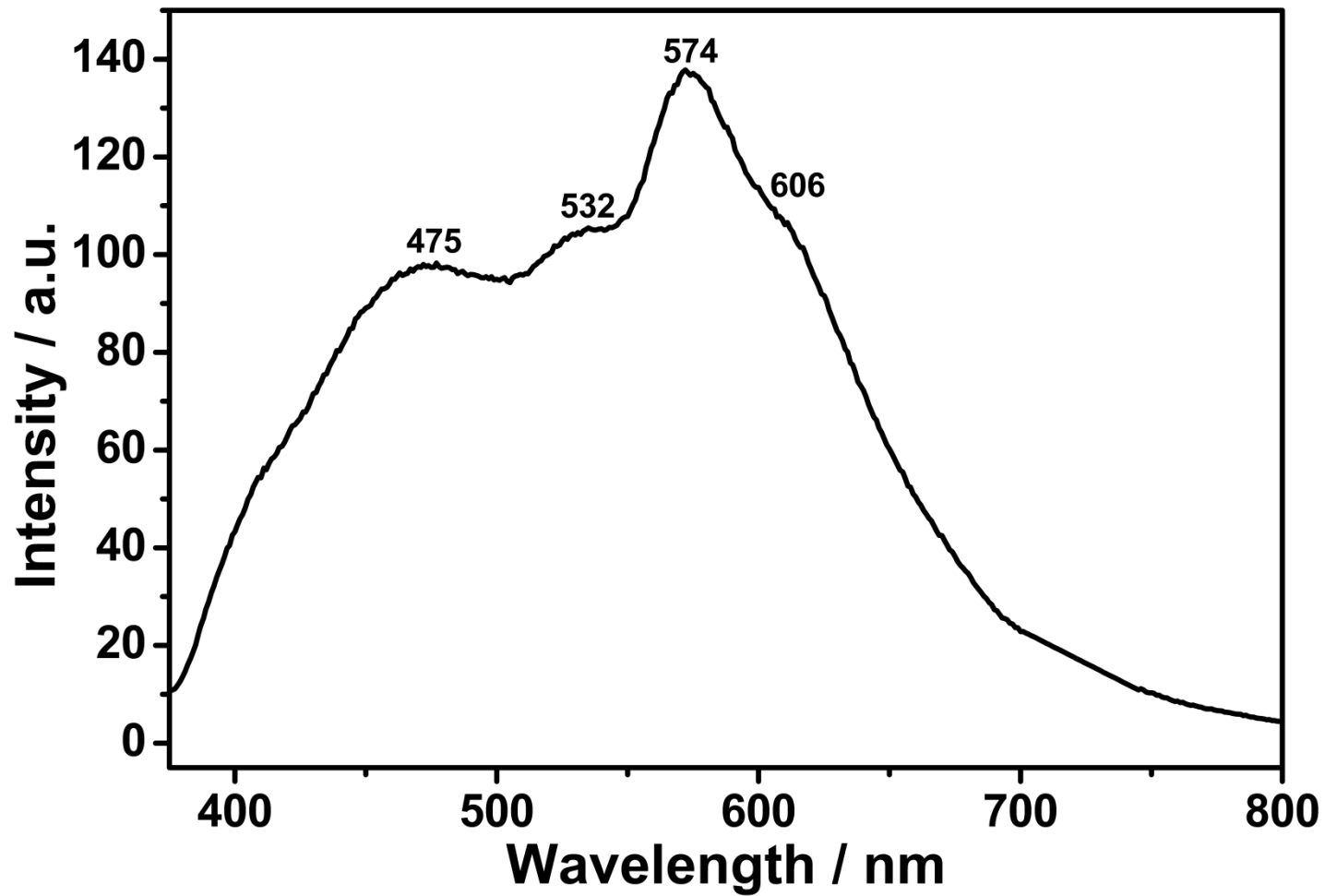


Figure 4.56: Emission Spectrum of TANPI in Pyridine ($C = 1 \times 10^{-5}$ M; $\lambda_{\text{exc}} = 360$ nm)

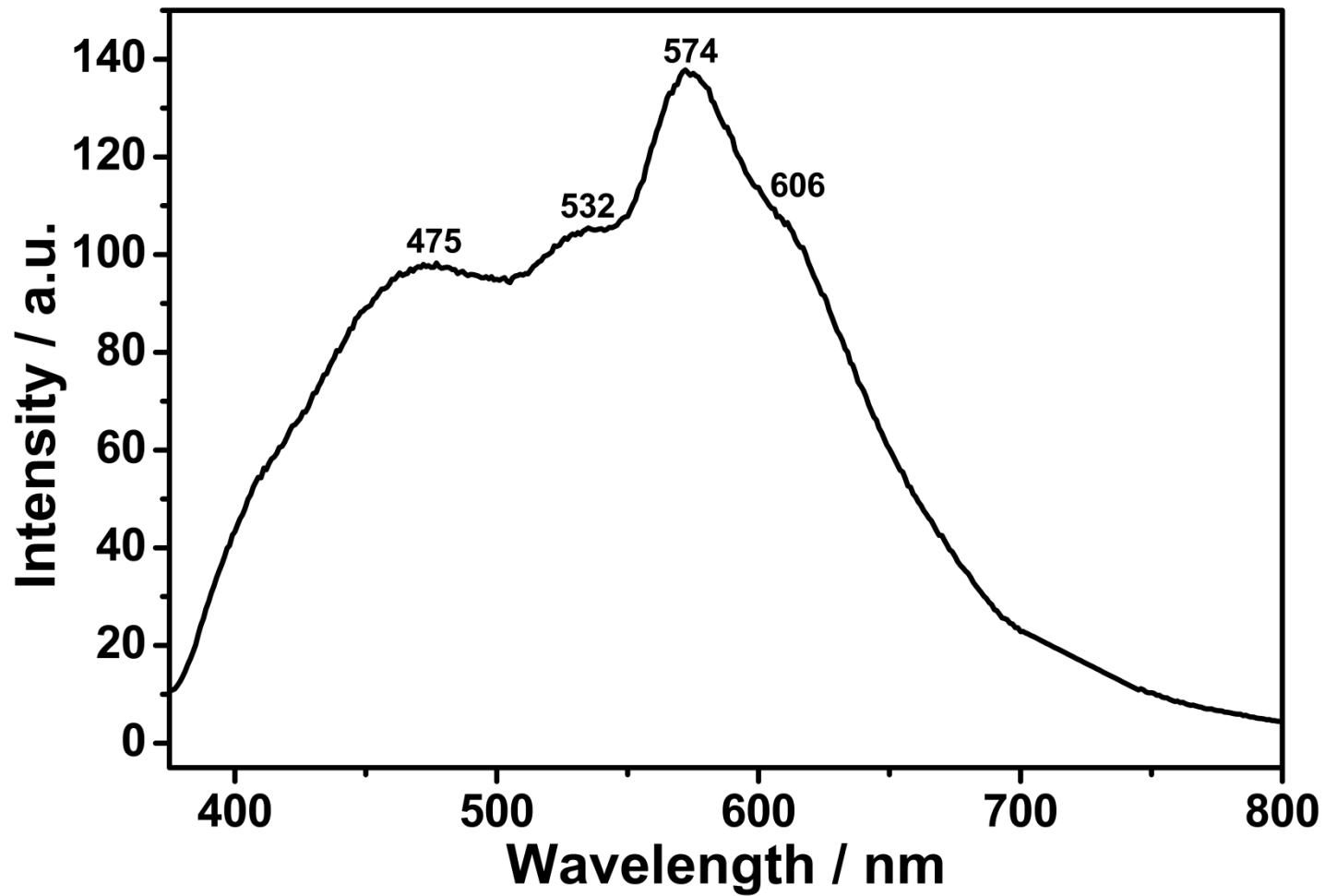


Figure 4.57: Emission Spectrum of TANPI in Pyridine (Microfiltered; $\lambda_{\text{exc}} = 360$ nm)

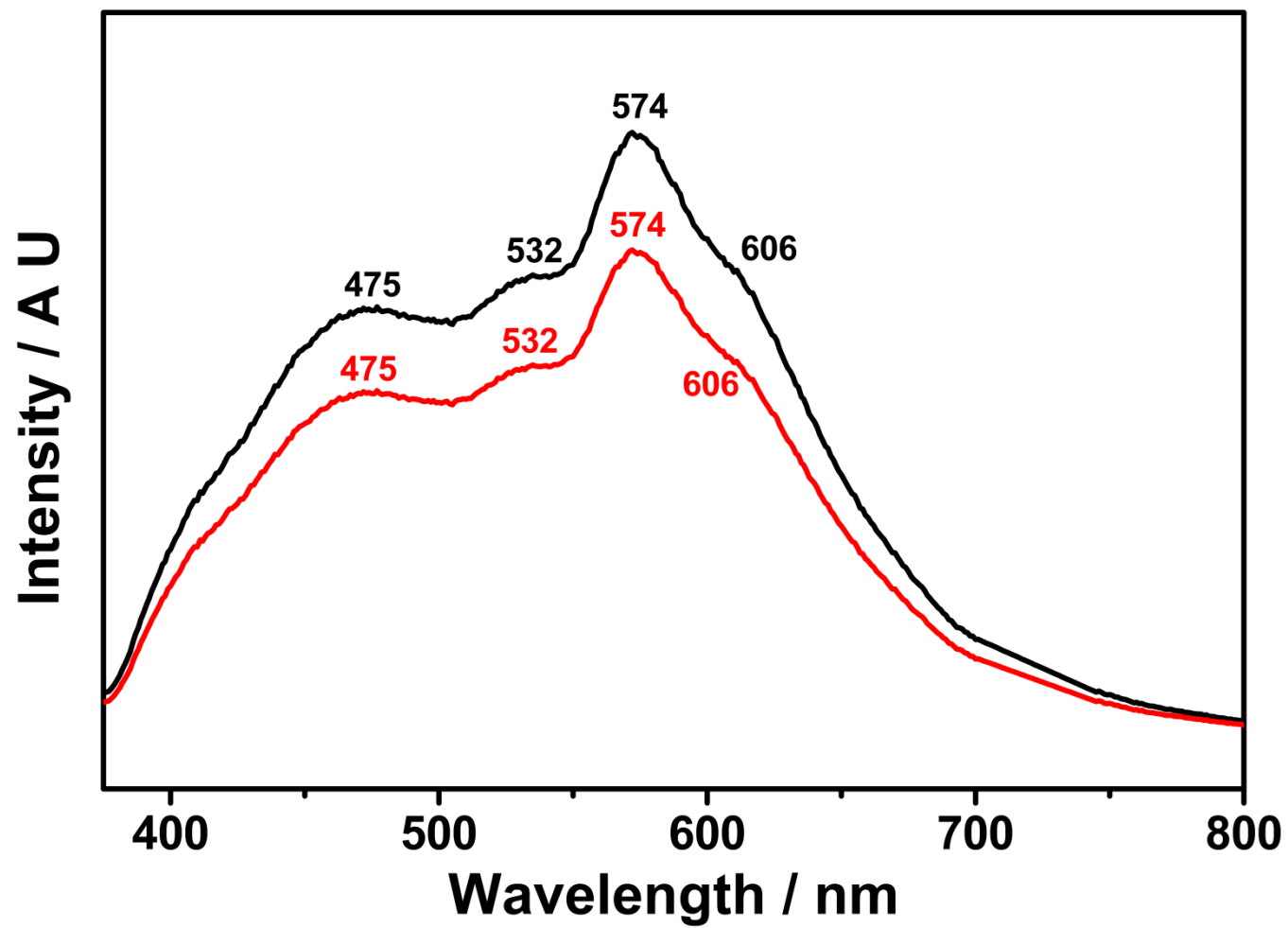


Figure 4.58: Emission Spectrum of TANPI in Pyridine (—: $C = 1 \times 10^{-5} \text{ M}$; —: Microfiltered; $\lambda_{\text{exc}} = 360 \text{ nm}$)

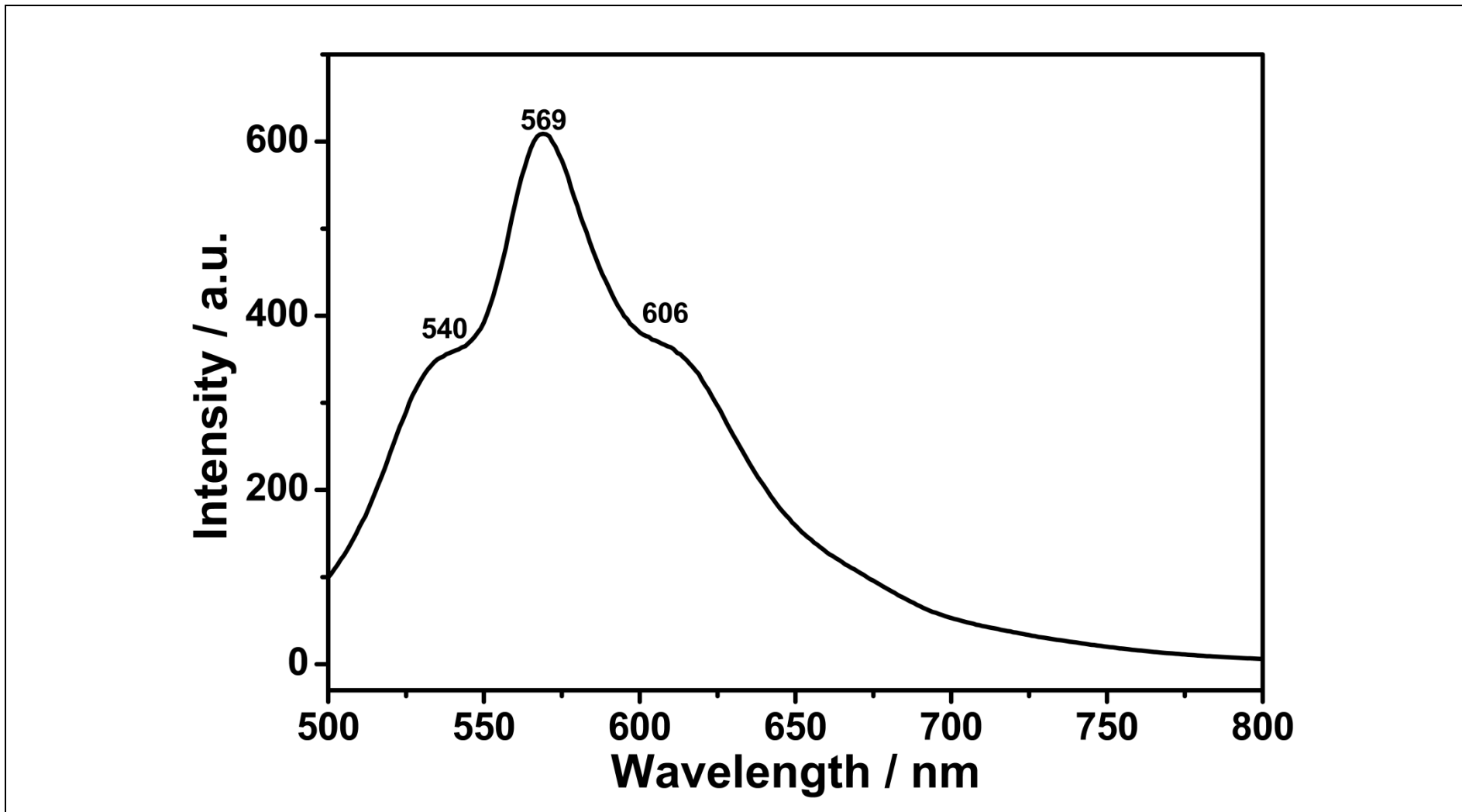


Figure 4.59: Emission Spectrum of TANPI in Pyridine ($C = 1 \times 10^{-5}$ M; $\lambda_{\text{exc}} = 485$ nm)

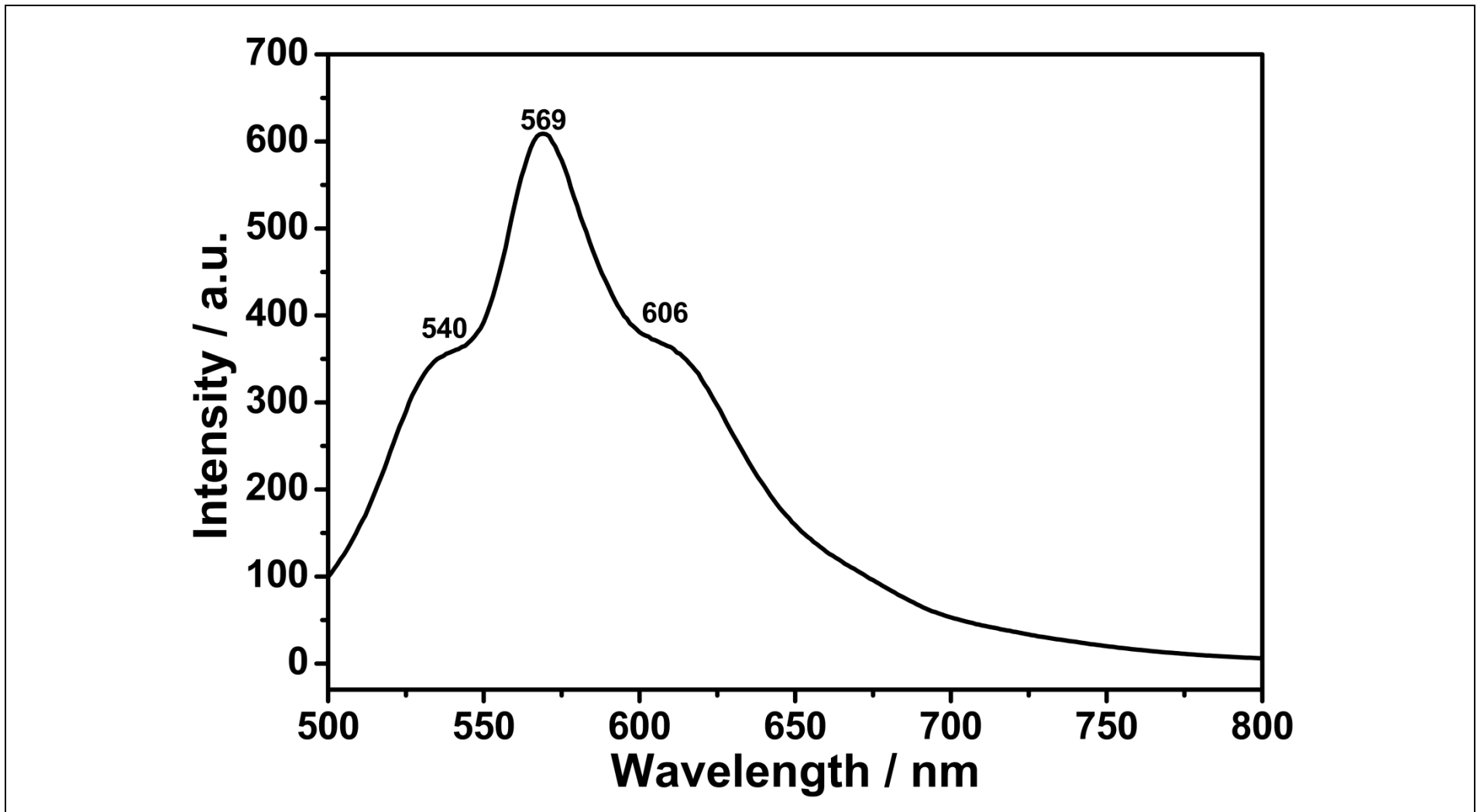


Figure 4.60: Emission Spectrum of TANPI in Pyridine (Microfiltered; $\lambda_{\text{exc}} = 360 \text{ nm}$)

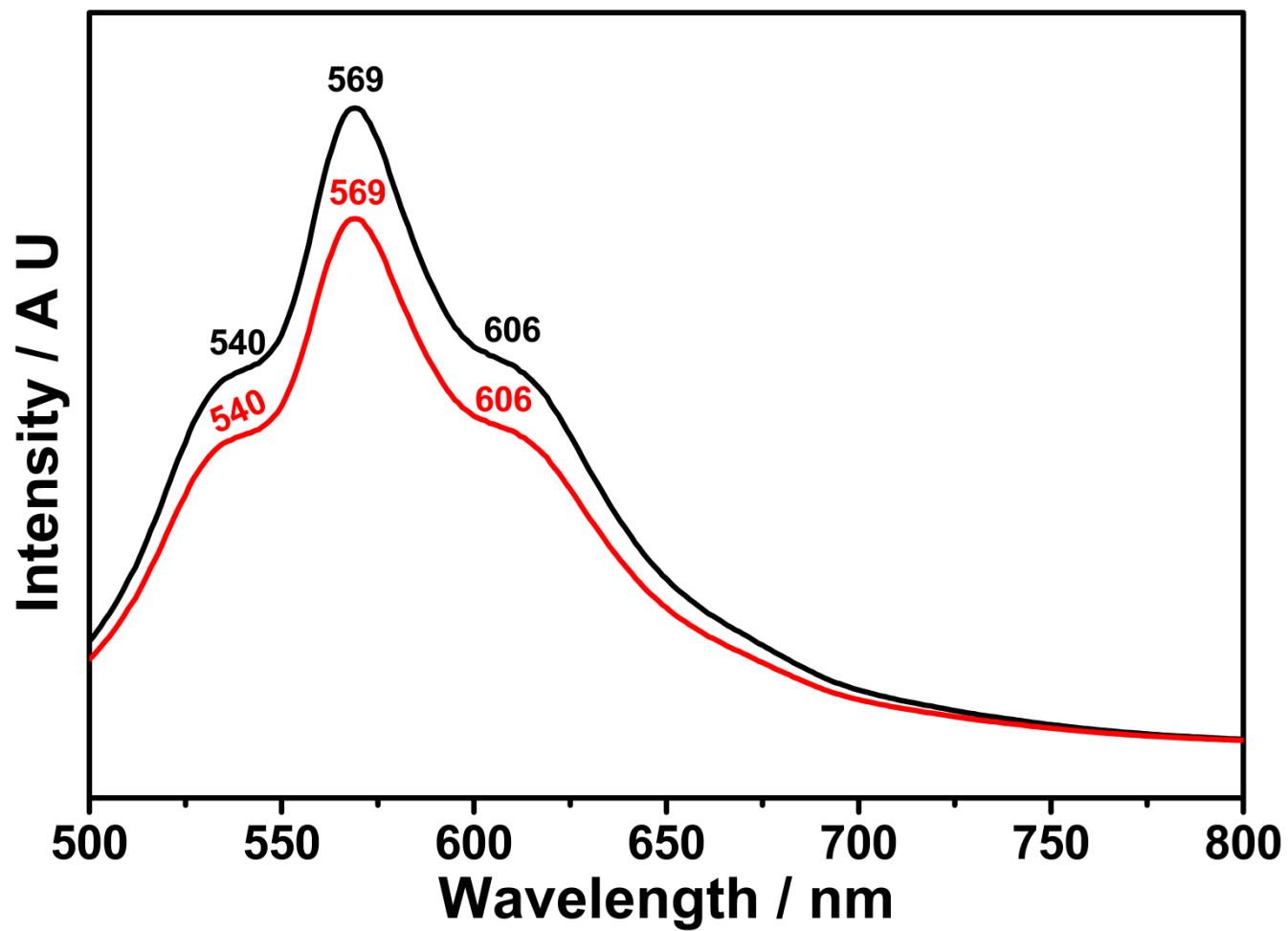


Figure 4.61: Emission Spectrum of TANPI in Pyridine (—: $C = 1 \times 10^{-5}$ M; —: Microfiltered; $\lambda_{\text{exc}} = 485$ nm)

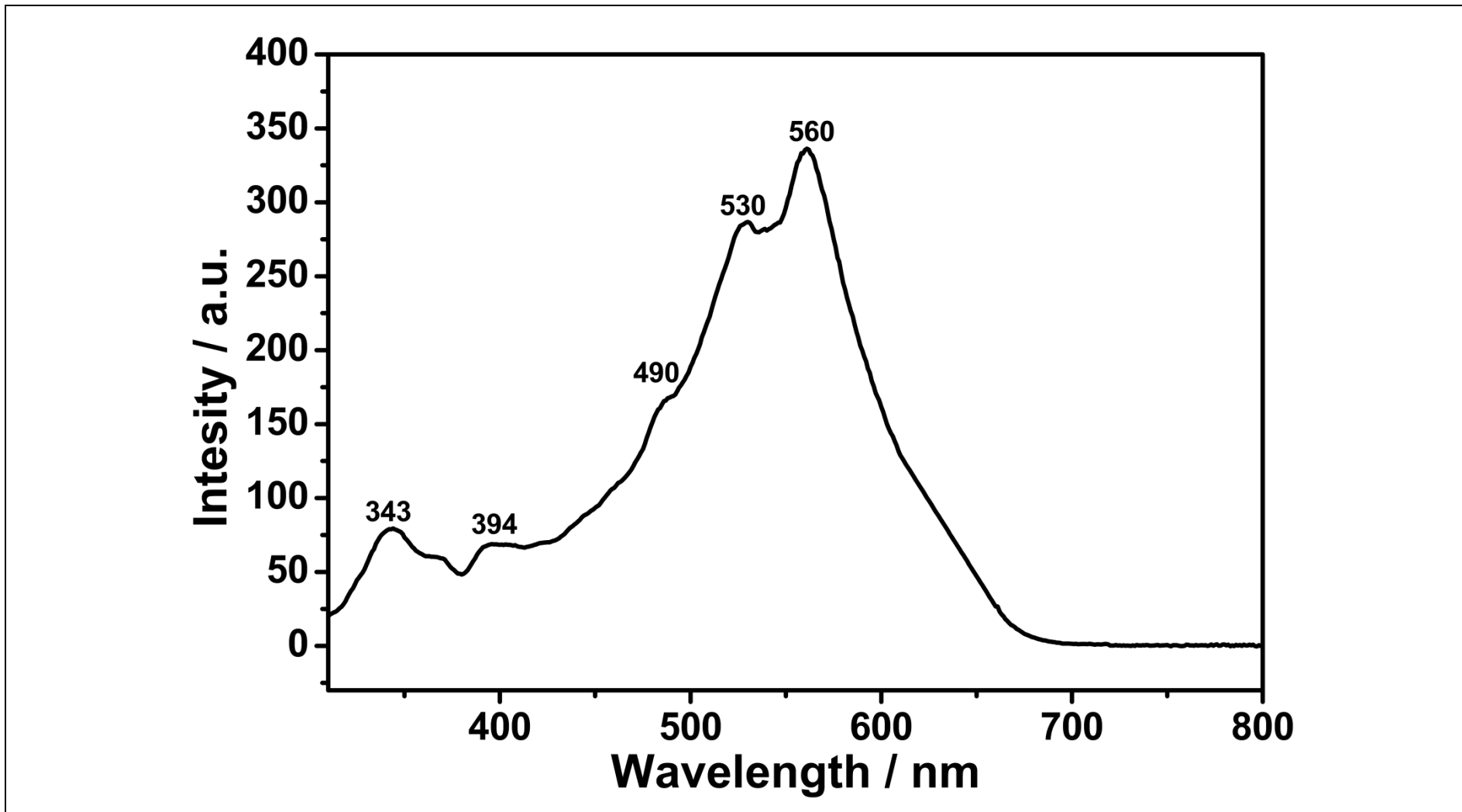


Figure 4.62: Excitation Spectrum of TANPI in Pyridine ($C = 1 \times 10^{-5}$ M; $\lambda_{\text{emis}} = 650$ nm)

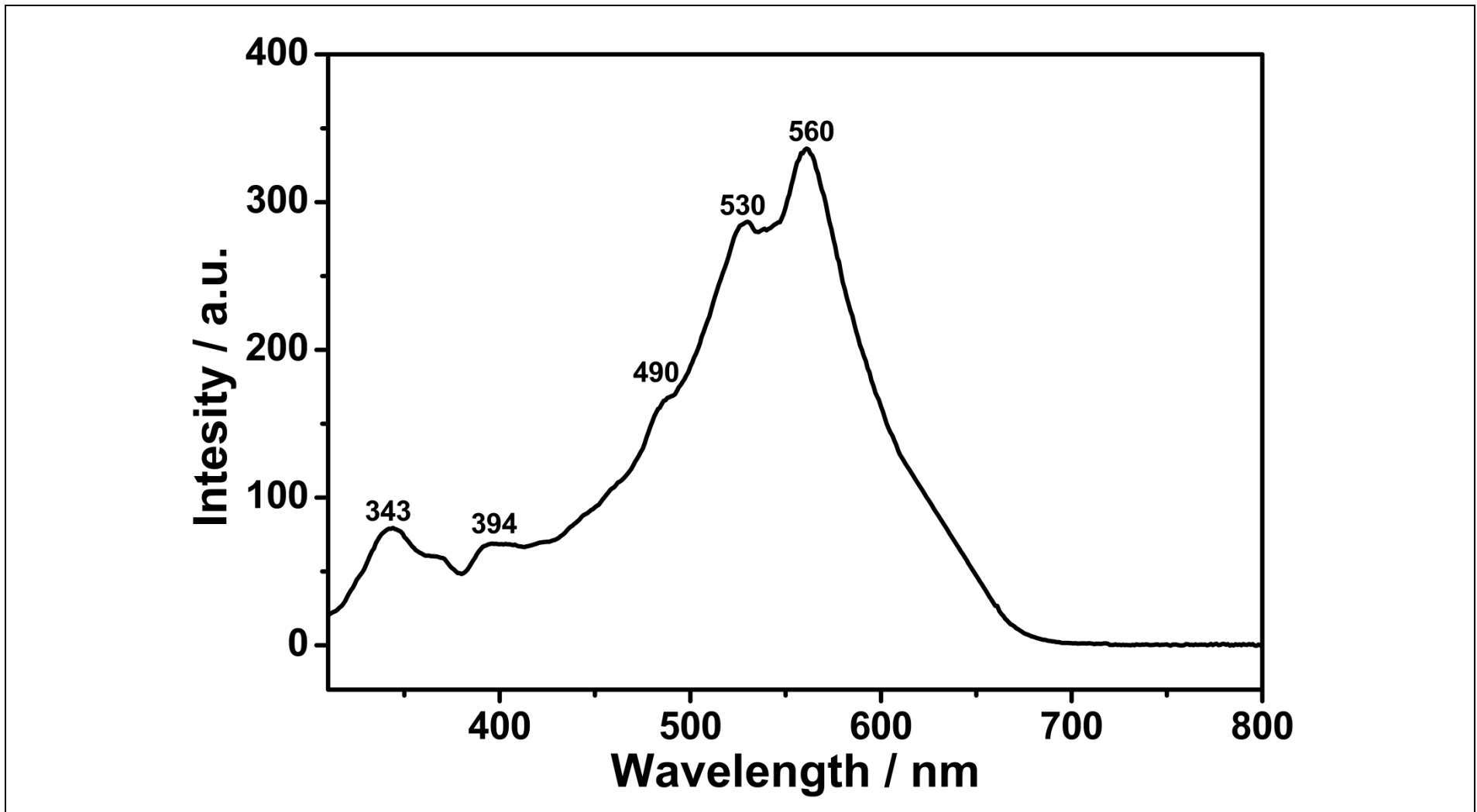


Figure 4.63: Excitation Spectrum of TANPI in Pyridine (Microfiltered; $\lambda_{\text{emis}} = 650 \text{ nm}$)

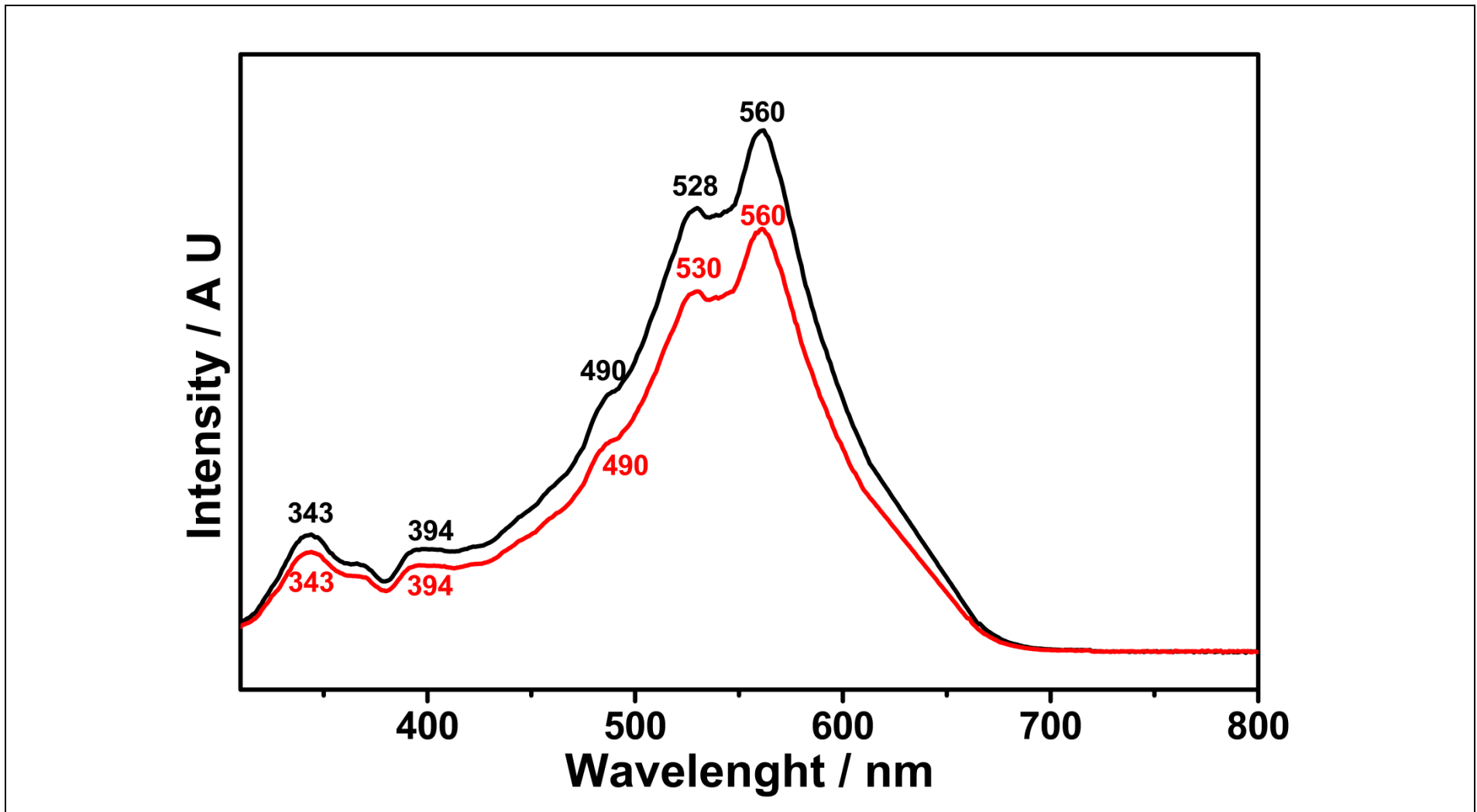


Figure 4.64: Excitation Spectrum of TANPI in Pyridine (— : $C = 1 \times 10^{-5}$ M; — : Microfiltered; $\lambda_{\text{emis}} = 650$ nm)

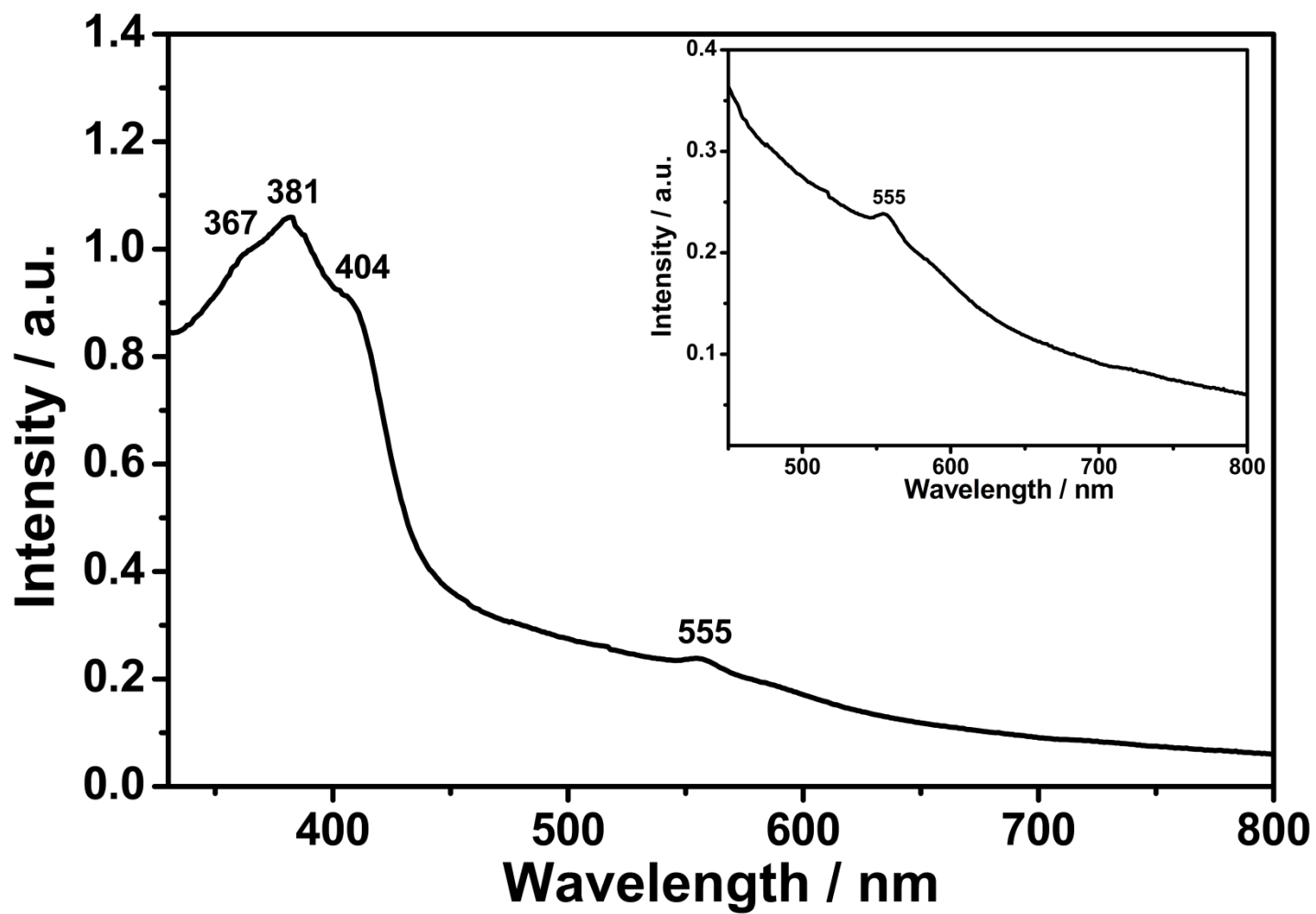


Figure 4.65: Absorption Spectrum of TANPI in M-cresol ($C = 1 \times 10^{-5} \text{M}$, Inset: Enlarged Spectrum, 450-800 nm)

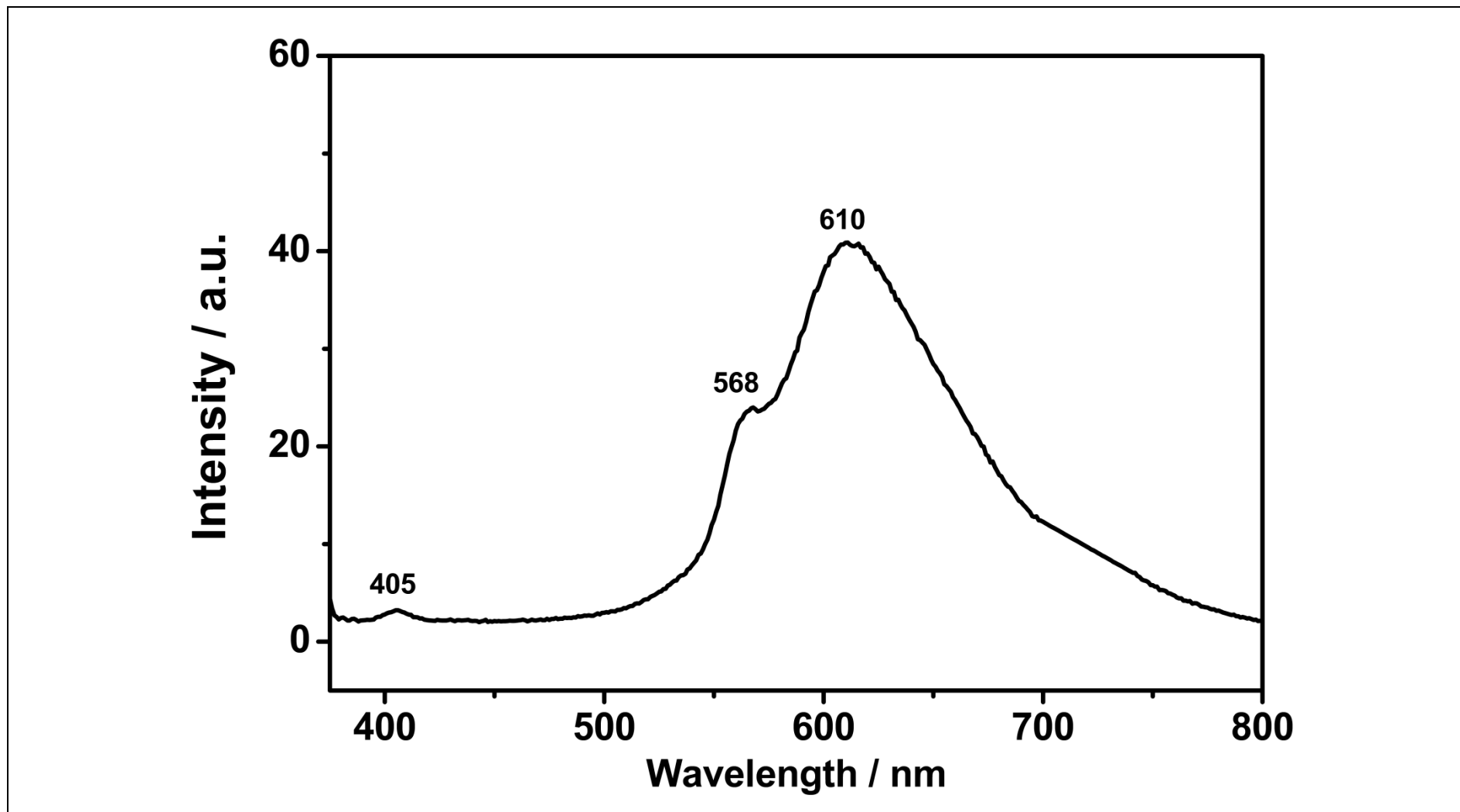


Figure 4.66: Emission Spectrum of TANPI in M-cresol ($C = 1 \times 10^{-5}$ M; $\lambda_{\text{exc}} = 360$ nm)

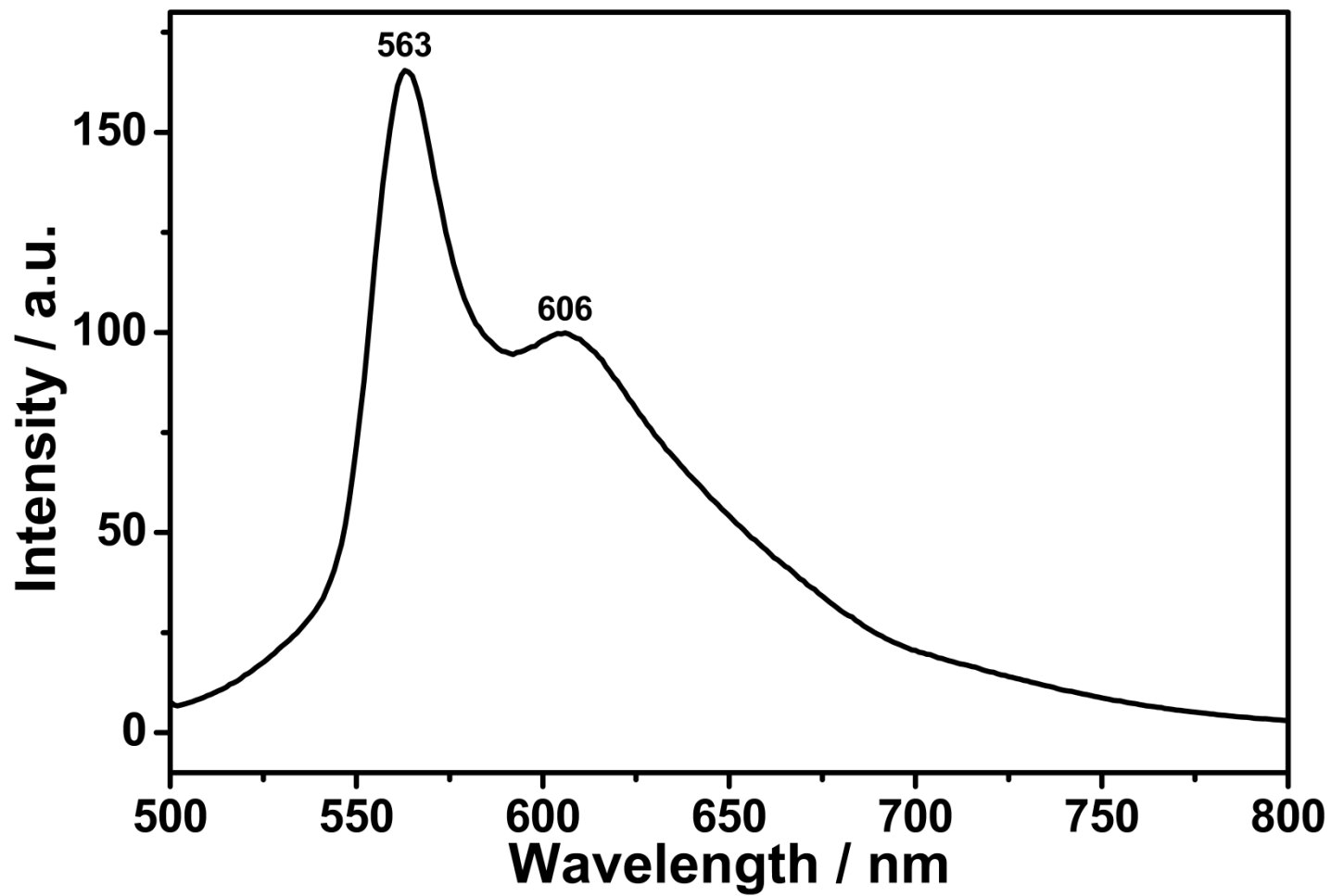


Figure 4.67: Emission Spectrum of TANPI in M-cresol ($C=1\times 10^{-5}$ M; $\lambda_{\text{exc}}=485$ nm)

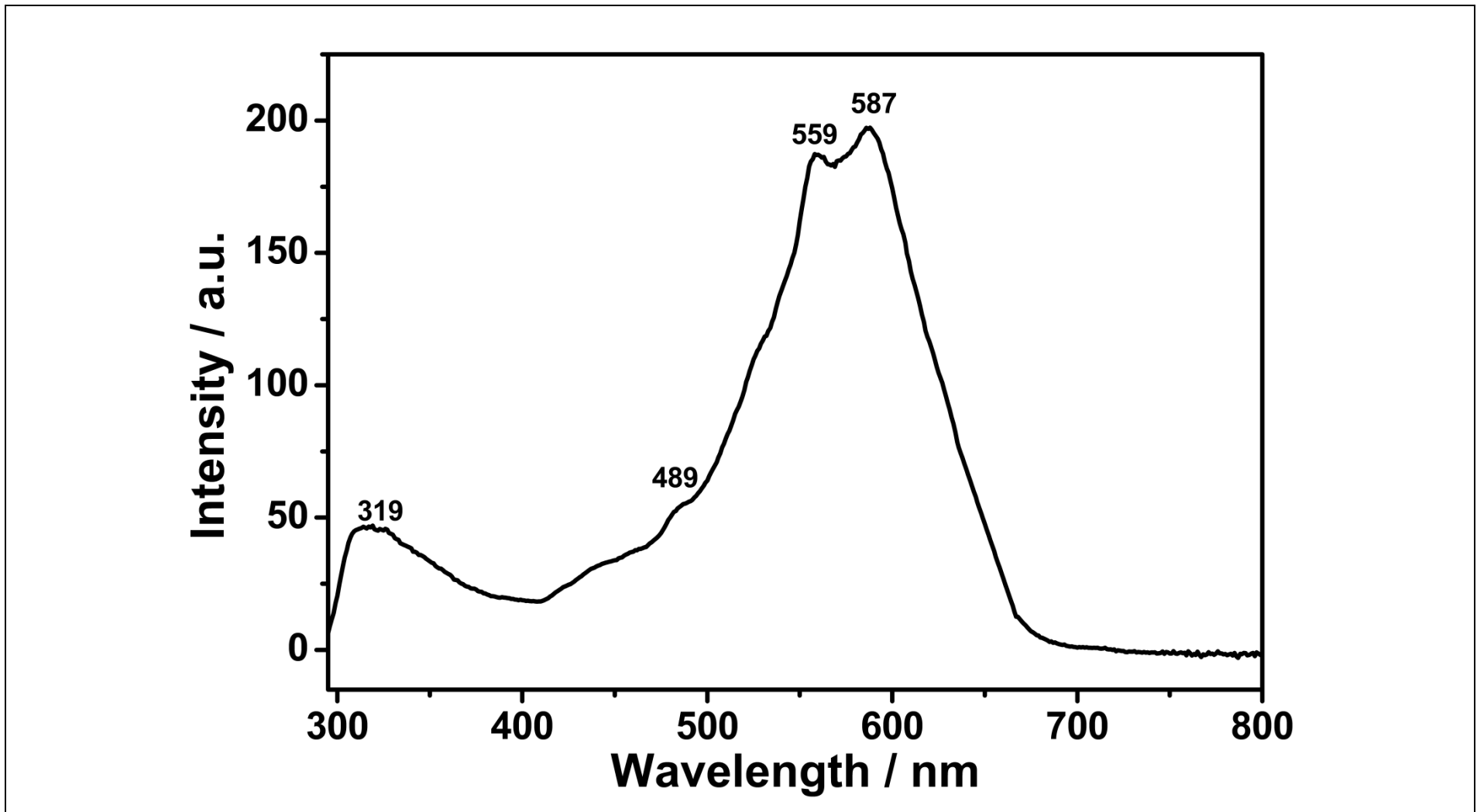


Figure 4.68: Excitation Spectrum of TANPI in M-cresol ($C = 1 \times 10^{-5}$ M; $\lambda_{\text{emis}} = 650$ nm)

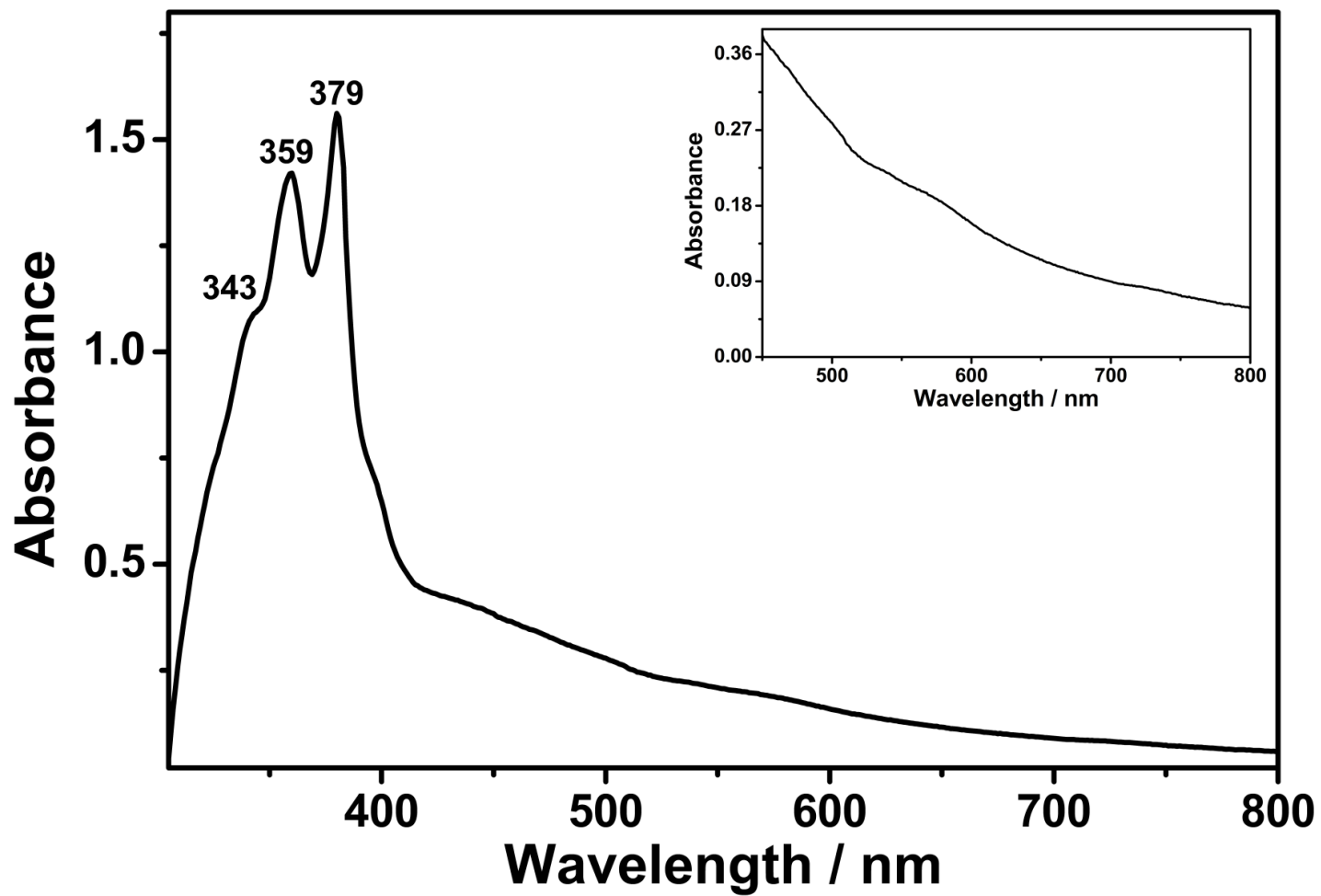


Figure 4.69: Absorption Spectrum of TANPI in TFA ($C = 1 \times 10^{-5}$ M, Inset: Enlarged Spectrum, 450-800 nm)

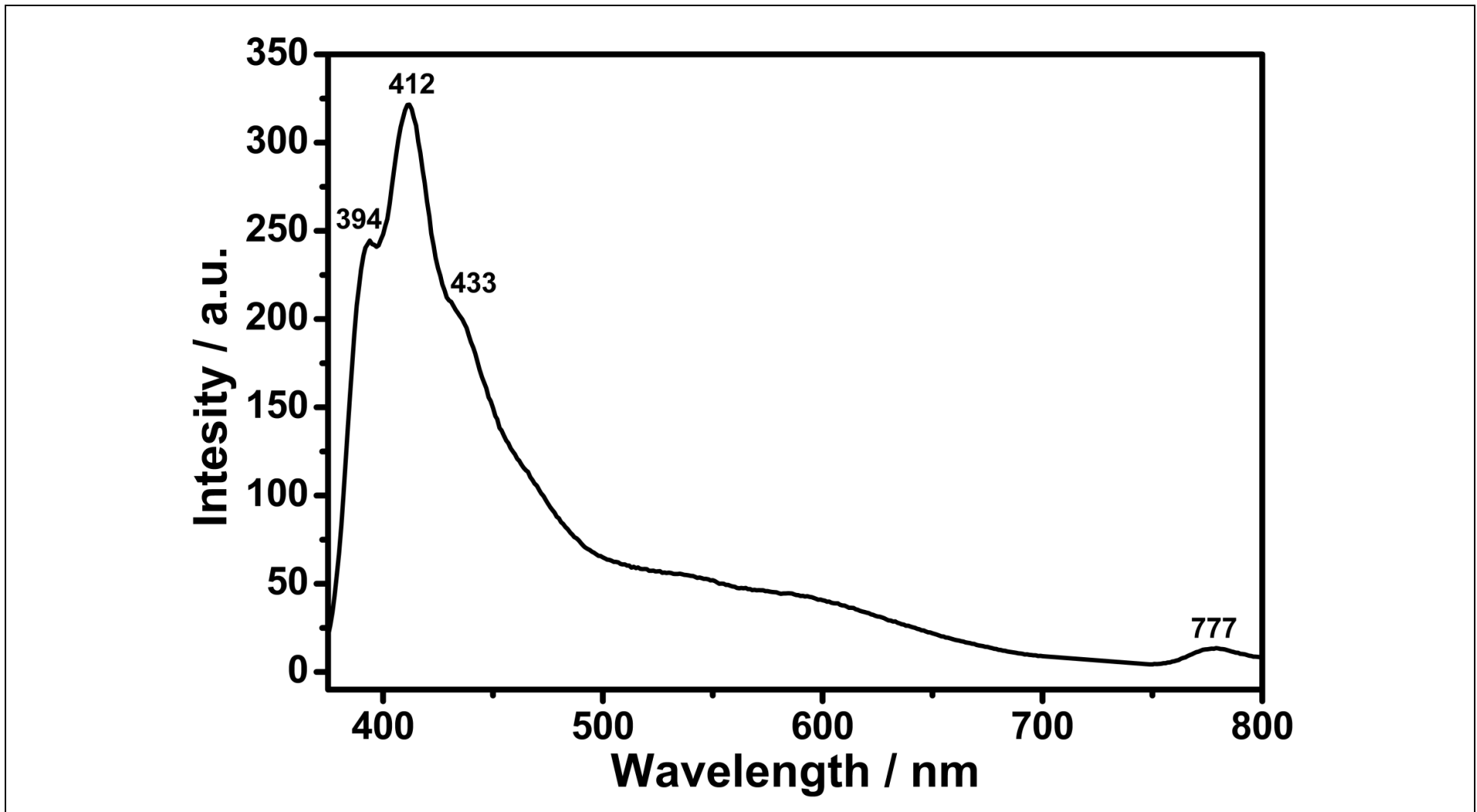
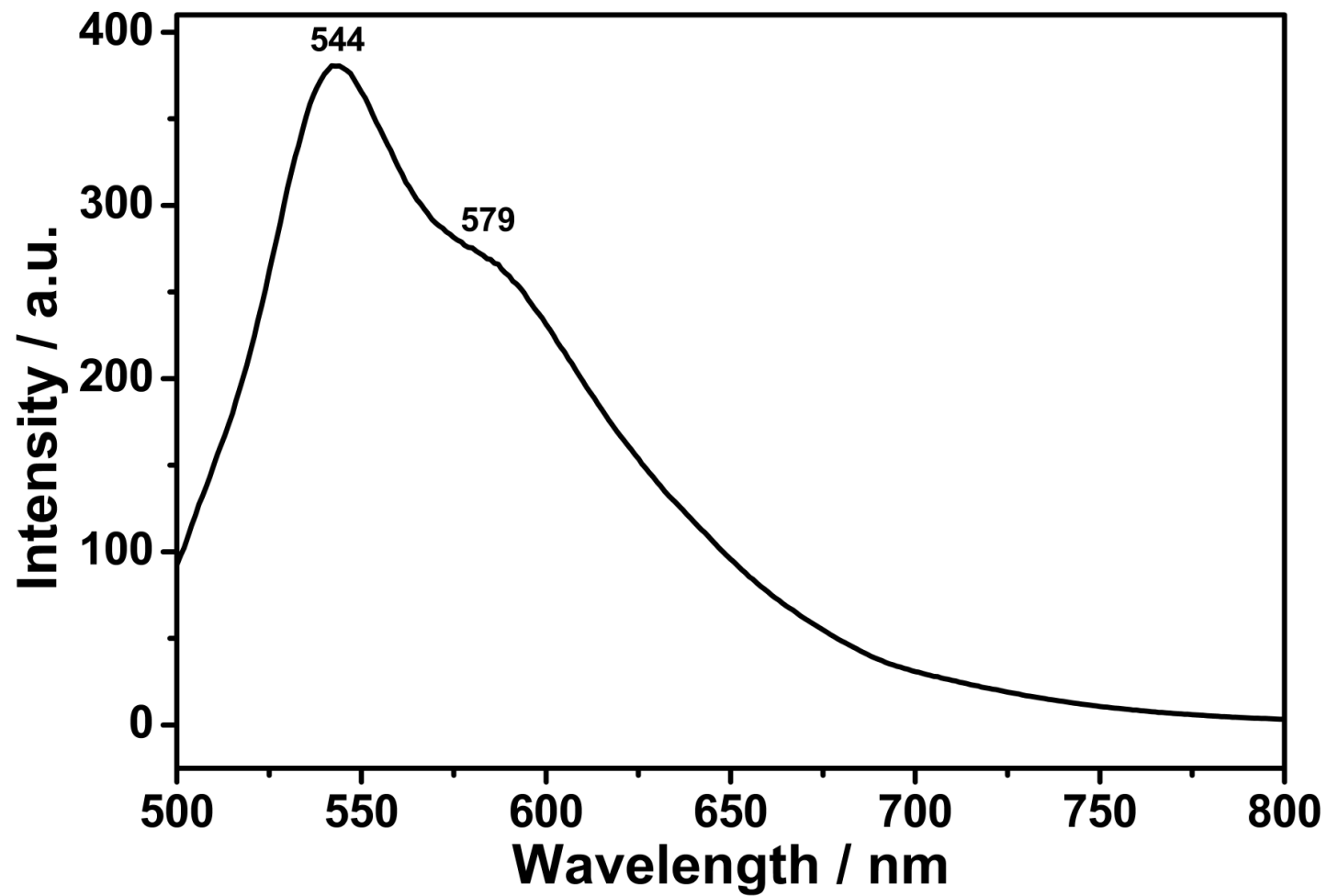


Figure 4.70: Emission Spectrum of TANPI in TFA ($C = 1 \times 10^{-5}$ M; $\lambda_{\text{exc}} = 360$ nm)



4.71: Emission Spectrum of TANPI in TFA ($C = 1 \times 10^{-5}$ M; $\lambda_{\text{exc}} = 485$ nm)

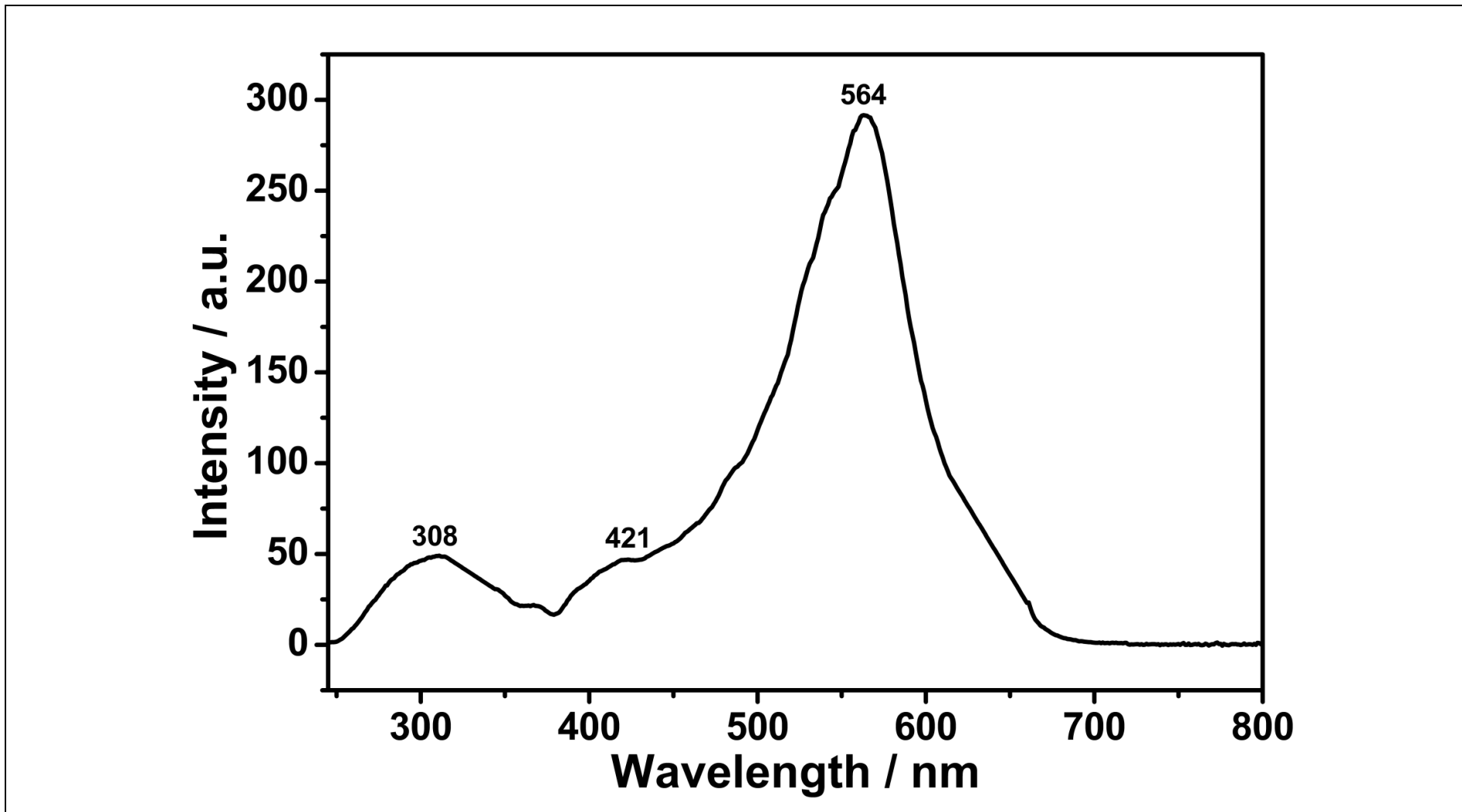


Figure 4.72: Excitation spectrum of TANPI in TFA ($C = 1 \times 10^{-5}$ M; $\lambda_{\text{emis}} = 650$ nm)

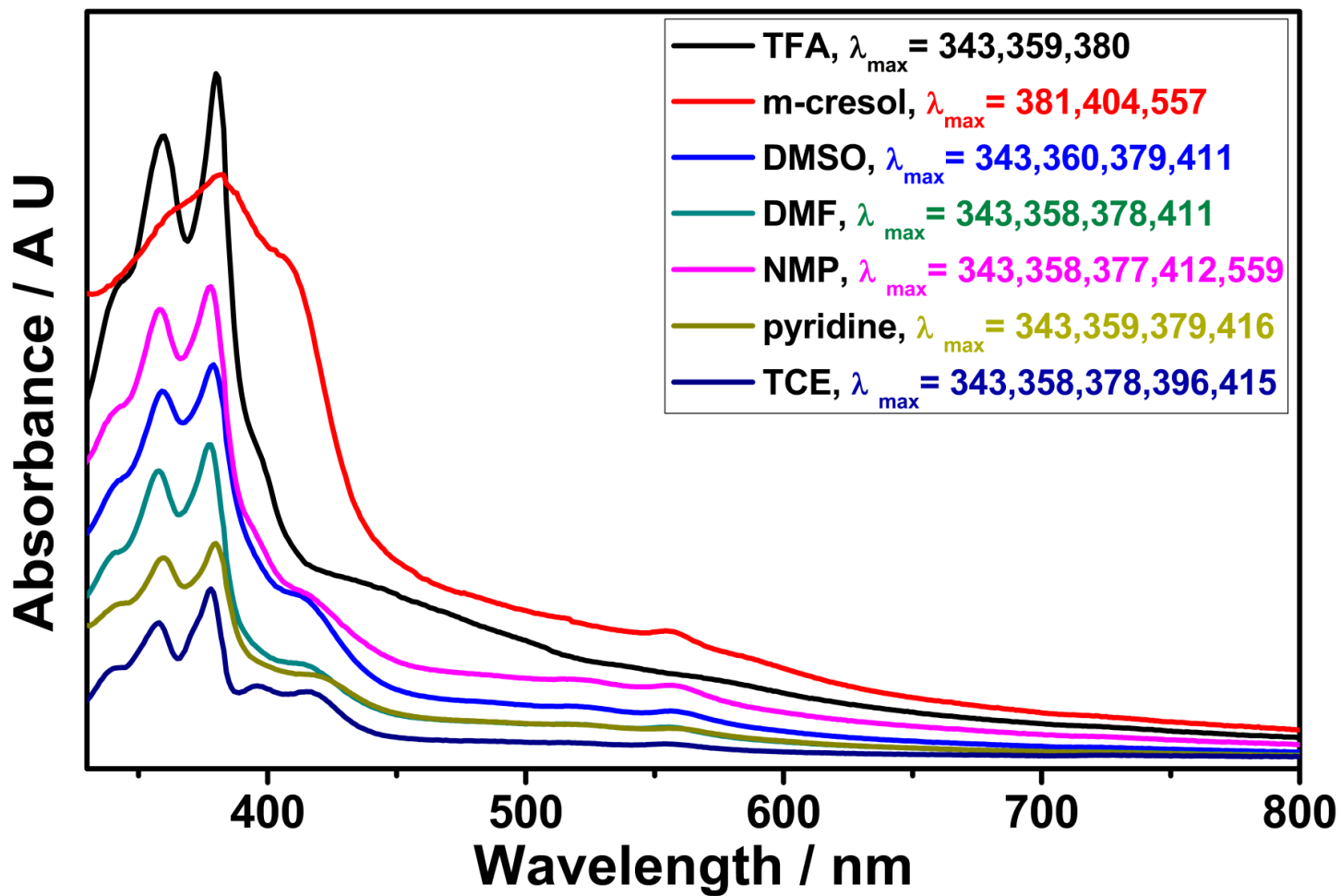


Figure 4.73: Absorption Spectrum of TANPI in TFA, M-cresol, DMSO, DMF, NMP, Pyridine, and TCE ($C = 1 \times 10^{-5} M$)

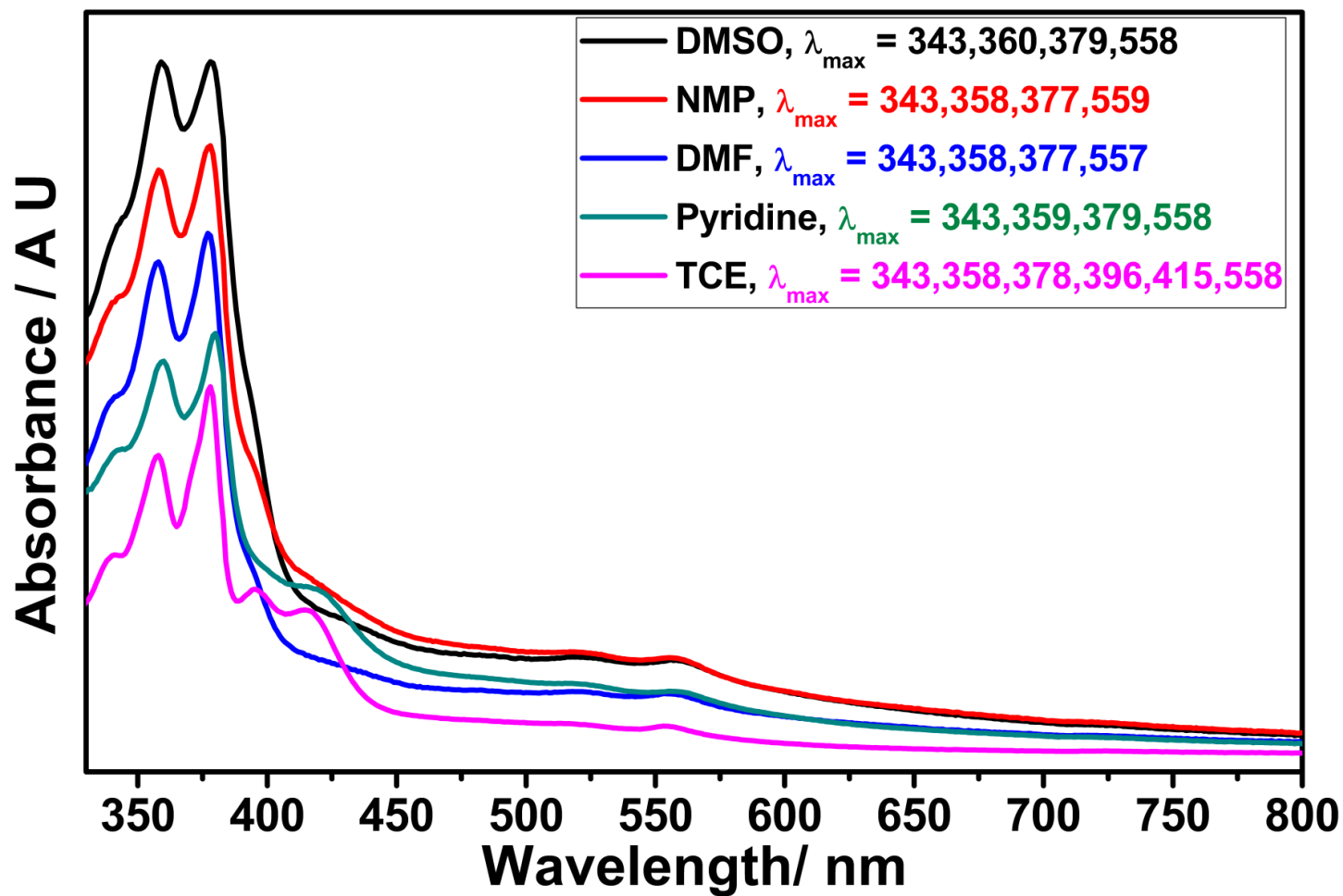


Figure 4.74: Absorption Spectrum of TANPI in DMSO, DMF, NMP, Pyridine, and TCE (Microfiltered)

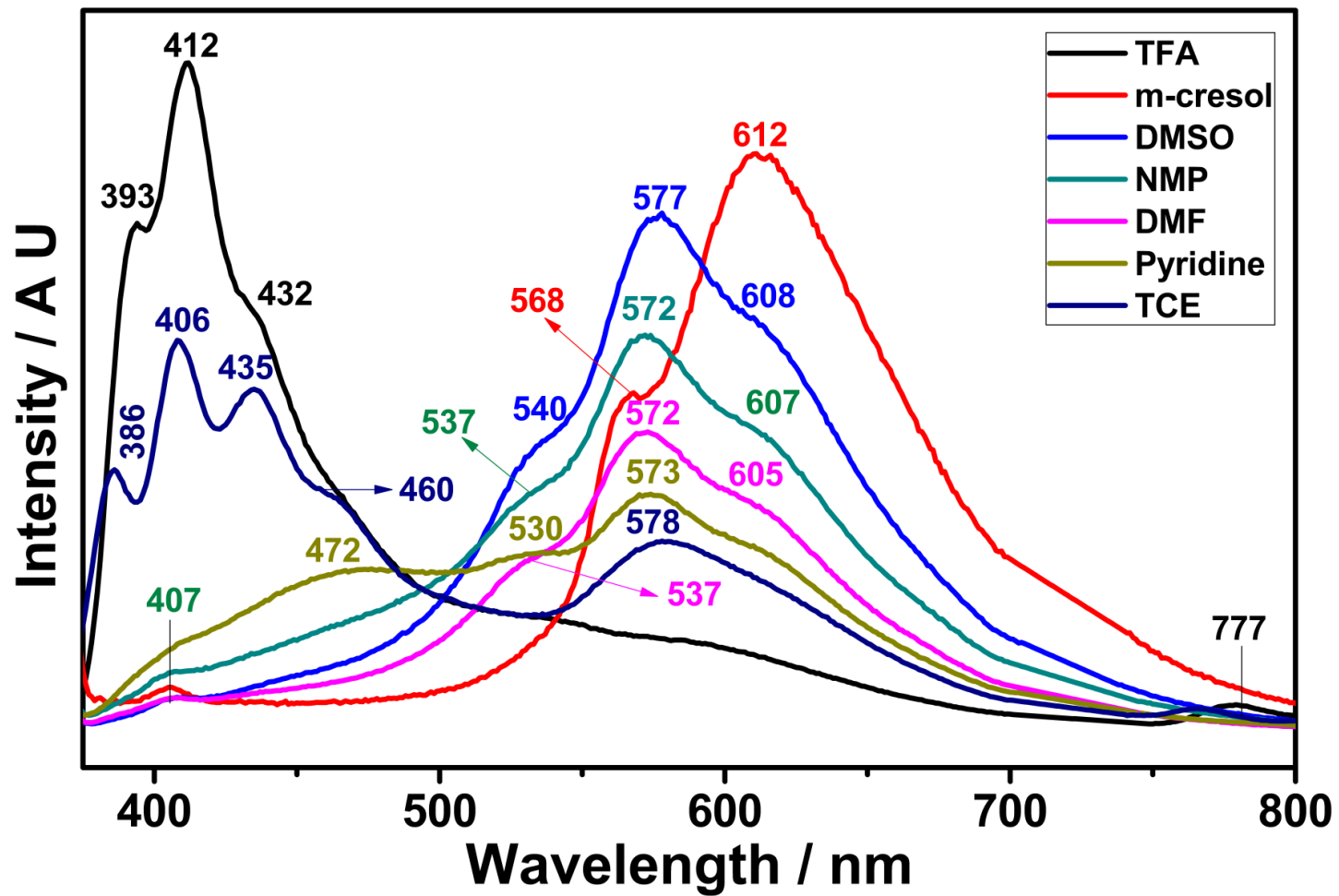


Figure 4.75: Emission Spectrum of TANPI in TFA, M-cresol, DMSO, DMF, NMP, Pyridine, and TCE ($C = 1 \times 10^{-5}$ M; $\lambda_{\text{exc}} = 360$ nm)

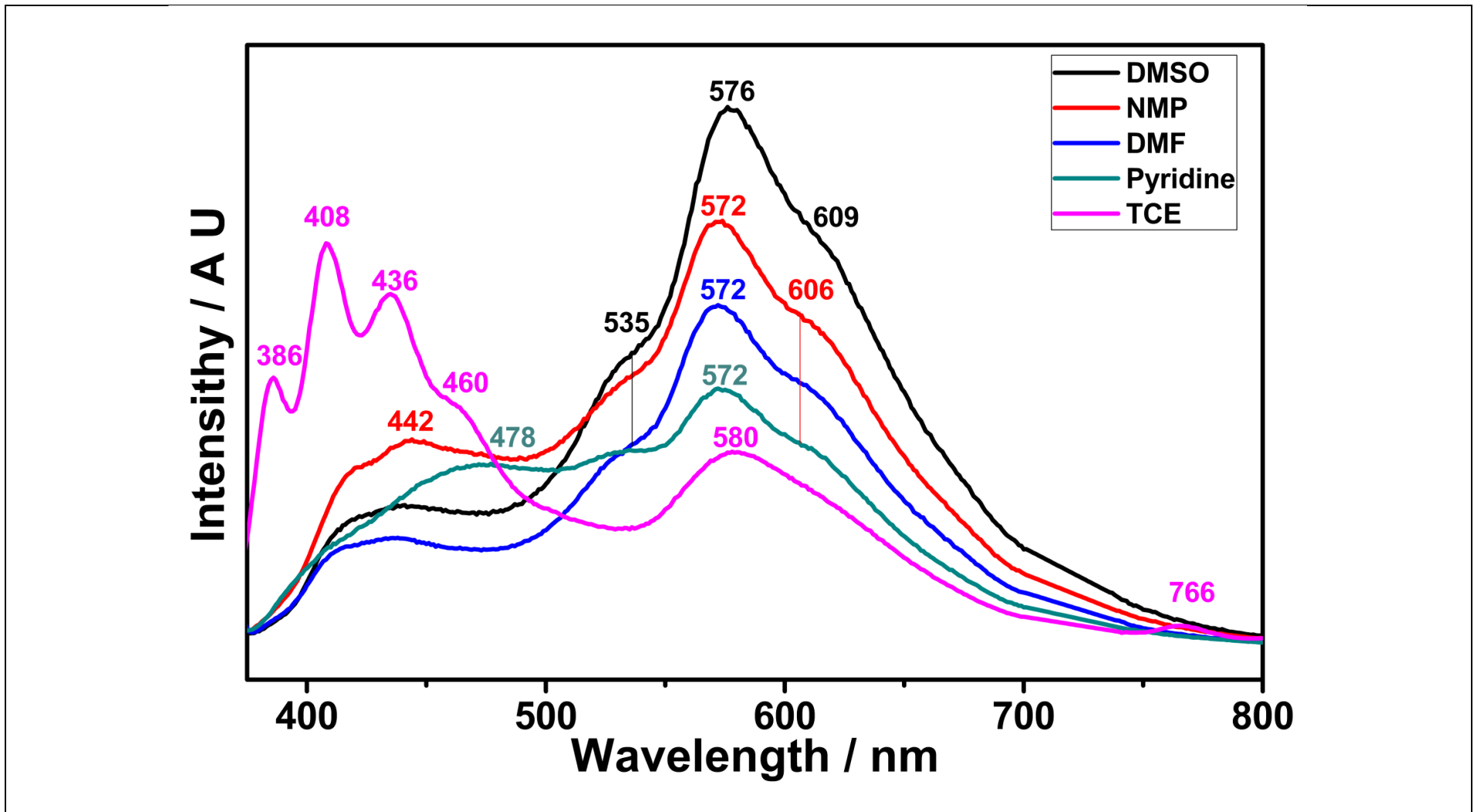


Figure 4.76: Emission Spectrum of TANPI in DMSO, DMF, NMP, Pyridine, and TCE (Microfiltered; $\lambda_{exc} = 360$ nm)

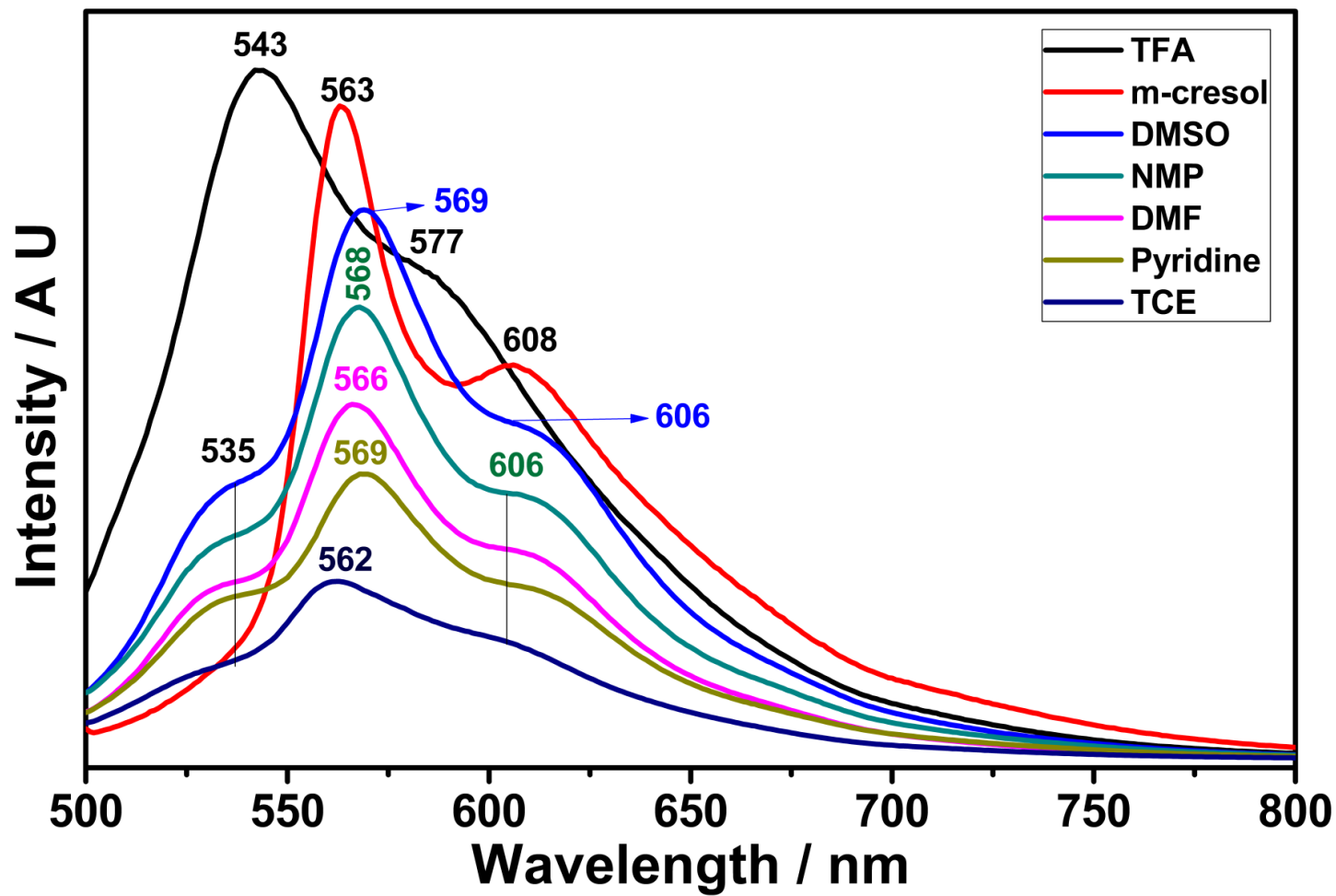


Figure 4.77: Emission Spectrum of TANPI in TFA, M-cresol, DMSO, DMF, NMP, Pyridine, and TCE ($C = 1 \times 10^{-5} \text{ M}$; $\lambda_{\text{exc}} = 485 \text{ nm}$)

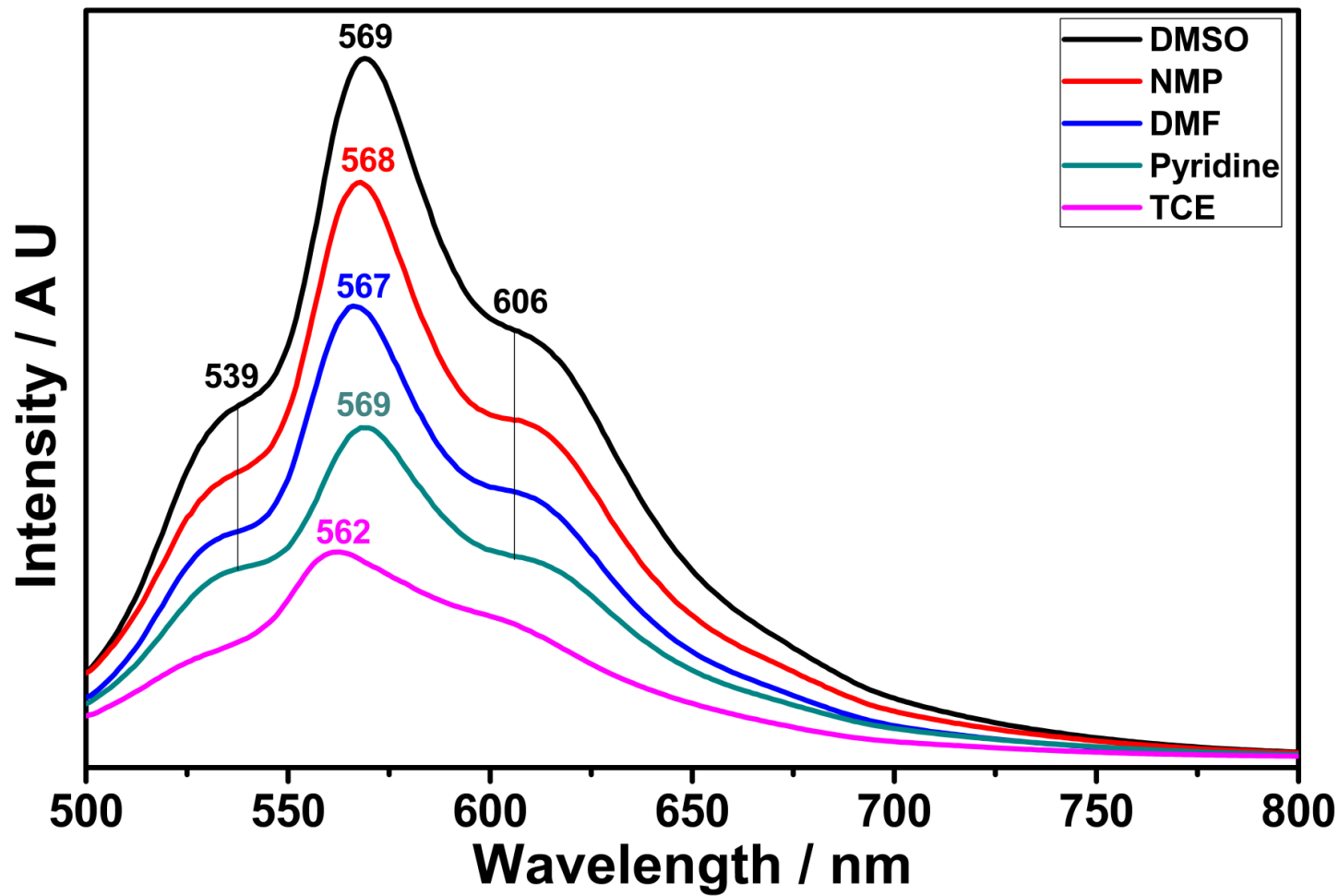


Figure 4.78: Emission Spectrum of TANPI in DMSO, DMF, NMP, Pyridine, and TCE (Microfiltered $\lambda_{\text{exc}} = 485$ nm)

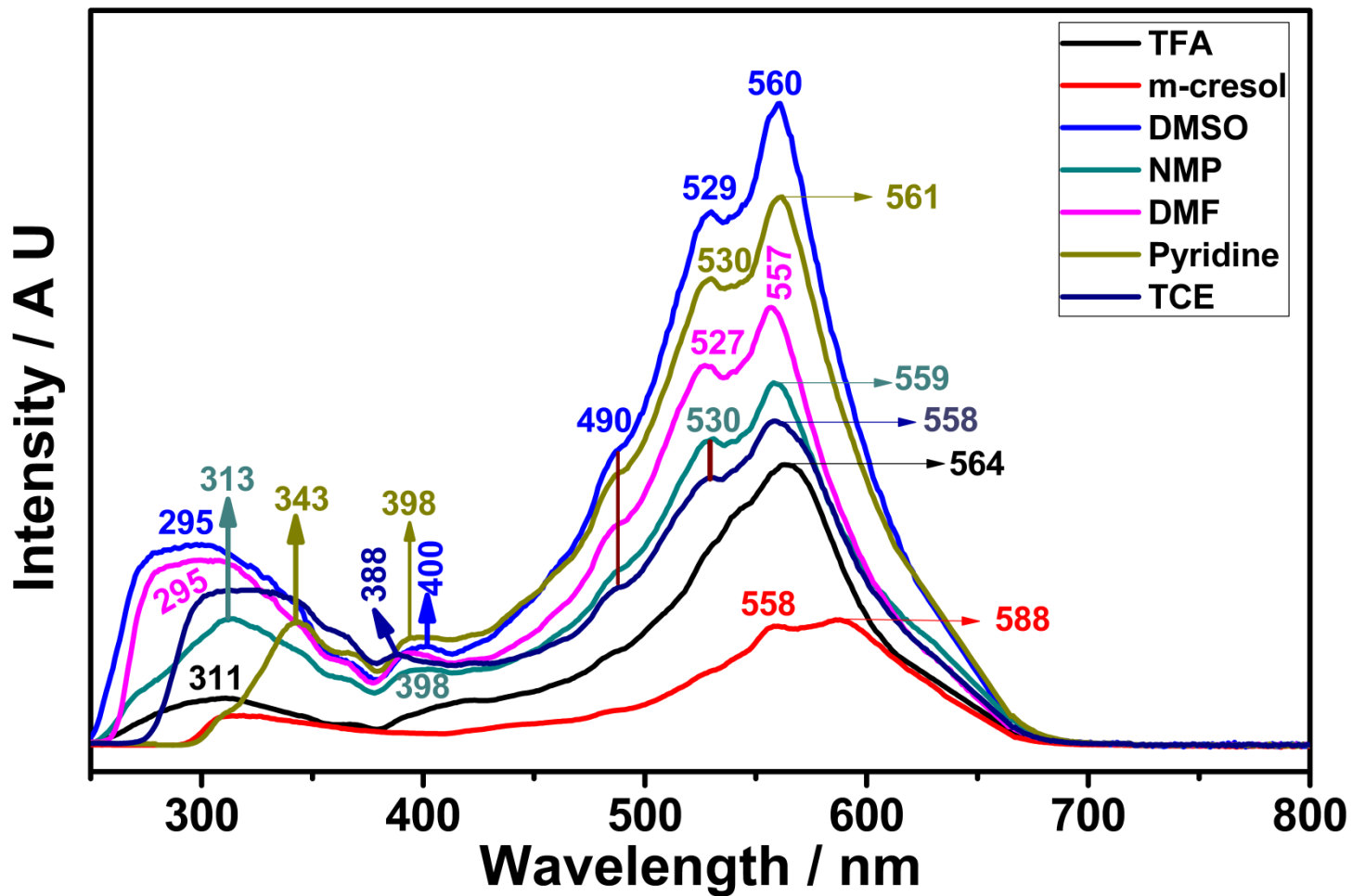


Figure 4.79: Excitation Spectrum of TANPI in TFA, M-cresol, DMSO, DMF, NMP, Pyridine, and TCE ($C = 1 \times 10^{-5} \text{M}$; $\lambda_{\text{emis}} = 650 \text{ nm}$)

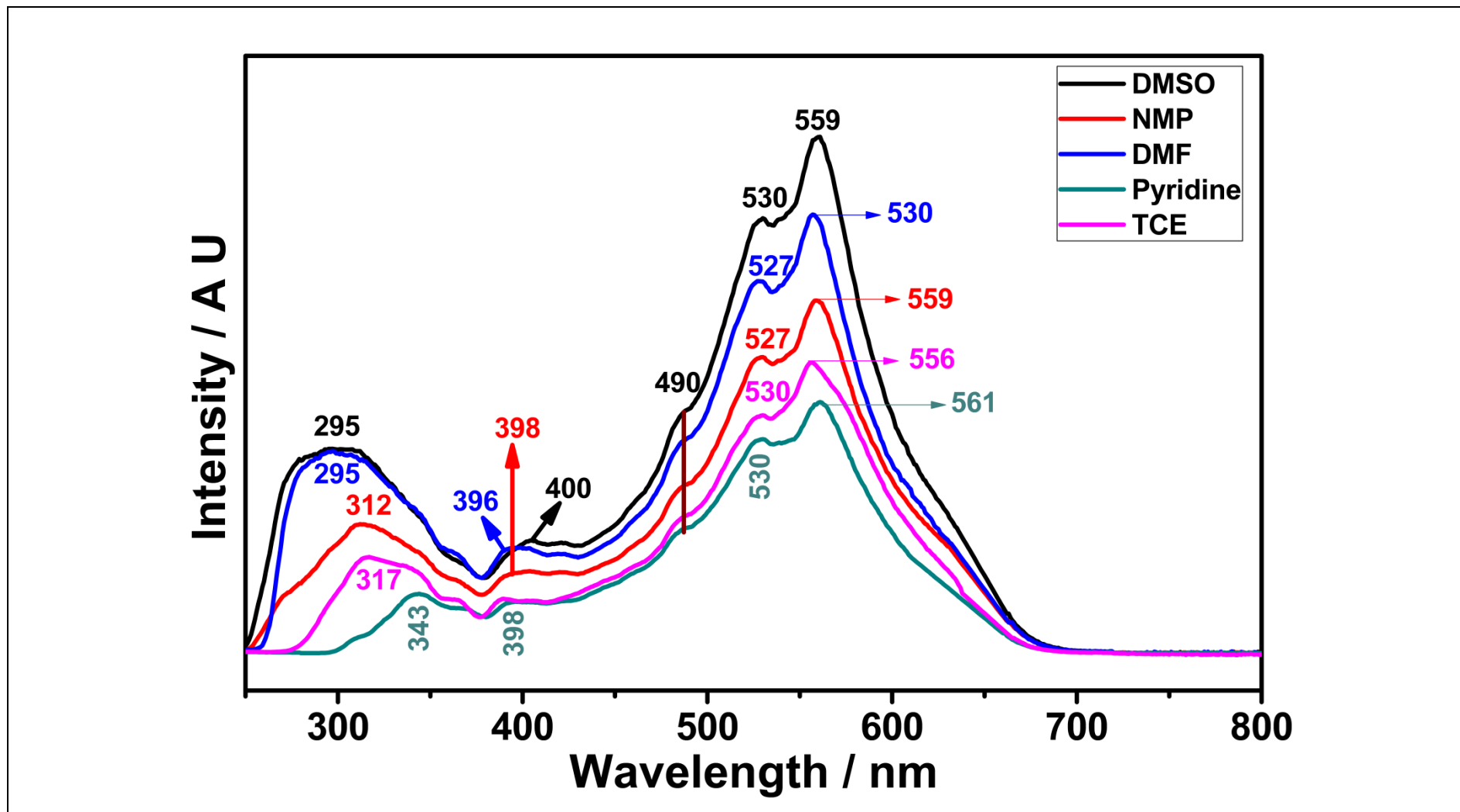


Figure 4.80: Excitation Spectrum of TANPI in DMSO, DMF, NMP, Pyridine, and TCE (Microfiltered; $\lambda_{\text{emis}} = 650 \text{ nm}$)

Chapter 5

RESULT AND DISCUSSION

5.1 Synthesis of the Compound TANPI

The synthetic route of TANPI compound is shown in Scheme 3.1. TANPI was synthesized by condensation of 1, 4, 5, 8-naphthalene tetracarboxylic dianhydride (NDA) with 2, 4-diamino-6-phenyl-1, 3, 5-triazine in isoquinoline solvent under argon atmosphere. The synthesized product was characterized through the data from IR, UV-vis, and elemental analysis. These characterizations confirmed the formation of a new polymer as a major product (Schemes 3.1).

5.2 Solubility of TANPI

The solubility of the product was studied in detail. The product TANPI is soluble mainly in polar solvents such as pyridine, NMP, DMF, DMSO, m-cresol and TFAC in brown colour (Table 5.1). The product was insoluble in polar protic solvents such ethanol and methanol.

Table 5.1: Solubility properties of TANPI in different solvents

solvents	Solubility^a / Color
DMSO	(+ +) Fluorescence, Light brown
NMP	(+ +) Fluorescence, Dark brown
DMF	(+ +) Fluorescence, Light brown
TFAC	(+ +) Fluorescence, Dark brown

m-cresol	(+ +) Fluorescence, Dark brown
Pyridine	(+ +) Fluorescence, Light brown
TCE	(- +) Light yellow
CHL	(- -) colorless
Me OH	(- -) colorless
EtOH	(- -) colorless
Acetone	(- -) colorless
H₂O	(- -) colorless

^a 1.0 mg of TANPI in 10ml of solvent; + + soluble at room temperature; - - insoluble; - + partial soluble at 60 °C.

5.3 Analysis of FTIR Spectra

The IR spectrum of TANPI was consistent with its chemical structure. As shown in Figure 4.4, the IR spectrum of TANPI exhibited characteristic absorption bands at 3448 (N–H stretch); 3175, 3070 (aromatic C–H stretch); 2860 (aromatic C–H stretch); 1696 (imide C=O stretch); 1632 (imide C=O stretch); 1578 (conjugated C=C stretch); 1526 (N–H bending); 1445 (C=N triazine); 1345 (C-N stretch); 1270 (CN) stretch; 1106 (CNC stretch); 855, 768 and 624 (C–H bend) cm⁻¹. Results of elemental analysis of compound in a good agreement with the calculated values.

5.4 Optical Properties

Figure 4.5, 4.6 and 4.7 shows that the shape of the absorption bands of TANPI in DMSO before ($\lambda_{\max} = 343, 360, 379$ with shoulder peaks at 411 and 560 nm) and after microfiltration ($\lambda_{\max} = 343, 359, 379$ with a red shifted shoulder peak at 560 nm) are almost same (all concentrations before microfiltration were 10^{-5} M, pore size of micro filter; 0.2 μm SPR). A red shifted shoulder at 411 nm were observed probably due to aggregation and disappeared upon microfiltration. Interestingly, the emission spectra monitored for the TANPI are different in shapes and in wavelength range. Before microfiltration, the red-shifted excimer-like fluorescence indicate the presence of intermolecular π -stacking of the compound in solution ($\lambda_{\max} = 577$ nm, shoulder peaks; 408, 536, 610 nm, Figure 4.8, 4.9, 4.10, $\lambda_{\text{exc}} = 360$ nm). The shoulder peak at 408 nm shifted to 440 nm and intensified upon microfiltration. Emission measurement of TANPI in DMSO was repeated at $\lambda_{\text{exc}} = 485$ nm. A blue shifted similar excimer-like emission was monitored before and after microfiltration ($\lambda_{\max} = 569$ nm, shoulder peaks; 536, 609 nm, Figure 4.11, 4.12, 4.13, $\lambda_{\text{exc}} = 485$ nm). The absorbance peak at 560 nm indicates the presence of energy transfer also. Additionally, the product has shown a very long Stoke shift (approximately 198 nm) which could be important in photonic applications (Table 5.2). Respective excitation spectrum was not similar to the UV-vis absorption spectra both before and after microfiltration ($\lambda_{\max} = 300, 400, 490, 529$ and 560 nm, Figure 4.14, 4.15, 4.16, $\lambda_{\text{emission}} = 650$ nm).

Similar optical properties were observed in DMF solution. The shape of the absorption bands of TANPI in DMF before ($\lambda_{\max} = 343, 358, 378$ with shoulder peaks at 411 and 560 nm) and after microfiltration ($\lambda_{\max} = 343, 358, 378$ with a red

shifted shoulder peak at 557 nm) are almost same (Figure 4.17, 4.18, 4.19. A red shifted shoulder at 411 nm were observed probably due to aggregation and disappeared upon microfiltration. The emission spectra monitored for the TANPI in DMF are different in shapes and in wavelength range as in the case of DMSO solution. Before microfiltration, the red-shifted excimer-like fluorescence indicate the presence of intermolecular π -stacking of the compound in solution ($\lambda_{\text{max}} = 572$ nm, shoulder peaks; 407, 536, 604 nm, Figure 4.20, 4.21, 4.22, $\lambda_{\text{exc}} = 360$ nm) with a 195 nm Stoke shift (Table 5.2). Upon microfiltration, the shoulder peak at 408 nm shifted to 437 nm and intensified. Emission measurement of TANPI in DMF was repeated at $\lambda_{\text{exc}} = 485$ nm. A blue shifted similar excimer-like emission was monitored before and after microfiltration ($\lambda_{\text{max}} = 566$ nm, shoulder peaks; 536, 606 nm, Figure 4.23, 4.24, 4.25, $\lambda_{\text{exc}} = 485$ nm). The absorbance peak at 557 nm indicates the presence of energy transfer also. Respective excitation spectrum was not similar to the UV-vis absorption spectra both before and after microfiltration ($\lambda_{\text{max}} = 300, 395, 489, 527$ and 557 nm, Figure 4.26, 4.27, 4.28, $\lambda_{\text{emission}} = 650$ nm).

Figure 4.29, 4.30 and 4.31 show the UV-vis absorption spectra of the product in NMP before and after microfiltration. Except the aggregation peak (414 nm), the values of the absorption wavelengths maxima of TANPI were exactly same (343, 358, 377 nm) before and after microfiltration. In fluorescence spectra measured in NMP, an excimer-like peak at 572 nm was observed (additional shoulder peaks at 408, 536 and 606 nm) with 194 nm Stoke shift (Figure 4.32, 4.33 and 4.34, Table 5.2). The fluorescence spectra of TANPI taken at $\lambda_{\text{exc}} = 485$ nm in NMP showed blue shifted similar shape excimer-like emission (568 nm, shoulder peaks; 537 and 606; Figure 4.35, 4.36 and 4.37). Respective excitation spectrum was different than the

UV-vis absorption spectra taken in NMP (313, 398, 490, 530 and 559 nm; Figure 4.38, 4.39 and 4.40, $\lambda_{\text{emission}} = 650$ nm).

Interestingly, TANPI showed new two absorption peaks at 396 and 415 in 1,1,2,2-tetrachloroethane (TCE) and did not disappear upon microfiltration (343, 358, 378, 396, 415 and 555 nm, Figure 4.41, 4.42, 4.43). Moreover, the fluorescence spectra of TANPI taken at $\lambda_{\text{exc}} = 360$ nm has shown broad excimer-like emission in a range of 400-800 nm before and after microfiltration ($\lambda_{\text{max}} = 387, 408, 435, 461, 579$ and 767 nm, Figure 4.44, 4.45, 4.46, $\lambda_{\text{exc}} = 360$ nm) with a 30 nm Stoke shift. Additionally, the fluorescence spectra measured at $\lambda_{\text{exc}} = 485$ nm showed excimer-like emission with a $\lambda_{\text{max}} = 562$ nm (534, 562, 599 nm, Figure 4.47, 4.48, 4.49, $\lambda_{\text{exc}} = 485$ nm). Respective excitation spectrum was very different comparing to the UV-vis absorption spectra (320, 388, 490, 530 and 558 nm, Figure 4.50, 4.51 and 4.52, $\lambda_{\text{emission}} = 650$ nm). After the microfiltration maximum absorption wavelength has blue shifted only 2 nm.

The absorption spectra of the product in pyridine before and after microfiltration are shown in Figure 4.53, 4.54 and 4.55. Both of the spectra were completely same ($\lambda_{\text{max}} = 343, 359, 379, 414, 519$ and 559 nm). The fluorescence spectra were similar also with a broad excimer-like emission in the range of 400-800 nm (475, 532, 574 and 606 nm, Figure 4.56, 4.57 and 4.58, $\lambda_{\text{exc}} = 360$ nm) with a 198 nm Stoke shift (Table 5.2). The emission spectra taken at $\lambda_{\text{exc}} = 485$ nm showed an excimer-like emission with a maximum at 569 nm (540, 569 and 606 nm, Figure 4.59, 4.60 and 4.61 nm, $\lambda_{\text{exc}} = 485$ nm). Respective excitation spectrum was very different comparing to the UV-vis absorption spectra (343, 394, 490, 530 and 560 nm, Figure

4.62, 4.63 and 4.64, $\lambda_{\text{emission}} = 650 \text{ nm}$).

In the absorption spectra taken in m-cresol, a red-shifted charge transfer style broad absorption peak was observed ($\lambda_{\text{max}} = 381 \text{ nm}$, shoulder peaks; 367, 404 and 555 nm, Figure 4.65). The fluorescence spectra taken in m-cresol have shown one red shifted excimer-like emission (610 nm, shoulder peak; 405 and 568 nm, Figure 4.66, $\lambda_{\text{exc}} = 360 \text{ nm}$) with a 50 nm Stoke shift (Table 5.2). On the other hand, the fluorescence spectra taken at 485 excitation wavelength has shown excimer-like emission with a maxima at 563 nm (563 and 606 nm, Figure 4.67, $\lambda_{\text{exc}} = 485 \text{ nm}$). Respective excitation spectrum was different than the UV-vis absorption spectrum of the product (319, 489, 559 and 587 nm, Figure 4.68, $\lambda_{\text{emission}} = 650 \text{ nm}$).

In trifluoroacetic acid, TANPI showed 3 characteristic peaks at 463, 359 and 379 nm which are assigned to vibronic $0 \rightarrow 0$, $0 \rightarrow 1$ and $0 \rightarrow 2$ progressions of the electronic $S_0 \rightarrow S_1$ transition respectively (Figure 4.69). In fluorescence spectra of the compound in trifluoroacetic acid, two broader excimer-like peaks were observed at 394, 412 and 433 nm with a 33 nm Stoke shift (Figure 4.70, $\lambda_{\text{exc}} = 360 \text{ nm}$, Table 5.2). The excimer-like emission peak was observed at 544 nm when excitation wavelength kept at 485 nm (shoulder peak; 579, Figure 4.71). Respective excitation spectrum was very different than the UV-vis absorption spectrum of the product (308, 421 and 564 nm, Figure 4.72, $\lambda_{\text{emission}} = 650 \text{ nm}$).

It is important to note that, different absorption and emission properties have been observed due to different intermolecular interactions as can be observed in Figures 4.73 to 4.80. This important property can be used in different photonic applications.

The emission spectra of TANPI were taken at $\lambda_{\text{exc}} = 360$ nm and the relative fluorescence quantum yields were determined in NMP, DMF and DMSO using anthracene in ethanol as standard. Low fluorescence quantum yields of naphthalene derivatives (NMP: 2%, DMF: 5% and DMSO: 1%) are in good correlation with literature data [3] (Table 5.3).

Table 5.2: Stokes shifts of TANPI ($C = 1 \times 10^{-5}$ M) in different solvents

Solvent	UV-Vis Absorption	Emission	Stokes Shift (nm)	Stokes Shift (cm)
	(nm)	(nm)		
	λ_{max}	λ_{max}		
DMSO	379	577	198	1.98×10^{-5}
DMF	378	572	194	1.94×10^{-5}
NMP	377	572	195	1.95×10^{-5}
TCE	378	408	30	3.0×10^{-6}
Pyridine	379	574	196	1.96×10^{-5}
m-cresol	381	431	50	5.0×10^{-6}
TFAc	379	412	33	3.3×10^{-6}

Table 5.3: Optical and Photochemical Constant

solvents	λ_{\max}	ϵ_{\max} ($M^{-1}\cdot L$)	Φ_f	$\Delta\bar{\nu}_{1/2}$ (cm^{-1})	τ_o (ns)	τ_f (ns)	k_f (s^{-1})	k_d (s^{-1})	f	Es kcal.mol	Eg (ev)
DMSO	379	31062.10	0.01	1995.27	8.11	0.81	1.23×10^8	1.21×10^9	0.27	75.46	3.07
NMP	377	41648.80	0.02	1941.69	6.151	0.12	1.63×10^8	3.57×10^9	0.35	75.86	3.13
DMF	378	33987.32	0.03	1482.60	9.94	0.81	1×10^8	9.9×10^9	0.22	75.66	3.13

Chapter 6

CONCLUSION

A novel naphthalene polymer (TANPI) was synthesized by polycondensation of 1,4,5,8-naphthalene tetracarboxylic dianhydride (NDA) with hindered aromatic diamine, 2,4-diamino-6-phenyl-1,3,5-triazine successfully. The purity of the polymer was confirmed using elemental analysis, IR and UV-vis spectroscopy.

The product TANPI is soluble mainly in polar solvents such as pyridine, DMF and DMSO in light brown and NMP, m-cresol and TFAC dark brown colors.

The polymer has shown enhanced absorptions with aggregations and excimer emissions with long Stoke Shifts. Moreover, the observed excitation spectra were different than the UV-vis absorption spectra of the product in all solvents. The red-shifted excimer-like fluorescence has shown the presence of intermolecular π -stacking of the polymer in solution.

A red-shifted and broad charge transfer kind absorption peak was observed in m-cresol solvent. Its fluorescence spectrum has shown one red shifted excimer-like emission with a 50 nm Stoke shift.

Complete characterization of the naphthalene polymer and its optical and electrochemical properties will be explored in our future studies.

REFERENCES

- [1] Smith, B. H. (1964). Bridged Aromatic Compounds, *Academic Press, New York*.
- [2] Bhosale, S. V., Jani, C. H, & Langford, S. J. (2008). Chemistry of Naphthalene Diimides. *Chemical Society Reviews* **37**(2): 331–342.
- [3] Ozser , M. E., Elci, D. Uzun. I., & Icil, H. (2003). Novel Naphthalene Diimides and a Cyclophane Thereof: Synthesis, Characterization, Photophysical and Electrochemical Properties. *Journal of Photochemistry and Photobiology Science*. **2**: 218 –223.
- [4] Asir, S., Demir, A. S., & Icil, H. (2010). The Synthesis of Novel, Unsymmetrically Substituted, Chiral Naphthalene and Perylene Diimides: Photophysical, Electrochemical, Chiroptical and Intramolecular Charge Transfer Properties. *Dyes and Pigments*. **84**:1–13.
- [5] Aveline, B. M., Matsugo, S., & Remond, R. W. (1997). Photochemical Mechanisms Responsible for the Versatile Application of Naphthalene Imides and Naphthalene Diimides In Biological Systems. *Journal of the American Chemical Society* **119**(49): 11785–11795.
- [6] Ozser, M. E., Yucekan, I., Bodapati, J.B & Icil, H. (2013). New Naphthalene Polyimide with Unusual Molar Absorption Coefficient and Excited State Properties: Synthesis, Photo Physics and Electrochemistry. *Luminescence*. **143**: 542 – 550.

- [7] Mazzitelli, C. L., (2007). Screening of Threading Bis-Intercalators Binding to Duplex DNA by Electrospray Ionization Tandem Mass Spectrometry. *Journal of the American Society for Mass Spectrometry* **18**(2): 311–321.
- [9] Lehn, J. M., Eliseev, A.V. (1985). Supramolecular Chemistry: Receptors, Catalysts, and Carriers. *Science*.227: 849 –856.
- [10] Ying, J.Y., Mehnert, C., P., & Wong, M.S. (1999). Synthesis and Applications of Supramolecular-Templated Mesoporous Materials. *Chemical Society Reviews*. **38** (2): 56 –77.
- [11] Blacker, A.J., Jazwinski, J., Lehn, L.M., & Cesario, J. (1987). Binding Of Nucleosides Nucleotides and Anionic Planar Substrates By Bis-Intercaland Receptor Molecules. *Tetrahedron Letters*. **28**(1): 60 –67.
- [12] Pechlivanidis, Z., Hopf, H., Grunenberg, J., and Ernst, L. (2009). Planar Chiral Asymmetric Naphthalene Diimide Cyclophanes: Synthesis, Characterization and Tunable FRET Properties. *Journal of Organic Chemistry*. **2**: 3–8.
- [13] Brown, C., J., & Farthing, A. C. (1949). Paracyclophanes in Polymer Chemistry and Materials Science. *Nature*. **47**(51): 9–15.
- [14] Sekine, Y., Brown, M., & Boekelheide, V. (1979). [2.2.2.2.2](1, 2, 3, 4, 5, 6) Cyclophane: Superphone. *Journal of the American Chemical Society*. **101**(11): 3126–3127.

- [15] Wasielewski, M., R., & Betzen, L.J. (1994). Wire-Like Charge Transport At Near Constant Bridge Energy Through Fluorene Oligomers. *Chemical Reviews*. **92**(2): 435–461.
- [16] Hai-jun, N., Jing-Shan, M., Mi-lin, Z., Jun, L., Pei-Hui, L., Xu-Duo., & Wen, W. (2009). Naphthalene-Containing Polyimides: Synthesis, Characterization and Photovoltaic Properties of Novel Doner-Acceptor Dyes Used in Solar Cell. *Trans Nonferrous Society China*. **19**: 587 – 593.
- [17] Gawrys, P., Boudient, D., Malgorzata, Z., David, D., Verlhac, J. M., Horwitz, G., Pecaud, J., Pouget, S., & Pron, A. (2009). Solution Processible Naphthalene and Pylene Bisimides: Synthesis, Electrochemical Characterization and Application To Organic Field Effect Transistor (OFETs) Fabrication. *Synthetic Method*. **159**: 1478 – 1485.
- [18] Kim, Y.D, Cho, J.H., Park, C.R, & Yoon, C. (2010). Synthesis, Application and Investigation Of Structure–Thermal Stability Relationships of Thermally Stable Water-Soluble Azo Naphthalene Dyes. *Chemical Society of Korea*. **89**(1): 1 – 8.
- [19] Gorteau, V., Cuillaume, B., & Matile, S. (2006). Rigid Oligo-Naphthalene diimide Rods as Transmembrane Anion- π Slides. *Journal of the American Chemical Society*. **128**(46): 14788 – 14789.
- [20] Thalacker, c., Roger, C., & Wurther, F. (2006). Synthesis and Optical and Redox Properties of Core-Substituted Naphthalene Diimide Dyes. *Journal of organic Chemistry*. **71**(21): 8098 – 8105.

- [21] Andric, G., Boas, J. F., Bond, A. M., Fallon, G. D. (2004). Three-component zipper assembly of photoactive cascade architectures with blue, red and colorless naphthalene diimide donors and acceptors. *Australian Journal of Chemistry*. **57**: 1011–1019.
- [22] Polander, L.E., Pomanov, A.S., Barlow, S., Hwang, D. K, & Marder, S.R. (2012). Stannyl Derivatives of Naphthalene Diimides and Their Use in Oligomer Synthesis. *Organic Letters*. **14**(3): 918 – 921.
- [23] Pan, M., Lin, X. M, Guo, B. L., & Cheng-Yong ,S. (2011). Progress in The Study Of Metal–Organic Materials Applying Naphthalene Diimide (NDI) Ligands. *Journal of Organic Chemistry*. **255**(15–16):1921 – 1936.
- [24] Dixon, D. W., Thornton, N. B., Stenlet, V., & Netzel, T. (1999). Effect of DNA Scaffolding on Intramolecular Electron Transfer Quenching of a Photoexcited Ruthenium(II) Polypyridine Naphthalene Diimide. *Journal of Organic Chemistry*. **38**(24):5526 – 5534.
- [25] Zhan, X., Faccetti, A., Barlow, S., Marks, T. J., Rontner, M. A., & Marder, S.R. (2010). Rylene and Related Diimides for Organic Electronics. *Journal of Organic Chemistry*. **23**(2): 268 – 284.
- [26] Xie, H., Tansil, N. C., & Geo, Z. (2006). A Redox Active and Electrochemical Luminescent Threading Bis-Intercalator And Its Applications In DNA Assays.

Biochemistry. **11**: 1147 – 1157.

- [27] Clegg, R. M. (1995). Fluorescence Resonance Energy Transfer. *Journal of Inorganic Chemistry*. **6**(1): 130 –110.
- [28] Selvin, P. R . (2000). The Renaissance of Fluorescence Resonance Energy Transfer. *Nature Structural Biology* .**9**(1):58 – 63.
- [29] Lin, S. H., Xiao, W. Z., & Dietz ,W. (1993). Generalized Förster-Dexter Theory of Photoinduced Intramolecular energy transfer. *Physical Reviews*. **47** :36 – 98.
- [30] Marcus, R.A. (1993). Electron Transfer Reactions in Chemistry. *Review Modern Physics*. **65**(21): 95 – 99.
- [31] King, G., & Warshel, A. (1990). Investigation of the free energy functions for electron transfer reactions. *Journal of Chemical Physics*.**93**:86 – 82.
- [32] Albinsson , B., & Martensson , J. (2008). Long-range electron and excitation energy transfer in donor–bridge–acceptor systems. *Journal of photochemistry review*. **9**(3): 138 – 155.
- [33] Kavarnos, G. L. & Turro, N. J. (1986). Photosensitization by Reversible Electron Transfer: Theories, Experimental Evidence, and Examples. *Chemistry Review*. **86**: 401 – 449.
- [34] Erten, S., Alp, S., & Icli, S. (2005). Photooxidation Quantum Yield Efficiencies

of Naphthalene Diimides Under Concentrated Sun Light in Comparisons With Perylene Diimides. *Journal of photochemistry*. **175** (2-3):214 – 220.

[35] Ramamurthy, V., & Mondal, B. (2015). Supramolecular Photochemistry Concepts Highlighted with Select Examples. *Photochemistry Review*. **23**: 68 – 102.

[36] Matthew, C., Fyfe, T., & Stoddart, J. F. (1997). Synthetic Supramolecular Chemistry. *Accounts of Chemical Research*. **30** (10):393 – 401.

[37] Aleshiloye, A. O., Bodapati, J. B, Icil, H. (2105). Synthesis, Characterization, Optical And Electrochemical Properties of A New Chiral Multi Chromophoric System Based On Perylene And Naphthalene Diimides. *Journal of Photochemistry and Photobiology A: Chem* **300**: 27 – 37.

[38] Cai, C. B., Han, Q. J., Tang, L.J., Xu, L., Wu, H. L., Jiang, J. H., & Yu, R. Q. (2009). The Spatial Effect Of Near-Infrared Spectroscopy and Its Application To The Study Of Supramolecular Chemistry. *Talanta*. **78**(2): 337 – 341.

[39] Craig, D. C., Ghiggino, K. P., Jolliffe, K.A., Langford, S. J., & Paddon-Row, M. N. (1997). Photoinduced Electron Transfer in Rigid Supramolecular Systems – Synthesis, Structure and Properties of a Novel Rigid Bichromophoric System Bearing a Viologen. *Journal of organic chemistry*. **62**: 2381 – 2386.

[40] Ruland, G . E, (1997). PhD Thesis, State University of New York.

- [42] Zhan, X., Facchetti, A., Barlow, S., Marks, T. J., Ratner, M. A., Wasielewski, M. R., & Marder, S. R. (2011). Rylene And Related Diimides For Organic Electronics. *Advance Mater.* 23: 268 – 284.
- [43] Ozser, M. E., Yucekan, I., Bodapati, J. B & Icil, H. (2013). New Naphthalene Polyimide With Unusual Molar Absorption Coefficient And Excited State Properties: Synthesis, Photophysics And Electrochemistry. *Luminescence.* 143: 542 – 550.
- [44] Uzun, D., Ozser, M. E., Yuney, K., & Icil, H. (2003). Synthesis and Photophysical Properties of N,N' – Bis-(4-Cyanophenyl) – 3,4,9,10- Perylenebis (Dicarboximide) and N,N'–Bis-(4-Cyanophenyl)–1,4,5,8-Naphthalene Diimide. *Journal of Photochemistry and Photobiology A: Chemistry.* **156**: 45 – 54.

APPENDIX

APPENDIX A: CURRICULUM VITAE CV

Personal details:

Full name	Kawa Hama Sharif Mahmood
Gender	Male
Date of birth	19 April 1984
Place of birth	Sulaimaniyah-kurdistan , Iraq
Marital status	Married
Nationality	Kurdish
Mobile phone	+9647702485115 and +9647503740845
Email address	Chemistkawa@gmail.com
Postal Address	House No.18 , street No.46 , Azadi quarter ChamchamaL, Sulaimaniyah , Iraq
Driving license	Full Iraqi-kurdistan driving license

Education:

1990-1996	Akhter primary school
1997-1999	Chamchaml secondary school
2000-2003	Hallo high school

Training

- 🚦 2007 – I participated in a summer course in Shahid peshraw Hospital in chamchamal on analyzing diseases by using chemical materials in laboratories.

Academic Qualifications

2008 – Obtained Bachelor Degree (B.S) with distinction in chemistry from Salahaddin University – College of science – chemistry department, Erbil, Iraq

Work Experiences

✚ 2008 – 2013 I have been teaching chemistry at several high schools in (Chamchamal , peshraw , Shwan ,)

✚ 2011 – 2013 I have been the headmaster of peshraw preparatory school.

✚ 25/5/2010 - 11/12/2011 I was worked at the Lab. of Mass cement factory in sulaymaniyah testing cement quality using my procedure .

2013- Present EASTERN MEDITERRANEAN UNIVERSITY, Department of Chemistry (Research Assistant)

